Translated to English from paper in Japanese, originally published in:
Gijutsu Houkoku, Vol.28, No.3 (No.86), 1-77, 1989 with permission of authors.

Geoelectric Observation used by the Telegraphic Facilities of NTT Corporation

by

Toshio MORI

Abstract

Unique geoelectric observations have been conducted in land and on the sea floor in the Kanto and Tokai districts in Japan, and progress has been made on original research. The geoelectric observations on land were conducted using the telegraphic facilities of Nippon Telegraph and Telephone Public Corporation (now NTT Company). The geoelectric observations on the sea floor have been observed by making use of the power-feeding arrangement of Permanent Ocean-Bottom Seismograph Observation Systems off Tokai and off the Boso Peninsula installed by the Japan Meteorological Agency. These geoelectric data are fairly high quality in comparison with conventional geoelectric data.

A comparison examination of the geoelectric data observed by NTT facilities was carried out with geomagnetic changes, geoelectric changes, seismic and volcanic activities, tide level changes, the weather elements, etc. Moreover, examination of the use of geoelectric noises was also performed.

The geoelectric observations using the electrodes and the underground metallic cables of NTT have been performed mainly in the Mito and Numazu telephone offices. The observations have the following two advantages in comparison with conventional methods: (1) The contact electric potential between the electrode and the soil seems very stable. Therefore, we can obtain stable data over a long time which is not affected by precipitation. (2) The base lengths for the observation are very long. The base lengths are 10 to 100 times longer than those for other ordinary observations in Japan. So, the observed field is affected by a large-scale structure.

The data observed at the Mito group are fairly noiseless, while the data at the Numazu and Fujinomiya groups contain large amplitude noises. In order to improve the detectability of self-potential variations related to tectonic activities, various methods were tried and developed by making use of these data. Especially, emphasis was placed on analysis by the method of real-time detection of anomalous geoelectric changes by removing components induced by geomagnetic variations with a stochastic difference equation.

As a result of investigating the relations between the observed geoelectric variations and tectonic activities, although no related change was observed in the Mito group, some abnormalities were found in the Numazu group. Anomalous electric potentials at the Numazu group took place simultaneously with the start of the earthquake swarm off the east coast of Izu on October, 1985. The electrical potential changes that took place ranged up to 300 mV in Atami, and 100 mV in Ito and Shuzenji. The Izu-Oshima volcano erupted on November 15, 1986. Before the start of the eruption, the geoelectric potentials at ODW were estimated to have decreased abruptly by 500 mV on November 6 and attained a maximum decrease of 800 mV on November 9.

Electrical potential changes relevant to tide level changes, and constituents of geoelectric change unrelated to geomagnetic change and long cycle change, were also detected.

It was shown that the observed electric noises are applicable to investigate the underground

structure and to detect underground electrical characteristic changes. If the earth potential is observed near the conductivity anomaly boundary, it will be thought possible to detect unusual sensitivity phenomena relevant to tectonic activities.

Comments on the English translation

The following will be noticed if a paper of about 15 years ago is put into English and read over again.

Mistakes were made in clarity and in some unsuitable expressions, such as in the names of places which are considered to be common sense by Japanese people, and in expressions where a simplified term was found. Corrections were made for those parts and explanation was added. Although notations of figures had portions which are not unified, since correction was difficult, the notation was left as it is, but explanations were added as much as possible.

As it is described in the "Circumstances of observation and acknowledgements," this paper was written when research business was being replaced with administrative business. Since it was thought that it would be difficult to return to research business as before, the data and ideas were hurriedly adjusted. In addition, since there was no Abstract in the text, it was written at this time.

Finally, the author is thankful to the personnel of the Magnetic Observatory who gave us this opportunity.

Geoelectric Observation used by the Telegraphic Facilities of NTT Corporation

CONTENTS

1. Introduction
2. Observation method
3. Outline of the observed records
   3-1 Outline of the records at each observation group
   3-2 Comparison of the observed record in the same time of a different day
4. Long-term stability
5. Impedance tensor and transfer function
   5-1 Impedance tensor at the Shimodate group and at Kakioka
   5-2 Impedance tensor at the Mito group and transfer function at Kakioka
6. Time changes of impedance tensors and transfer functions
7. Elimination of the electrical fields induced by geomagnetic variations - Detection of the anomalous earth potential -
   7-1 Analysis method by a stochastic differential equation
   7-2 For geoelectric fields between Kasama and Mito
   7-3 Application to the data of electrical fields at the Mito group and Z at Kakioka
   7-4 Spectral analysis
   7-5 When using per-minute data
   7-6 Use of the transfer function and impedance tensor
8. Relation to tectonic activities
   8-1 Relation to the earthquake swarms off the east coast of the Izu Peninsula
   8-2 Relation to eruptions of Izu-Oshima volcano
   8-3 Other changes
9. Relation to tide, atmospheric pressure and others
10. Application for research of fault structure
   10-1 Iriyama fault
   10-2 Tanna fault
   10-3 Fujikawa fault
11. Anomalous geoelectric change observed near CA (conductivity anomaly) boundary
12. Electrical observation on the sea floor by making use of the power-feeding arrangement of the Permanent Ocean-Bottom Seismograph Observation System off Boso Peninsula (BSOBS)
13. Conclusions
14. Circumstances of observation and acknowledgements

References

1. Introduction

Geoelectric observation is very simple, on the principal target, in order to measure the potential differences between two arbitrary points on the earth. But it is not so easy to recognize the significant geophysical signals, because the observed electrical field involves various other factors: meteorological factors (temperature, rainfall, moisture, etc.), artificial electrical noises from electric trains, factories, etc., troubles in the observation system (electrodes, insulation of the circuit, recorder, etc.) and so on. Especially, the contact potential between the electrodes and the soil are affected by the closeness of contact between the surface of the electrode and the surrounding soil, and also affected by the changes in meteorological conditions involving temperature, precipitation, content of soil moisture and so on. So we were not able to have confidence, especially in changes that occurred over several hours or more. Many authors have claimed that "anomalous changes" in earth potential prior to earthquakes were precursors. However, it has been debatable whether or not those anomalous changes were truly precursors, because of problems in the reliability of those data.

Unique geoelectric observations have been conducted in land and on the sea floor, which were originally developed by the author (Mori, 1982, 1985, 1987). The geoelectric observations on land were conducted by lengths of several 10 km, using the telegraphic facilities of Nippon Telegraph and Telephone Public Corporation (now NTT Company). The geoelectric observations on the sea floor have been observed by making use of the power-feeding arrangement of Permanent Ocean-Bottom Seismograph Observation Systems off Tokai (TKOBS) installed by the Japan Meteorological Agency (JMA). These geoelectric data are fairly high quality in comparison with conventional geoelectric data because of the stable contact potential. Therefore, we can get very useful data for geophysical research.

Geoelectric observation is sometimes called earth current observation. The history of earth current observation was summarized by Hatakeyama (1940), Chapman and Bartels (1940), Garland (1960) and others. It is said that the first earth current observation was performed in Britain in 1847 using a telephone wire by Barlow (1849). He used the telephone wires which connected with various points to Derly, and recognized the existence of earth currents. In August 1859, telegraphic systems throughout the world were considerably disturbed by irregular currents induced by remarkable geomagnetic storms. It is said that research of earth currents were ignited by it and prospered. The record of the geoelectric field was performed at Greenwich by Airy for two years after 1865. Also, the earth current observations were performed as the work of the First International Polar Years from 1882 to 1883. In Japan, Shyda (Shyda, 1886) observed electrical fields by using the telegraphic line between Nagasaki and Fuzan, and found clear daily variations in the electrical field. In the early history of earth current research, observations were conducted by telegraphic lines longer then 100 km. However, those observations had to be discontinued because of the disturbing effects of stray currents which resulted from electrical railways and other artificial sources. After that, routine observations of electrical fields have been continued by specific magnetic observatories.

Recently, geoelectric and geomagnetic observations on land have been actively conducted for research of underground conductivity, tectonic activities such as seismic precursors, etc. Most geoelectric observations have their base length less than a few hundred meters, and the observation periods are short except in routine observatories. The observations have also been actively conducted on the ocean floor. On the ocean floor, the lengths of the base lines of the observation are ordinarily short and the observation periods are also short, although the contact potential is stable. Therefore, it is difficult to study all of the events related to geoelectric variations.

As mentioned above, the specific electrical observations on the sea floor have been conducted by making use of the power-feeding arrangement of TKOBS installed by JMA. The results of the observations were reported by Mori (1982, 1987), and stable observation has been conducted over a long period of time. This observation length is about 110 km and very long, but there is only one component. Therefore, we can not discuss current direction. In 1986, Permanent Ocean-Bottom Seismograph Observation Systems off Boso Peninsula (BSOBS) were installed by JMA in the same system of TKOBS, so we can measure the electrical field on the sea floor. The length is about 80 km. Since Katsuura Weather Station installed the shore ground close to a direct-current train railroad, the electrical noise is very large in the day time. However, at midnight, the noise is not so large, so the electrical field records might be usable.

Many authors have reported anomalous changes of the geoelectric field preceding or accompanying earthquakes (e.g., Myachkin et al., 1972 ; Sobolev, 1975; Molnar et al., 1977; Corwin and Morrison, 1977; Varotsos and Alexopoulos, 1984). However, there is a problem in the reliability of the data, and it is truly doubtful in many cases whether it is the precursor of an earthquake. Consequently, we still do not have general concepts about the anomalous changes in the electrical fields as precursors of the tectonic activities, that is, how long, how intense and what type.

The geoelectric observations using the electrodes and the underground metallic cables of NTT were made not very long after these observations started. However, the data obtained from these observations is high quality, and especially seem to be epoch-making in their stability over a long period of time. These data are very useful for geoelectric research as compared with ordinary observations. The previous workers seem to have made an effort to calculate the electrical field induced by the observed magnetic variations and detect anomalous changes according to tectonic activities such as earthquakes. The author thinks that they could not have very reliable data for analysis. In this paper, emphasis is placed in the analysis on removing the induced electrical field from the observed one. That is how valuable data came to be obtained in such analysis. Geoelectric observations based on the use of long telegraph lines were made earlier in history, but no detailed analysis was done. The geoelectric observation which is described in this paper has not been performed in Japan recently.

In Japan, it is considered that the geoelectric observations at Kakioka Magnetic Observatory and other branch observatories of JMA are first class observations, but those observations have also been affected by heavy precipitations. It will be described in Section 4 that the observations using NTT facilities have not been affected by precipitation. The author had almost given up on long time variations in the geoelectric data before taking these data, while coming to hold great expectations for these new reliable data.

Though the observations using NTT facilities have been conducted with the good will of NTT, it was heard that the underground metallic cables of NTT would be replaced with optical fiber cables in the near future. Therefore, the author felt strongly a pressing need to learn whether the new geoelectric observations would be available for research. Therefore, the author has randomly studied for the purposes which investigate relations with tectonic activities such as seismic and volcanic activities. The paper is in an intermediate stage, so further intense studies are expected.

This observation method has the following two advantages in comparison with conventional methods:

(1) The contact electrical potential between the electrode and the soil seems very stable.

For conventional observation, the electrical potential between the electrodes and soil is unstable, especially due to precipitation. The present observation is hardly affected by precipitation. It seems to have originated from the fact that the contact resistance between the electrode and the soil is less than 2 ohms, and that the installation depth is more than 5 meters. We can therefore obtain stable data over a long time.

(2) The base lengths for the observation are very long.

The base lengths are ten to several tens of kilometers, and these are 10 to 100 times longer than those for other ordinary observations in Japan. The amplitude of the variation of earth potential due to tectonic activity is roughly proportional to the distance, while noise due to industries, railways, etc., and noise associated with the electrodes themselves is primarily local. Therefore, we can expect a high ratio of signal to noise when we use long electrode spacing. In contrast, the sensitivity for the so-called “effective point” with tectonic activities might be blunt. The observed electrical field is affected by the large scale structure.

The detail about the observation due to the facilities of NTT will be described in Section 2. The locations used as associated data are listed in the next page.

These observations have been conducted by JMA except for the tide level meter at Ooarai (by Ibaraki Prefecture) and at Ito (by Geographical Survey Institute). The manometer at Youkaichiba has been observed for the compensation to the volume strain meter. The tsunami-meters are made of a quartz pressure gage attached to the terminal apparatus of TKOBS and BSOBS, and

	Longitude	Latitude
Kakioka Magnetic observatory (KAK)	36° 13.75’	140° 11.38’
TKOBS　Shore earth (OMZ)	34° 35.73’	137° 35.40’
TKOBS　Sea earth（TSI）	33° 45.90’	137° 35.40’
BSOBS　Shore earth (KTU)	35° 08.75’	140° 18.79’
BSOBS　Sea earth（BSI）	34° 39.21’	140° 58.68’
Volume strain meter at Fuji	35° 11’	138° 44’
Manometer at Youkaichiba	35° 45’	140° 32’
Volume strain meter at Higashi-Izu	34° 49’	139° 03’
Tide level meter at Ooarai	36° 19’	140° 04’
Tide level meter at Ito	34° 58’	139° 04’
Tide level meter at Uchiura	35° 01’	138° 54’

the pressure values are converted into the sea level from the bottom.

Throughout this paper, JST (Japanese Standard Time) is used. JST can be calculated by adding 9 hours to GMT (Greenwich Mean Time).

2. Observation method

Outline of the observation methods using the NTT facility is described on the previous reports (Mori, 1985, 1987). Fig. 2-1 shows the observation networks for the geoelectric field and the location of Kakioka Magnetic Observatory (KAK) in the Kanto and Tokai districts of Japan. The electrical fields on the sea floor are measured between shore earth (OMZ and KTU) and sea earth (TS1 and BS1). The electrical fields on the sea floor are not principally discussed in this paper, although the electrical fields on land are affected by oceanic electrical currents and the motion of the sea water. Marine data is also required in order to study the causes of the geoelectric variations.

The geoelectric fields using the NTT facilities are measured between NTT key stations (SMO, MTO, FJM and NMZ in Fig. 2-1) and the connected sub-stations. The observations between that are connected with the thick lines have been conducted at present in September, 1987. But the stations connected with dotted lines have not yet had the observations conducted. In this paper, the observation networks will be called the “Shimodate group,” “Mito group,” “Fujinomiya group” and “Numazu group,” taking the name of the key station for each group. The locations of the NTT stations for the observation are shown in Table 2-1, and the distances and the directions of the observation lines in Table 2-2.

The observations have been conducted with digital recorders at the Mito, Fujinomiya and Numazu groups, so we can calculate the mutual electrical potential differences between two arbitrary stations belonging to the same group, as shown in Table 2-2. The input channels of the digital recorder at each key station are as follows:

Key station	1ch	2ch	3ch	4ch	Input range
MTO	ISI	KSM	HIO	ISI*	10 V
NMZ	SUZ	ITO	ATM	ODW	10 V
FJM	KOF	MNB	FJI	KOF**	10 V

* ：using low-pass filter of 30 seconds

** ：using low-pass filter of 10 seconds

The observation periods and the methods are as follows:

(1) Shimodate group

The observation was conducted over a distance of 26.8 km from Shimodate (SMO) to Kasama (KSM) and a distance of 15.7 km from SMO to Oyama (OYA). The observation period was from November 29, 1983, to March 3, 1984. The electrical fields were recorded with a two-pen recorder through low-pass filters with a cut-off frequency of 0.003Hz (about 1/6 cycle/minute). It was the test observation for whether or not to get usable data, for the reasons that such observations have not been done in recent years in Japan and also that the NTT repeater stations are located in the central part of an electrically noisy city. Though the records were not completed because of trouble with the pen recorder, the purpose has been accomplished.

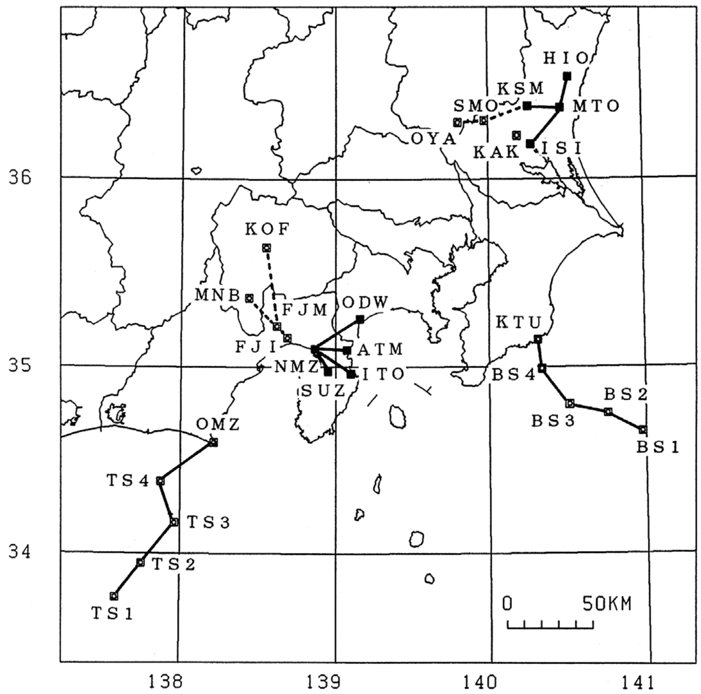

Fig. 2-1 Observation networks for geoelectric fields and the location of Kakioka Magnetic Observatory (KAK) in the Kanto and Tokai regions of Japan.
Electrical fields at the Shimodate (SMO), Mito (MTO), Fujinomiya (FJM) and Numazu (NMZ) regions have been observed using electrodes and underground metallic cables of NTT Company.
Electrical variations between Omaezaki (OMZ) and TS1 off Tokai, and between Katsuura (KTU) and BS1 off Boso Peninsula are carried out using the power feeding arrangement of the ocean bottom seismographs of JMA.

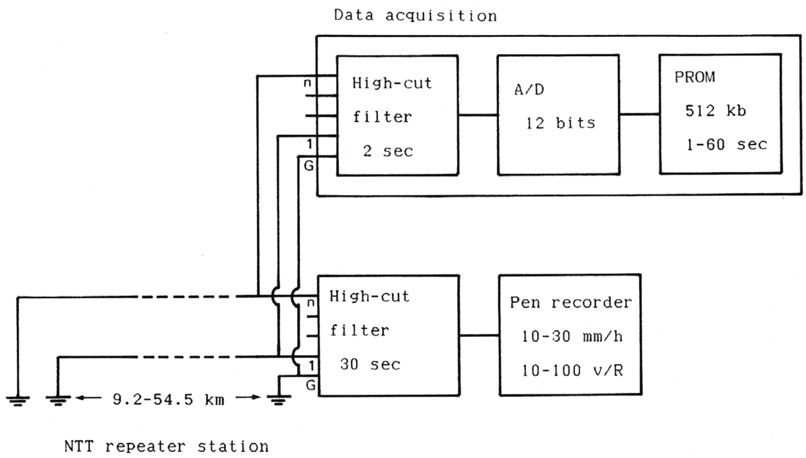

Fig. 2-2 Schematic diagram of the geoelectric observation system.

Table 2-1 Location of the NTT repeater stations used for the geoelectric observation in the Kanto and Tokai regions of Japan

Station	Symbol	Lat. N	Long. E
Mito	MTO	36° 22.50’	140° 28.34’
Ishioka	ISI	36° 11.08’	140° 16.62’
Kasama	KSM	36° 23.03’	140° 15.57’
Hitachiota	HIO	36° 32.36’	140° 31.50’
Shimodate	SMO	36° 18.51’	140° 58.56’
Oyama	OYA	36° 17.95’	139° 48.12’
Numazu	NMZ	35° 5.91’	138° 51.90’
Syuzenji	SUZ	34° 58.56’	138° 56.92’
Ito	ITO	34° 57.93’	139° 5.88’
Atami	ATM	35° 5.47’	139° 4.34’
Odawara	ODW	35° 15.51’	139° 9.44’
Fujinomiya	FJM	35° 13.14’	138° 37.19’
Kofu	KOF	35° 38.17’	138° 32.98’
Minobu	MNB	35° 22.10’	138° 26.34’
Fuji	FJI	35° 9.49’	138° 41.28’

Table 2-2 Distance and direction of the geoelectric observation lines

Station group	Line Symbol	Distance	Direction
Mito group	ISI-MTO	27.4 km	N 40°E
	ISI-HIO	45.1 km	N 29°E
	ISI-KSM	22.1 km	N -4°E
	MTO-HIO	18.8 km	N 15°E
	KSM-MTO	19.0 km	N 93°E
	KSM-HIO	29.3 km	N 54°E
Shimodate group	SMO-KSM	26.8 km	N 72°E
	OYA-SMO	15.7 km	N 86°E
Fujinomiya group	FJI-KOF	54.5 km	N -13°E
	FJI-FJM	9.2 km	N -42°E
	FJI-MNB	32.5 km	N -44°E
	FJM-KOF	46.7 km	N -8°E
	FJM-MNB	23.3 km	N -45°E
	MNB-KOF	31.4 km	N 19°E
Numazu group	NMZ-ODW	32.0 km	N 56°E
	NMZ-ITO	25.9 km	N 125°E
	SUZ-ITO	13.7 km	N 95°E
	ITO-ODW	32.9 km	N 9°E
	ATM-ODW	20.1 km	N 23°E
	ITO-ATM	14.1 km	N -10°E
	SUZ-ODW	36.6 km	N 31°E
	SUZ-ATM	17.0 km	N 41°E
	SUZ-NMZ	15.6 km	N -29°E

(2) Mito group

The electrical fields have been observed at the Mito key station connecting with Ishioka (ISI), Kasama (KSM) and Hitachiota (HIO). The observation using a multi-pen recorder through the same filters at SMO was conducted from January 17 to March 6, 1985. Since March 6, 1985, the observation has been conducted with a multi-pen recorder and a digital recorder as shown in Fig. 2-2. The continuous data were passed through a 0.5 Hz low-pass analog filter for anti-aliasing, and were converted to 12-bit digital data. Although data were available every second, per-minute data were usually obtained by averaging and stored in a 512 kB PROM (Programmable Read Only Memory). At the same time, the continuous data were passed through a 1/30 Hz low-pass analog filter and recorded on a multi-pen recorder.

(3) Fujinomiya group

Electrical potentials had been observed at the Fujinomiya (FJM) key station for Kofu (KOF), Minobu (MNB) and Fuji (FJI). The observation period was from June 10 to August 26, 1985. The observation system is same as in the Mito group in Fig. 2-2. The Fujinomiya and Numazu groups are located in the Tokai district which might be affected by the Tokai earthquake with magnitude 8 class considered likely to happen in the near future. Also, this area is in a tectonically active region including Mt. Fuji, which is an active volcano and the highest mountain in Japan, and a volcanically and seismically active area. The line from FJM to KOF via MNB is selected in order to research for volcanic activities of Mt. Fuji. At that time, NTT Company decided to exchange the underground metallic cables for optical fiber cable in the near future for connections with FJM and the other repeater stations. It was unfortunate that the cable from FJM to KOF via MNB was inundated with heavy rain by the typhoon on June 30, 1985, and it was not restored. At result, the observations at FJM were stopped on August 26, 1985.

(4) Numazu group

Electrical potentials have been observed at the Numazu (NMZ) key station for Shuzenji (SUZ), Ito (ITO), Atami (ATM) and Odawara (ODW) since August 26, 1985. The observation method is the same as for the Mito group, except for a part of the filter to a multi-pen recorder.

3. Outline of the observed records

3-1 Outline of the records at each observation group

The outline of the records in each group is described below.

(1) Shimodate group

Fig. 3-1 shows an example of the analog records for about 50 seconds without any filtrations at SMO. The most outstanding noises have a period of 1 second. These short-period noises have been observed at various parts of Japan (Mori and Hasegawa, 1979). The origin of those noises seems to be from the charge counters for telephone usage time by customers of NTT Company. In order to eliminate those short-period noises, high-cut filters of around 6 minutes have been applied. Electrical variations observed at the Shimodate group are compared with the geoelectric and geomagnetic variations at KAK.

The upper part of Fig. 3-2 shows the geoelectric variations at the Shimodate group and the geoelectric and geomagnetic variations at KAK. The records of the geoelectric fields at the Shimodate group and KAK were digitized by a curve-reader because of analog records. The electrical variations are expressed in mV/km, and a positive sign is taken when the current flows to the north and to the east. OYAMA denotes the electrical field variations at OYA-SMO, while KASAMA denotes those at SMO-KSM. EW and NS at KAK denote the east (N85°E) and north (N5°W) components of the geoelectric field. The length for the EW base line is 1200 meters, while that for the NS base line is 900 meters. X, Y and Z at KAK denote the geographic north, east and downward components of the geomagnetic field. X and Y are converted from the horizontal component and declination. The electrical variations at SMO-KSM and EW at KAK are very similar, and well correlated to geomagnetic variations at KAK. The greater part of these geoelectric variations are induced by geomagnetic variations.

The bottom of Fig. 3-2 shows the power spectrums of the geoelectric fields due to the AR model (Akaike, 1969). At OYAMA, the power in a cycle of several 10 seconds is relatively large, and the main part seems to be due to artificial electrical noises of electric trains, because OYA is located near the Tohoku-railway where the trains are driven by DC electric power.

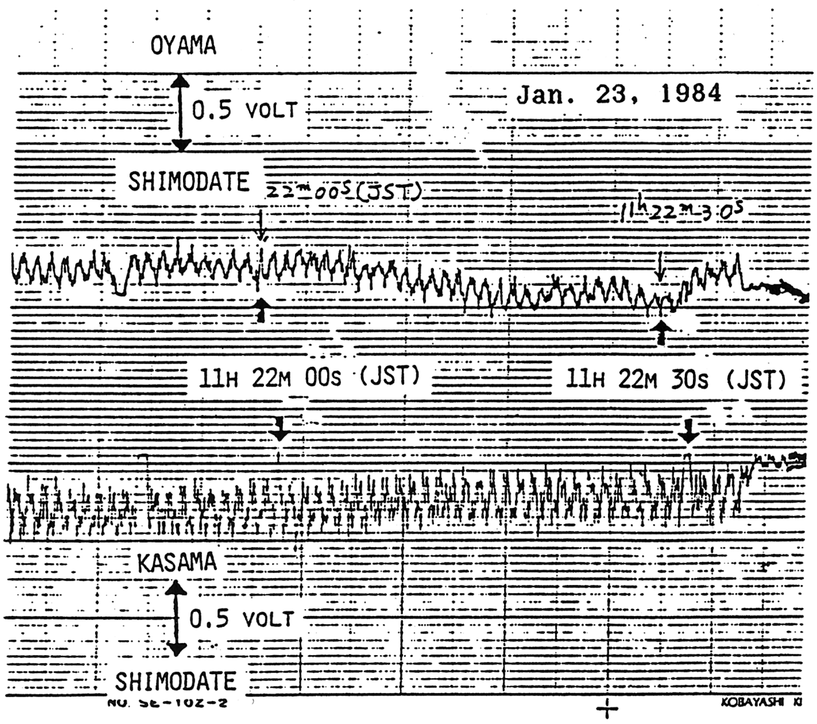

Fig. 3-1 The analog records without any filtrations for about 50 minutes on January 23, 1984, at SMO.

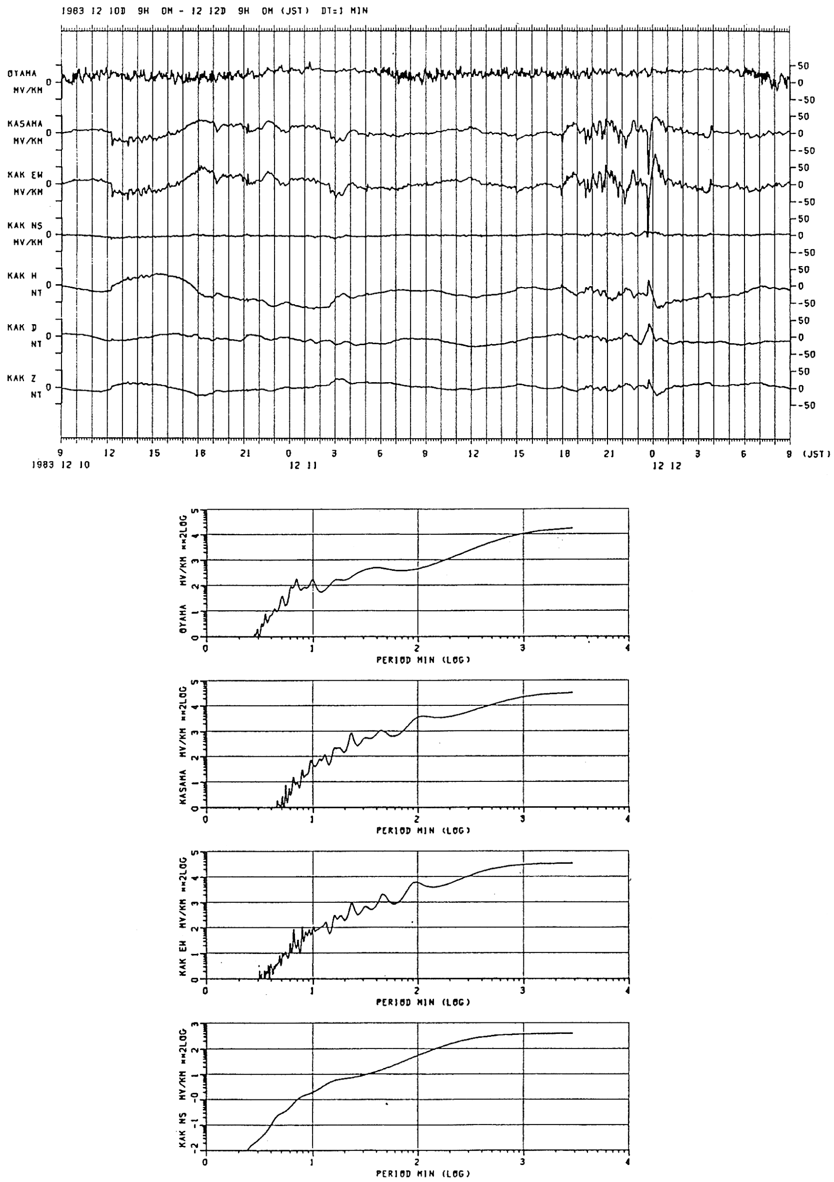

Fig. 3-2 Top shows the geoelectric variations at the Shimodate group and the geoelectric and geomagnetic variations at KAK. OYAMA and KASAMA stand for the electrical field at OYA-SMO and SMO-KSM, respectively. KAK EW and KAK NS stand for the east-west and the north-south components of the electrical field at Kakioka. KAK H, KAK D and KAK Z stand for the horizontal component, declination and vertical component of the magnetic field at Kakioka, respectively. The bottom shows the power spectrum due to the AR model.

(2) Mito group

Fig. 3-3 shows the geoelectric fields at the Mito group at intervals of 1 second. FC = 2S and FC = 30S show the record through a 2 second low-pass filter and a 30 second low-pass filter, respectively. In this figure, there are very remarkable noises with a period of 18 seconds on the record of FC = 2S at HIO-MTO. These noises also seem to be from the charge counters of NTT Company. Fig. 3-4 shows an example of short-period fluctuations in the geoelectrical fields at the Mito group and the geomagnetic fields at KAK. The figure is illustrated by the 10-second average value of a sampling per second, and the data period is 2 hours. The records are of a bay-type event and of Pi2 pulsation with a period of about 60 seconds. Short-period variations such as Pi2 are observable, despite the fact that the electrodes are located in such a noisy area as Mito City. This fact shows that the present observation gives us highly accurate data. The observation stations of the Mito group are located along the Joban Line, which uses AC electricity. Therefore, the leak current from a train does not affect the observation.

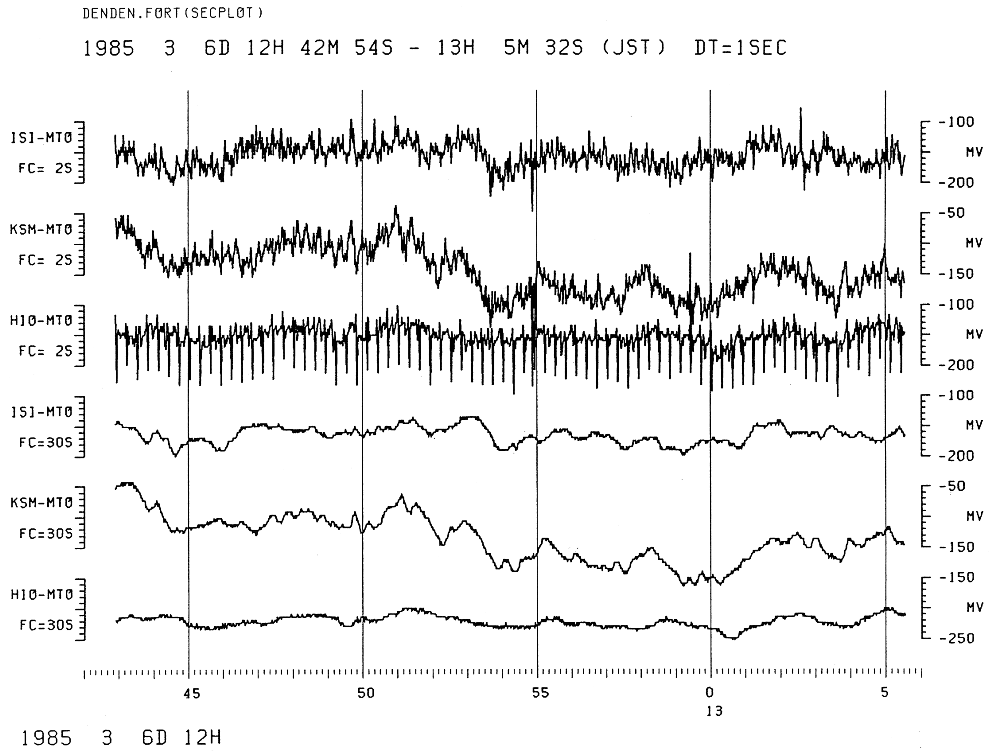

Fig. 3-3 Geoelectric fields at the Mito group at 1-second intervals from 12:42 to 13:06 on March 6, 1985. FC=2S, FC=30S show the record through 2-seconds low-pass filter and 30-seconds low-pass filter, respectively.

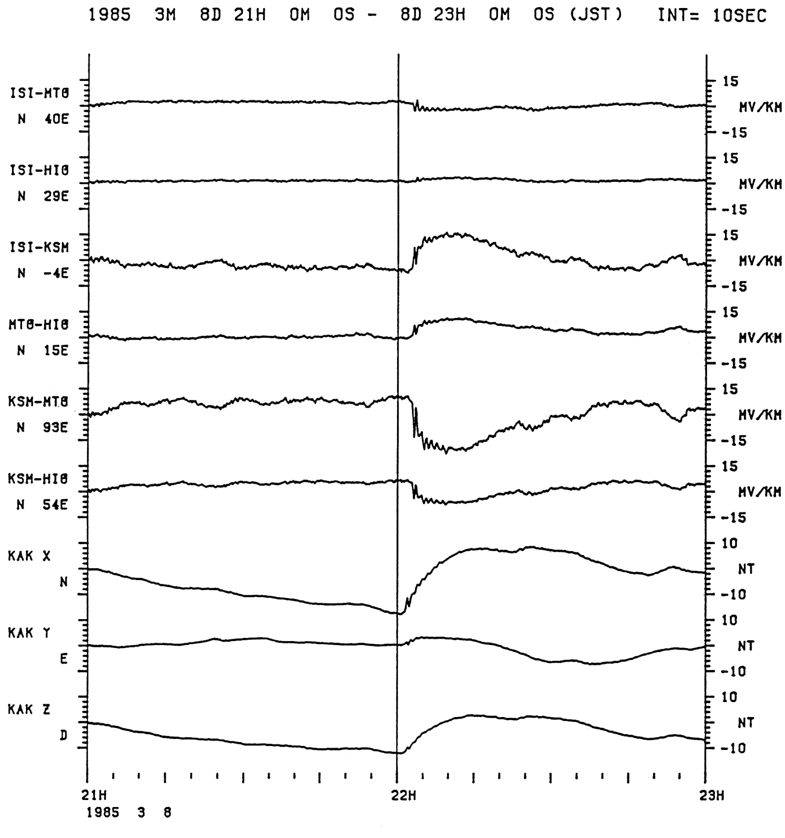

Fig. 3-4 Example of short period variations (Pi2 and bay-type events) of the electrical fields between the various pairs among the Mito group from 21:00 to 23:00 on March 8, 1985. The magnetic fields at Kakioka (KAK) are also shown. The figure is illustrated by the 10-second average value of a sampling per second

(3) Fujinomiya group

Fig. 3-5 shows the electrical field in the sampling interval of 2 seconds. Almost all the fluctuations seem to be artificial noises. The fluctuations at FJM-MNB are pulse-like variations and different from other records. MNB and FJM are located near the Itoigawa-Shizuoka tectonic line and the Fujikawa seismic fault, and those areas might have low resistivity. Fig. 3-6 shows the electrical fields at the Mito group and Fujinomiya group and the magnetic fields at KAK at 1-minute intervals. In this figure, the record at FJM-MNB is almost straight because of the few seconds fluctuations as seen in Fig. 3-5. The records of the Fujinomiya group have very large artificial noises except for the late night periods, and the geoelectric variations induced by geomagnetic variations can be detected only when remarkable geomagnetic changes take place between 0:00 and 5:00 local time.

(4) Numazu group

Fig. 3-7 shows the magnetic and electrical fields at KAK and the electrical fields at the Mito group and Numazu group at 1-minute intervals. The bottom 10 records at the Numazu group are very noisy, so we can distinguish the geoelectric variations when a large geomagnetic disturbance occurred late at night. FJI, NMZ, ATM and ODW are along the Tokaido Line, where direct-current trains run. Moreover, the area has many big factories as compared with Mito.

3-2 Comparison of the observed record in the same time of a different day

It is interesting to consider whether or not those large artificial noises at the Fujinomiya group and Numazu group are the same noises every day. The top of Fig. 3-8 shows the records between 3:00 and 6:00, and the bottom shows the records between 8:00 and 11:00 on June 12 and 13, 1985, at intervals of 10 seconds. Those two lines are the first in time from the top. For example, the third and fourth upper lines of the figure show the record on June 12 and that on June 13, respectively, at FJI-FJM. The noises increase from around 5:15 every day, and the forms are similar. The same characteristics of noises can also be seen in the other cases of the Numazu group.

Fig. 3-9 shows the records at the Mito group in the same manner as in Fig. 3-8. The plotter sensitivities in the Mito group are 2 to 20 times that of the Fujinomiya group, as shown in the right sides of each figure. At ISI-KSM and MTO-HIO, some noises are likely on the 2 days, but the noises are fairly small in comparison with those at the Fujinomiya and Numazu groups.

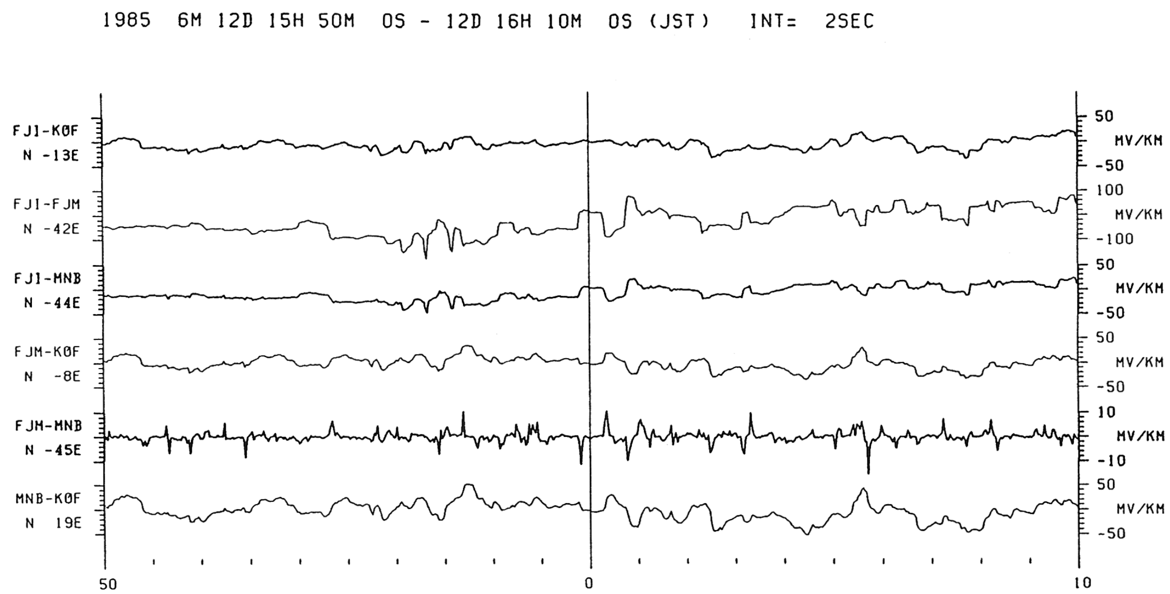

Fig. 3-5 Geoelectric variations between the various pairs among the Fujinomiya group at 2-second intervals from 15:50 to 16:10 in June, 1985. The vertical scale of FJM-MNB is 5 times as large as others.

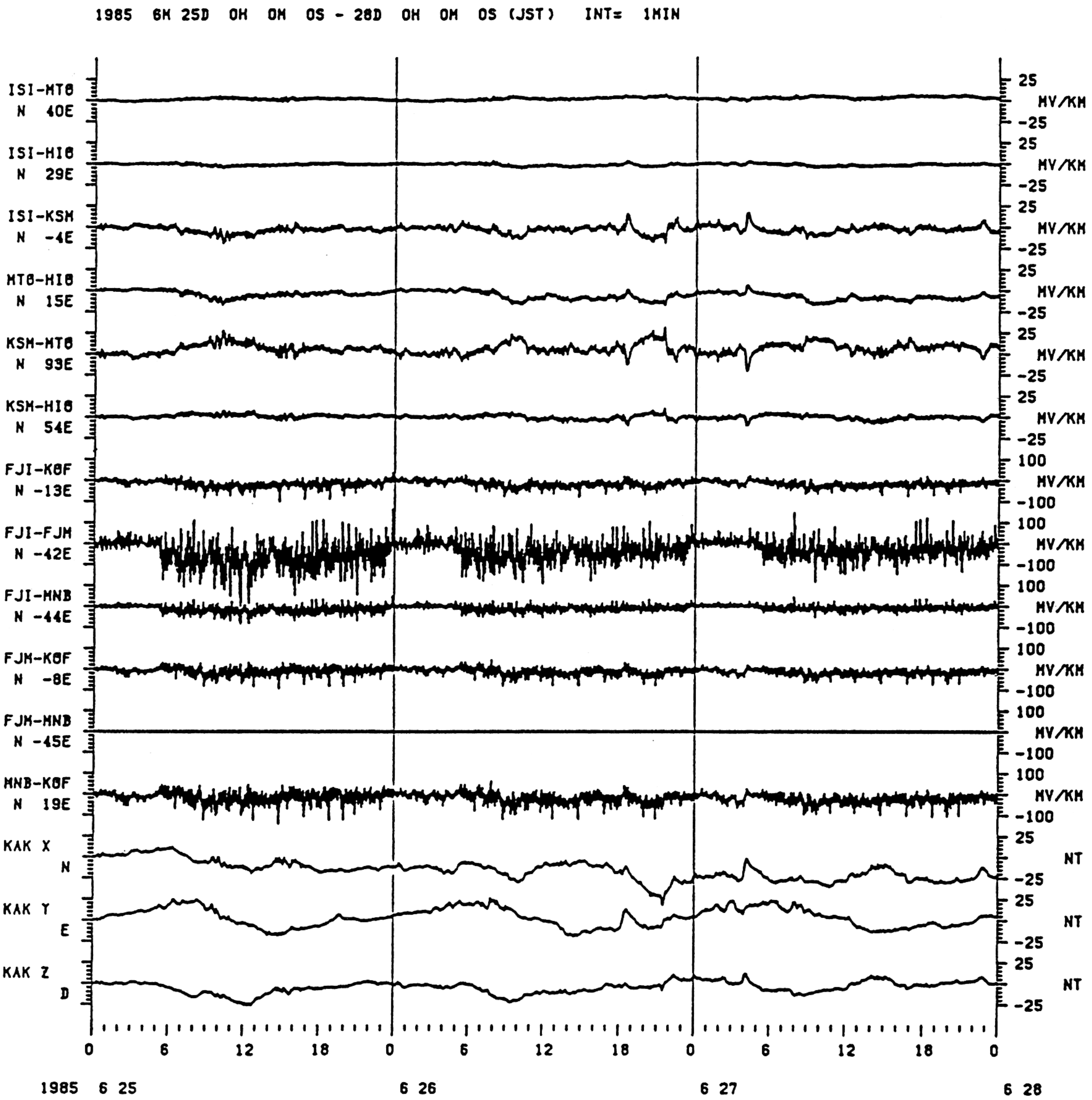

Fig. 3-6 Electrical fields between the various pairs among the Mito group (from ISI-MTO to KSM-HIO) and Fujinomiya group (from FJI-KOF to MNB-KOF) at 1-minute intervals from June 25 to 27, 1985. The magnetic fields at Kakioka (KAK X, KAK Y, KAK Z) are shown for convenience of comparison.

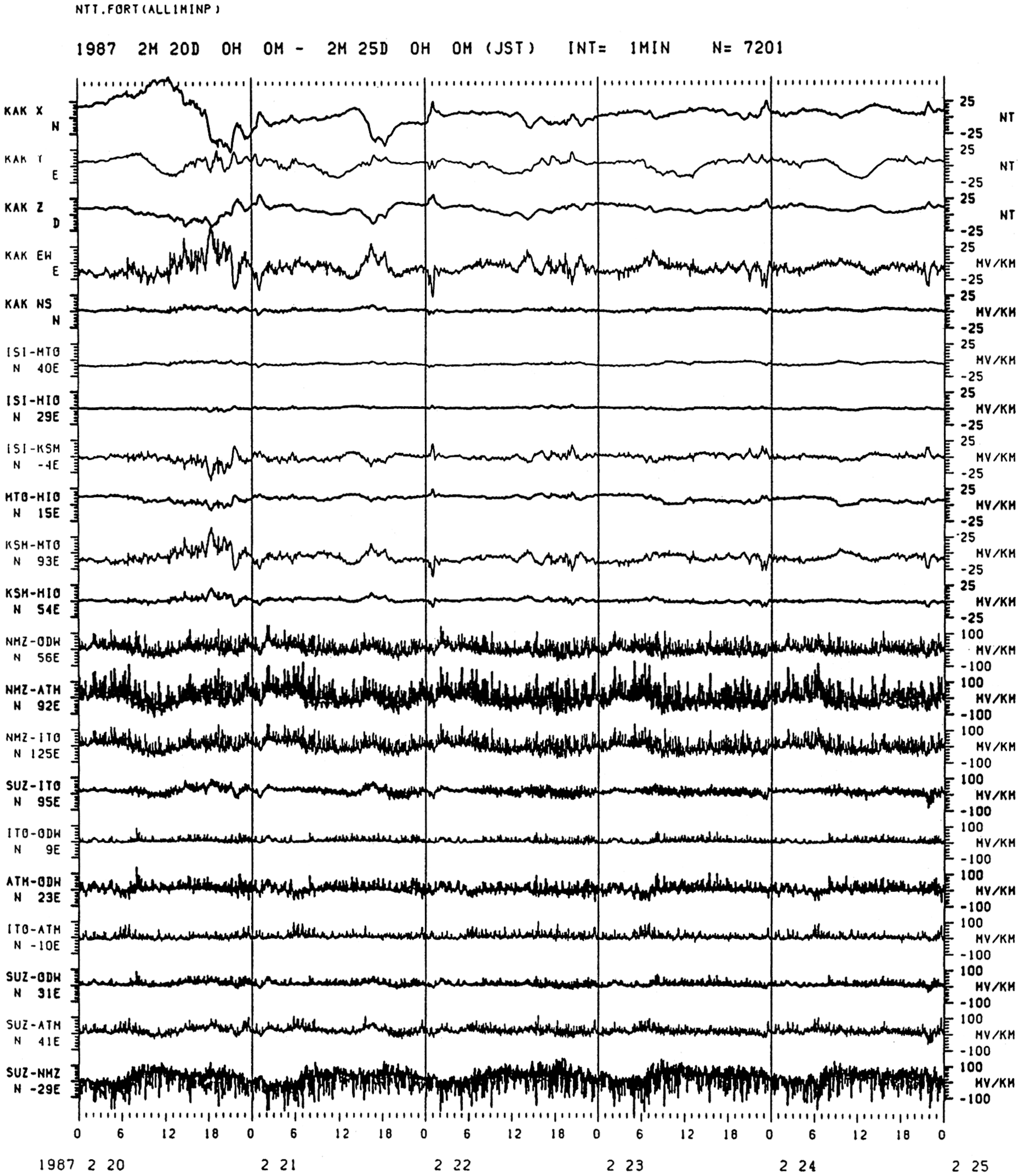

Fig. 3-7 Electrical fields between the various pairs among the Mito group (from ISI-MTO to KSM-HIO) and Numazu group (from NMZ-ODW to SUZ-NMZ) at 1-minute intervals from February 20 to 24, 1987. The magnetic and electrical fields at Kakioka (from KAK X to KAK NS) are shown for convenience of comparison.

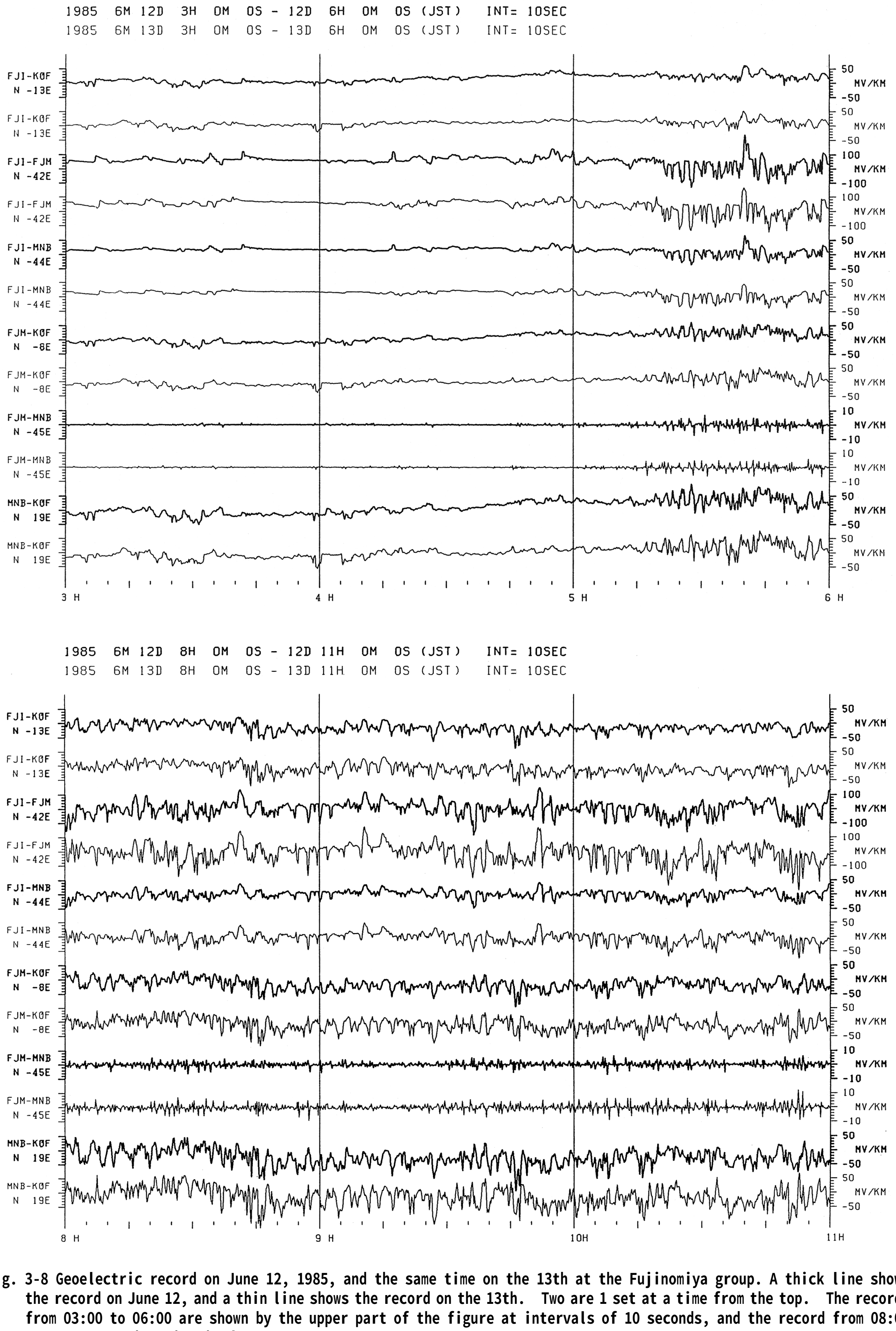

Fig. 3-8 Geoelectric record on June 12, 1985, and the same time on the 13th at the Fujinomiya group. A thick line shows the record on June 12, and a thin line shows the record on the 13th. Two are 1 set at a time from the top. The records from 03:00 to 06:00 are shown by the upper part of the figure at intervals of 10 seconds, and the record from 08:00 to 11:00 are shown by the lower part.

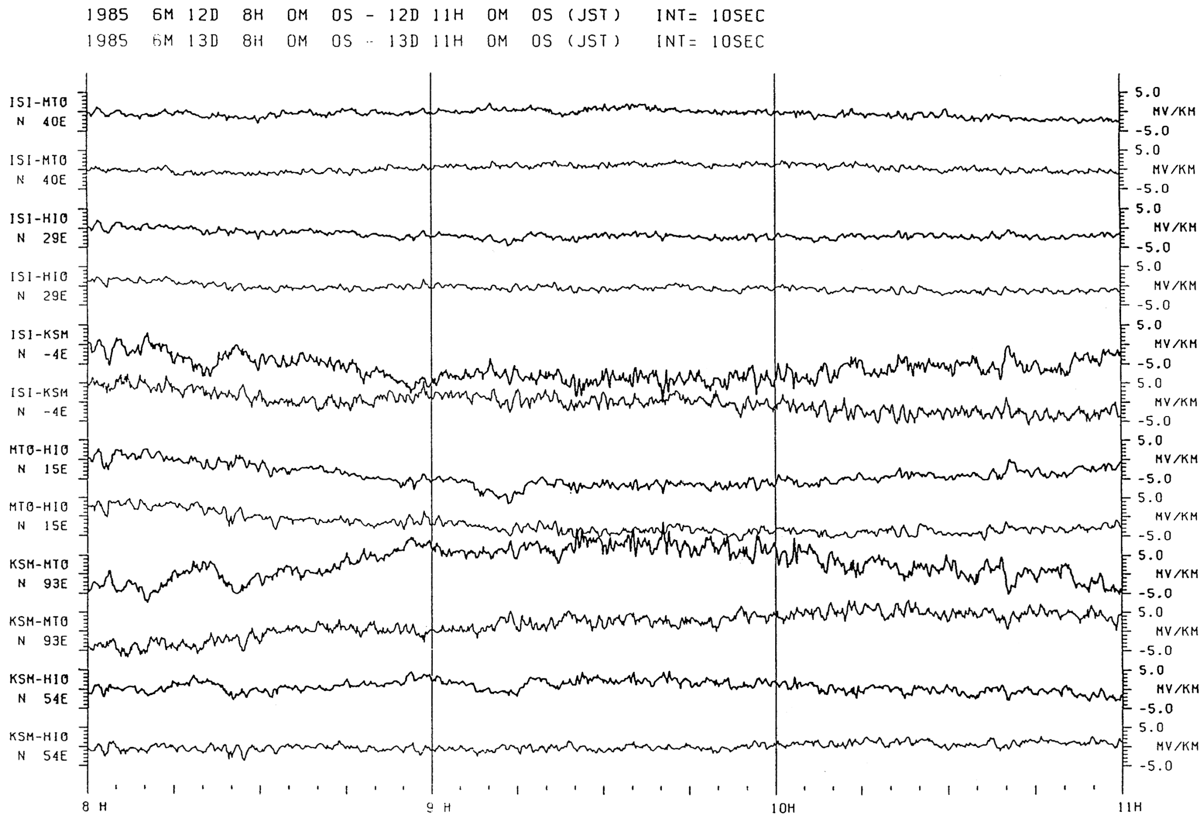

Fig. 3-9 Geoelectric record from 08:00 to 11:00 on June 12, 1985, and the same time on the 13th at the Mito group at intervals of 10 seconds. A thick line shows the record on June 12, and a thin line shows the record on the 13th. Two are 1 set at a time from the top.

4. Long-term stability

In order to inspect the long-term stability, the geoelectric variations at the Fujinomiya, Numazu and Mito groups and at KAK, and the geomagnetic variations at KAK are shown in Fig. 4-1 in the daily mean values from March, 1985, to November, 1986. The daily mean values averaged the sampling values for 1 minute, except for the geoelectric fields at KAK. Those at KAK are the mean values of the 25 hourly values in the vicinity of every hourly value. The upper 10 lines of the figure are the geoelectric fields at the Fujinomiya group until August 25, 1985, and since then those at the Numazu group. In the top part of the figure, vertical lines show heavy precipitation, and the numbers are the continued total precipitations in mm at Mishima Weather Station near Numazu, and those at Mito Local Meteorological Observatory are shown in the middle part.

The electrical variations at the Numazu group are changeable in comparison with those at the Mito group because of artificial noises due to direct-current electric trains and large-scale factories, etc. Typhoons passed through the observation areas on June 30 and July 1, 1985, and on August 4, 1986, and considerable precipitation was observed at both Mishima and Mito. After those times, the geoelectric fields at KAK changed considerably. Precipitation has an adverse effect on the stability of the contact potential, and those deviations should be ascribed to precipitation at KAK. Geoelectric fields of the Mito group, however, show no anomalous changes at those times. This shows that precipitation does not change the contact potentials of electrodes.

The electrical field at FJI-FJM (second line from the top of Fig. 4-1) became lower from the beginning of July to the middle of August. The underground cable from FJM to KOF via MNB was inundated by heavy rain from a typhoon on June 30, 1985, and observations were stopped after that. Electrical resistivity observation of the Fujikawa fault in Fujinomiya-shi showed decreasing of the underground electrical resistivity around the same period (Earthquake Research Institute, University of Tokyo, 1987). So the decreasing of the electrical field at FJI-FJM may not be reflecting the changes of electrical conditions near the electrodes, but the wide change of the underground electrical conditions.

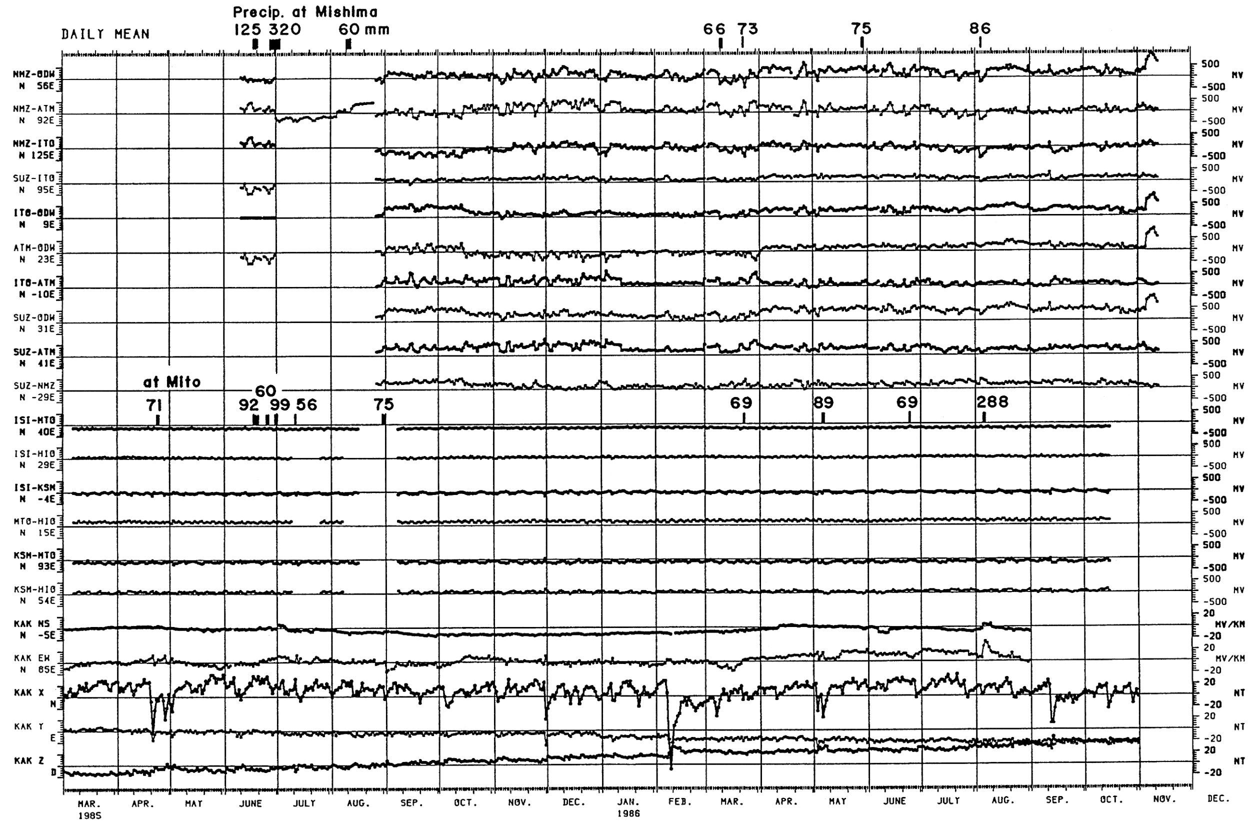

Fig. 4-1 Electrical variations in daily mean values at NTT stations and electrical and magnetic ones at Kakioka. The upper 10 lines are at the Fujinomiya and Numazu group, the middle 6 lines at the Mito group and the lower 5 lines at KAK. The vertical lines and the numbers (for example 125) on the top and on the middle of the figure show the heavy precipitation days and the continued total precipitations in mm at Mishima Weather Station (near Numazu) and those at the Mito Local Meteorological Observatory, respectively. These precipitations are shown in case the continued total ones exceeded 60 mm.

After the typhoon at the beginning of August, 1986, the electrical field at KAK showed anomalous change, and similar anomalous changes at the Numazu group had begun before the typhoon. As the electrical variations at the Numazu group seem to be affected by the change of sea level, as will be shown in Section 9, these anomalous changes may be due to the variations of the sea level with atmospheric pressure. Furthermore, since tectonic activities are active in the Tokai district, the influence by tectonic activities may also be included, so the cause cannot be specified. It is thought that there is at least no direct influence from precipitation.

5. Impedance tensor and transfer function

The following relation was introduced by Rikitake and Yokoyama (1955) as a result of analyses for short-period geomagnetic variations such as bay-type events:

$$Z = A \cdot H + B \cdot D.$$

Here, Z, H and D denote the amplitudes of the vertical component, horizontal components and declination in the geomagnetic variation, respectively. A and B are complex functions of frequency or period, and are called transfer functions.

In the same way, the geoelectric variations are expressed as

$$Ex = Z_{11} \cdot X + Z_{12} \cdot Y$$
$$Ey = Z_{21} \cdot X + Z_{22} \cdot Y.$$

Here, X represents the northward component, and Y represents the eastward component, of the geomagnetic variations. Ex and Ey represent the north-south and east-west components of the geoelectric variations respectively, and positive signs are taken when the currents flow northward and eastward. Z_{11}, Z_{12}, Z_{21} and Z_{22} are called impedance tensors.

In this paper, the direction of the geoelectric variations observed at the NTT stations are not exchanged for the north or east components. These equations are adopted for all periods of the variations, and the transfer functions and the impedance tensors are calculated by using the least square method (e.g., Mori, 1987).

5-1 Impedance tensor at the Shimodate group and at Kakioka

In the Shimodate group, the impedance tensors at SMO-KSM are calculated because the geoelectric field at KSM-OYA has been fairly contaminated by artificial noises, as described in Section 3-1.

The top of Fig. 5-1 shows the per-minute data of KASAMA (same as SMO-KSM), KAK EW, KAK H, KAK D from 8:00 on December 13 to 8:00 on December 14, 1983. The data of KASAMA and KAK EW are digitized by a curve-reader. KAK H and KAK D are the horizontal component and the declination in nT at KAK.

The elements of the impedance tensors are obtained by Fourier transform of geoelectric variations for 3 hours. The bottom of Fig. 5-1 shows the impedance tensors (Z21 and Z22) of SMO-KSM and KAK EW in mV/km/nT. R denotes the real part, and I denotes the imaginary part. The impedance tensors at SMO-KSM are almost the same as those at KAK EW, except for Z21(I).

The impedance tensors at SMO-KSM for five days were displayed on Fig. 5-2 in piles. ERRZ21 denotes the standard deviation of Z21, and ERRZ22 denotes that of Z22. Z21(R) shows almost the same values, except for December 12 ~ 13 (symbol +). Z22(I) is approximately zero for all periods.

Fig. 5-3 shows the impedance tensors at KAK EW in the same manner as in Fig. 5-2. The degree of scattering in the impedance tensors at KAK EW is compared with those at SMO-KSM. The degree of scattering of Z21(I) at SMO-KSM is in comparison with other elements, and those at KAK EW have especially large scattering. Although the origins are not clarified at present, artificial noises are considerably large. The impedance tensors at SMO-KSM and KAK EW become scattered for periods less than around 20 minutes, and the origin seem to be artificial noises.

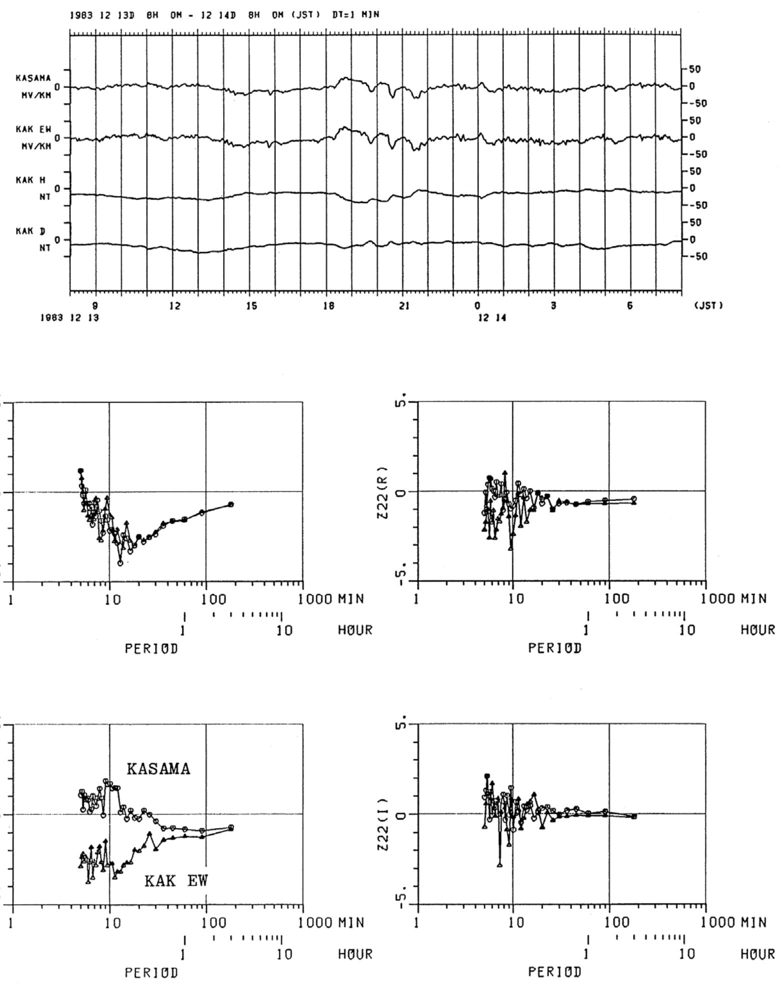

Fig. 5-1 Impedance tensors (Z21 and Z22) of KASAMA (SMO-KSM) and KAK EW for KAK H and KAK D in mV/km/nT. R and I denote the real and imaginary part, respectively. These impedance tensors were calculated by using the upper record from 08:00 on December 13 to 08:00 on December 14, 1983.

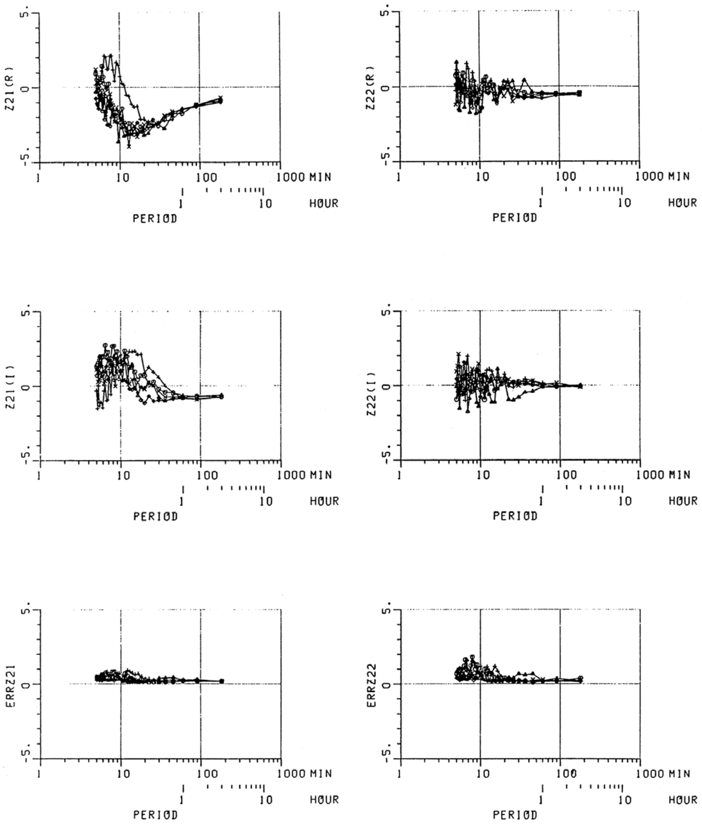

Fig. 5-2 Impedance tensors at SMO-KSM on the 5th are displayed in piles. ERRZ21 and ERRZ22 denote the standard deviations of Z21 and Z22, respectively. The symbols and the analysis times are as follows:
○ : 1983/12/10 08:00 ～ 12/11 08:00 △ : 1983/12/11 08:00 ～ 12/12 08:00 ＋ : 1983/12/12 08:00 ～ 12/13 08:00
× : 1983/12/13 08:00 ～ 12/14 08:00 ◇ : 1983/12/14 08:00 ～ 12/15 08:00

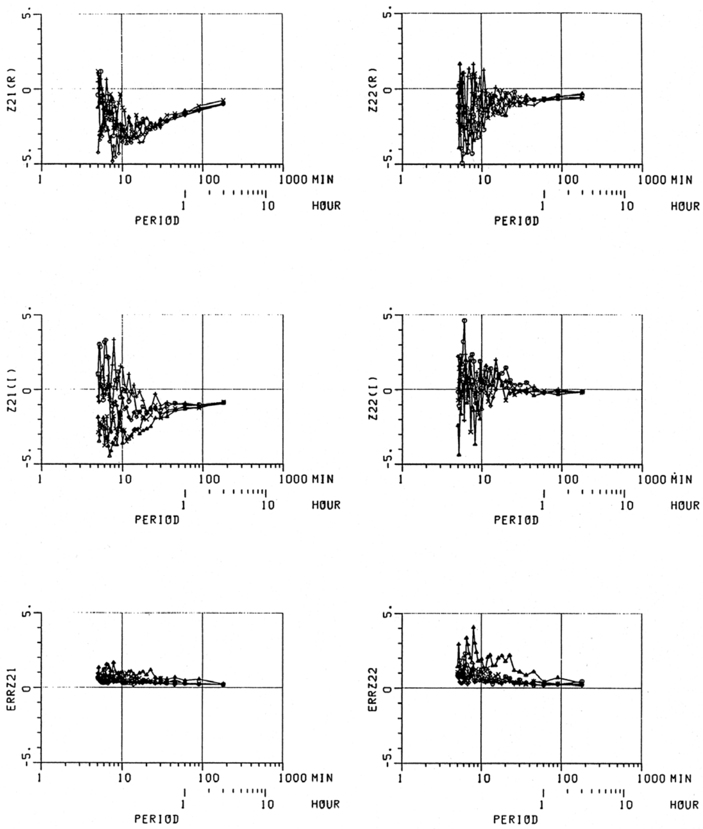

Fig. 5-3 Impedance tensor at KAK EW. The legends are the same as in Fig. 5-2.

5-2 Impedance tensor at the Mito group and transfer function at Kakioka

Geoelectric fields at the Mito group have usually been recorded to the PROM memory with 1-minute mean values of per-second sampling. However in this section, per-second records, as on the special observation, are used for research for the wide frequency range. Impedance tensors are calculated using 10-second, 1-minute and 10-minute average values based on the per-second data. Z transfer functions are also calculated in the same manner. Here, the impedance tensor and transfer function are expressed as follows:

$$E \text{ (or } Z) = (Au + i\,Av) \cdot X + (Bu + i\,Bv) \cdot Y.$$

Fig. 5-4 shows the geomagnetic fields at KAK and the geoelectric fields at the Mito group in 10-minute mean values from 13:00 to 17:00 on March 8, 1985 (the top of the figure), and the transfer function and the impedance tensors for the period from 0.8 to 40 minutes. These are computed using the values after passing through a digital band-pass filter of 50 ~ 3000 seconds.

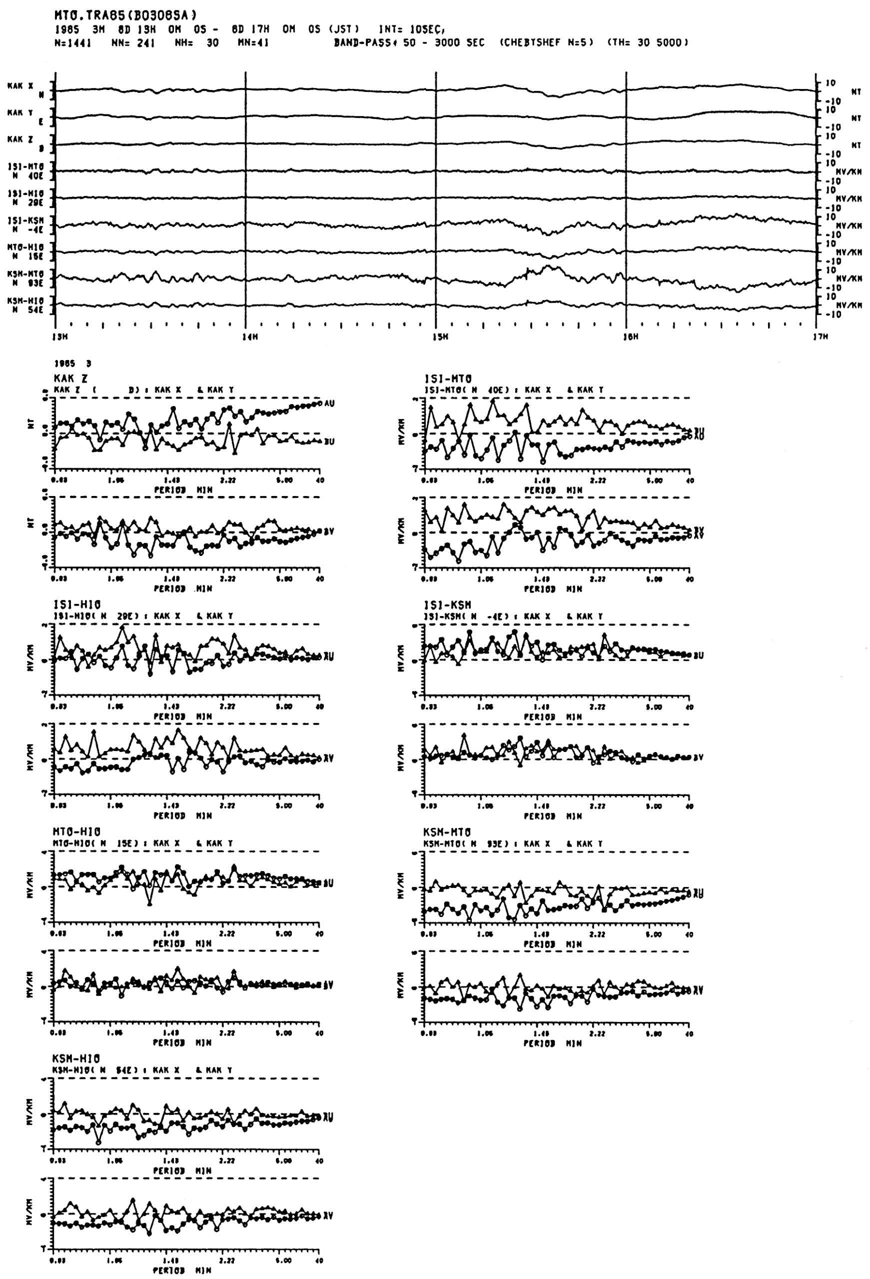

Fig. 5-4 Transfer functions at KAK and impedance tensors at the Mito group calculated through a band-pass filter of 50 ~ 3000 seconds. The top shows the geomagnetic variations at KAK and the geoelectric variations at the Mito group in 10-second mean values from 13:00 to 17:00 on March 8, 1985

Au, Av, Bu and Bv are calculated using each group of sampling data piled up in a figure. Fig. 5-5 shows Au, Av, Bu and Bv of the transfer function in piles, and Fig. 5-6(a) ~ (f) show Au, Av, Bu and Bv of the impedance tensor at the Mito group in piles. ERR-A represents the error of A, and ERR-B represents that of B. The periods and sampling times used are shown in the upper parts of each figure.

The transfer functions at KAK Z become scattered in periods shorter than several minutes and in periods longer than several hundred minutes. Usually Z components in the short period variations don't have so much of their origin external to the earth, but Z in the daily variations have considerable external origin. If there is a linear relation among X, Y and Z, the error of A and B become small. The same manner is in the geoelectric fields at the Mito group.

For impedance tensors, the errors become very large in periods shorter than around 10 minutes. Especially, in the period just around 10 minutes, the size of the error is remarkable. It might be dependent on artificial noises. In all of the impedance tensors, a tendency is seen that the errors become smaller with longer periods.

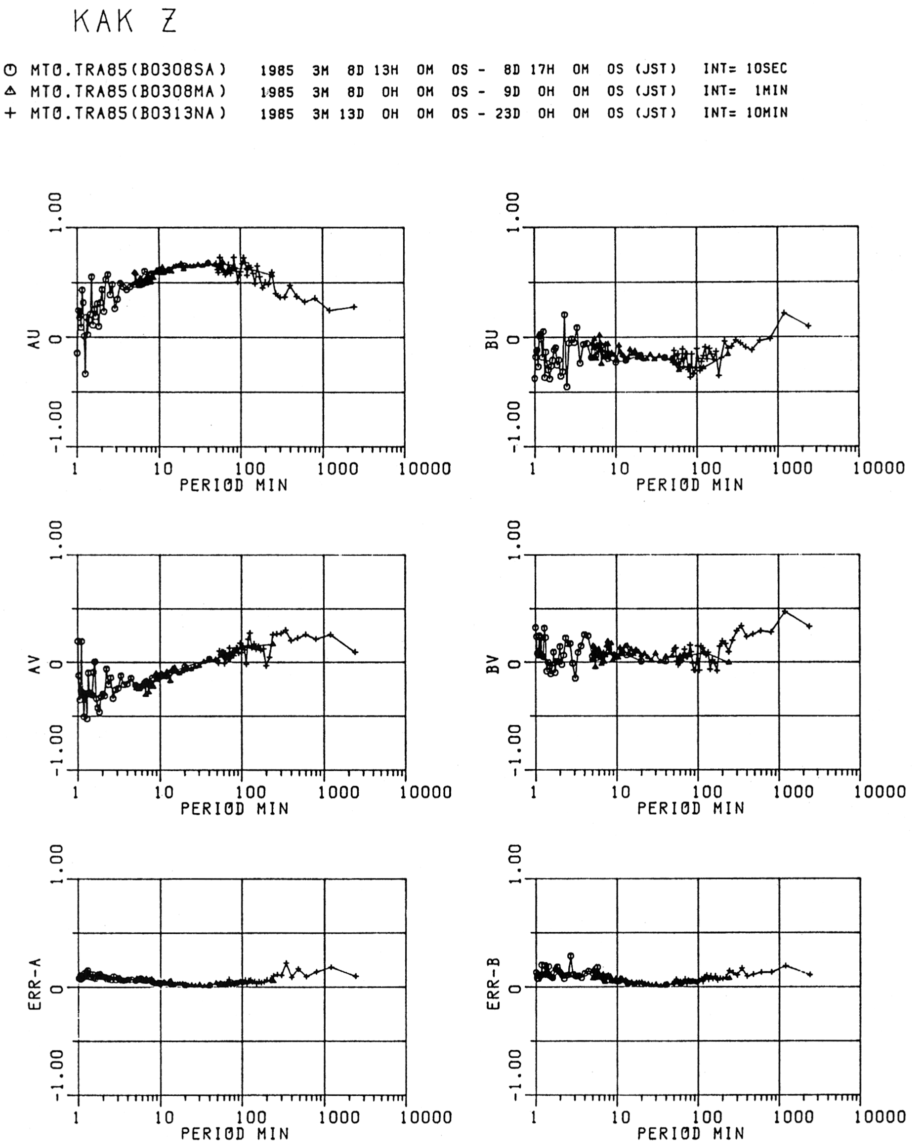

Fig. 5-5 Transfer functions using the 10-second (○), the 1-minute (△) and the 10-minute (+) mean values at KAK in piles.

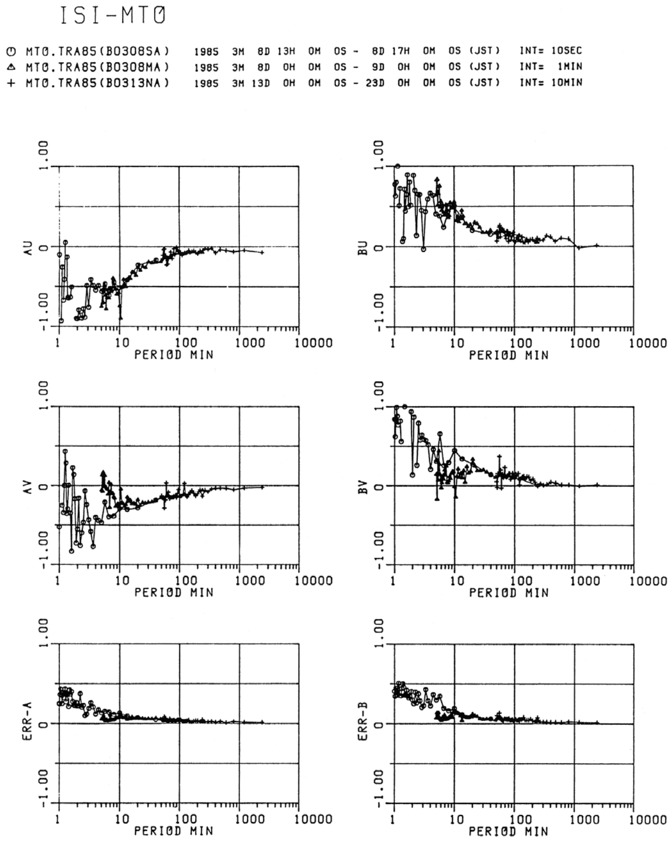

Fig. 5-6(a) Impedance tensors using the 10-second (○), the 1-minute (△) and the 10-minute (+) mean values at ISI-MTO in piles.

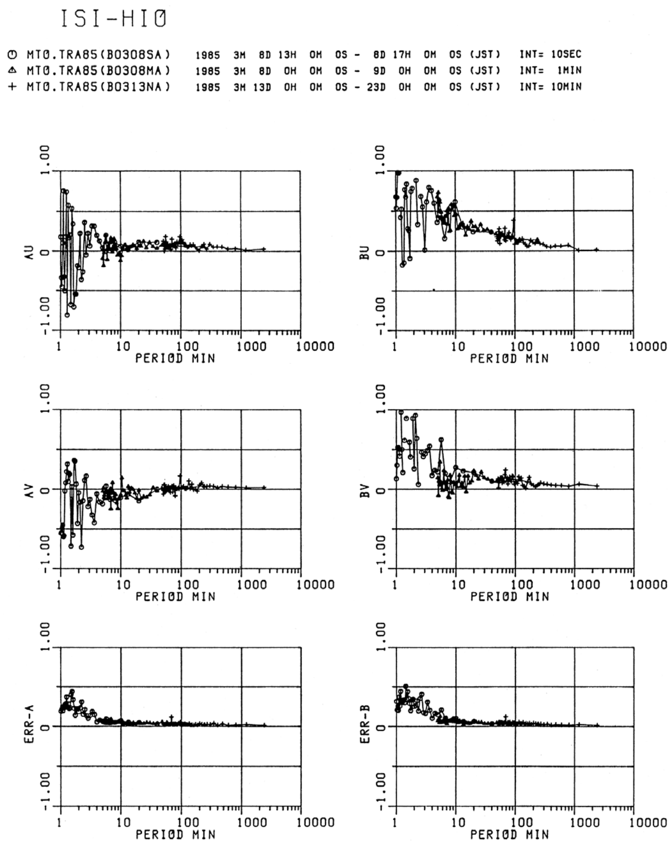

Fig. 5-6(b) Impedance tensors using the 10-second (○), the 1-minute (△) and the 10-minute (+) mean values at ISI-HIO in piles.

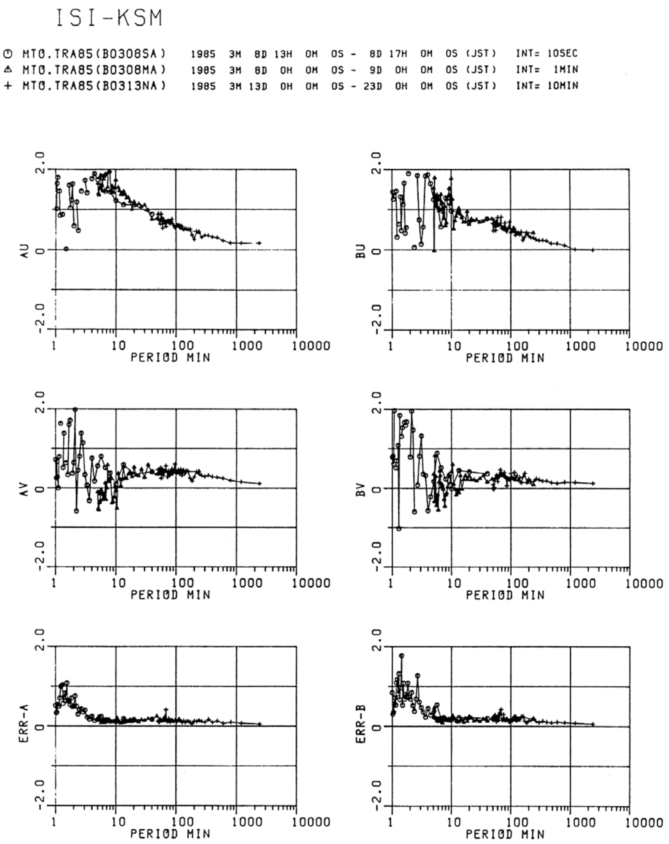

Fig. 5-6(c) Impedance tensors using the 10-second (○), the 1-minute (△) and the 10-minute (+) mean values at ISI-KSM in piles.

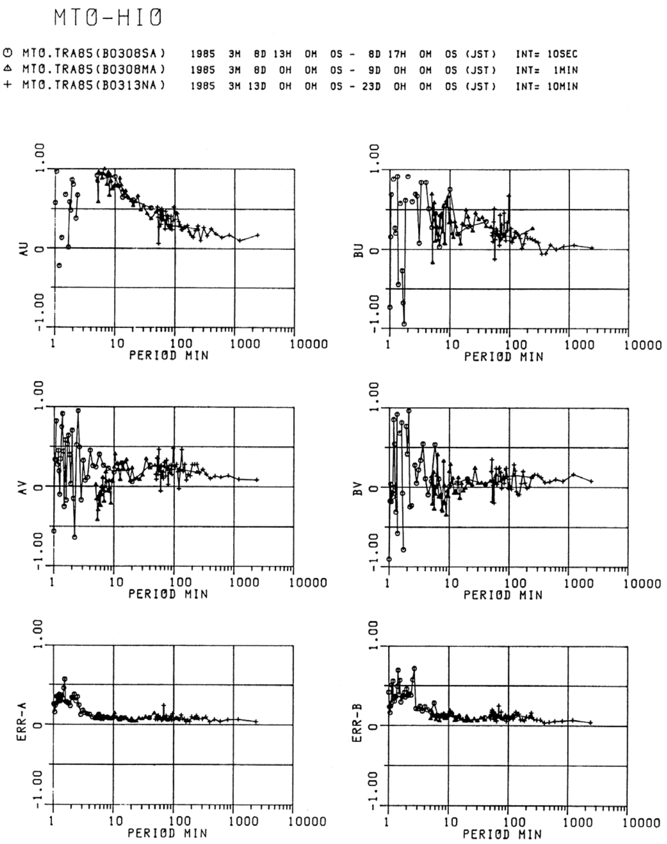

Fig. 5-6(d) Impedance tensors using the 10-second (○), the 1-minute (△) and the 10-minute (+) mean values at MTO-HIO in piles.

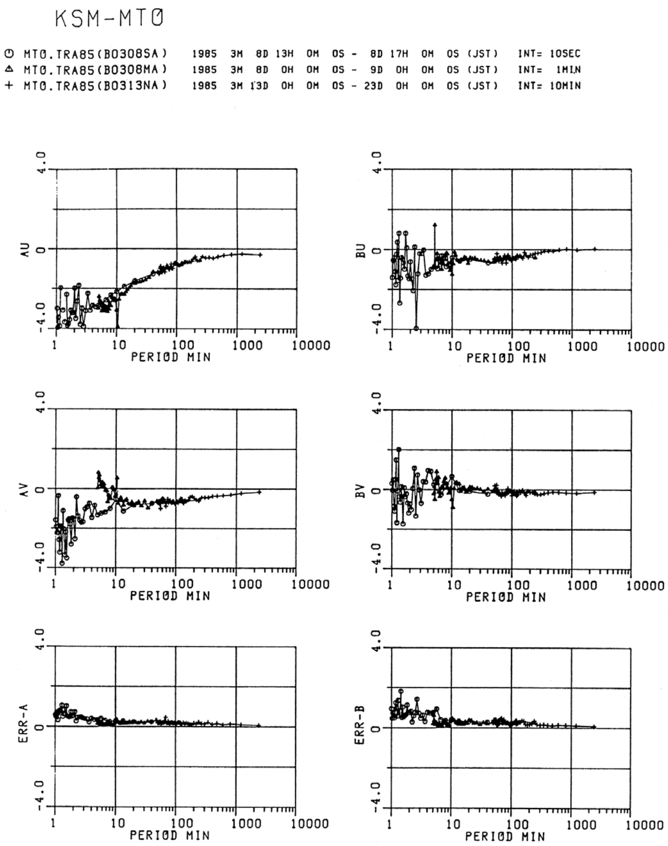

Fig. 5-6(e) Impedance tensors using the 10-second (○), the 1-minute (△) and the 10-minute (+) mean values at KSM-MTO in piles.

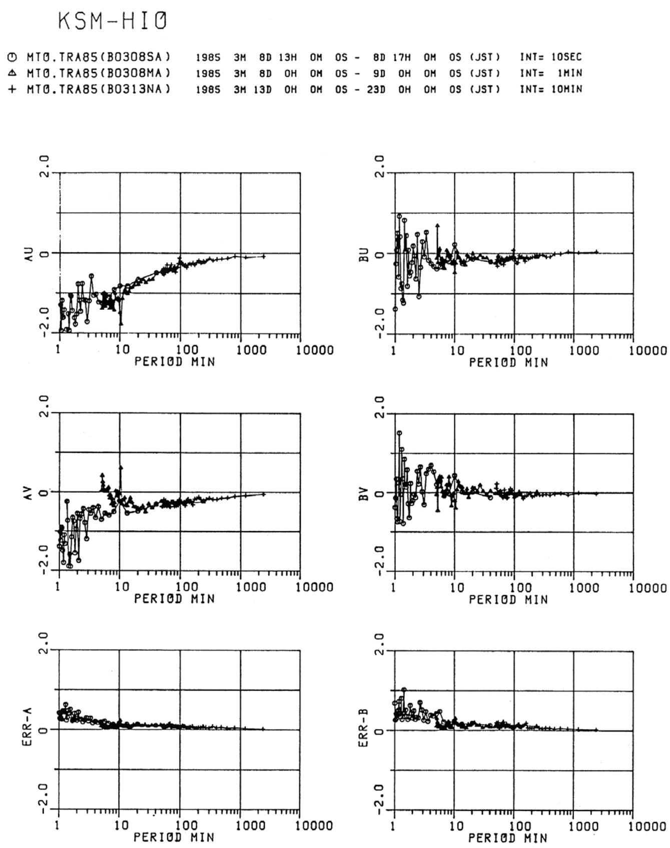

Fig. 5-6(f) Impedance tensors using the 10-second (○), the 1-minute (△) and the 10-minute (+) mean values at KSM-HIO in piles.

6. Time changes of impedance tensors and transfer functions

In order to attain the purpose of detecting abrupt changes of underground conductivity related to tectonic activities, it is important to get to know how much time change is usually there. In this section, time changes of impedance tensors and transfer functions are researched using geoelectric fields at the Mito group and geomagnetic fields at KAK.

Fig. 6-1(a) ~ (e) show the time changes of impedance tensors and transfer functions calculated by using 10-minute average values from March to August, 1985. Each mark plotted in the figures represents the average value for ten days, and the height of the mark is the error (±σ).

Changes are slowly seen in all of the components of impedance tensors and transfer functions, and these may be seasonal changes. The impedance tensors of 360-minute period (T = 360 m) in Fig. 6-1(d) are scattered relative to other periods.

Z transfer functions of 60-minute periods are fairly stable in time. Functions of 120- to 360-minute periods become scattered, and those of 720-minute periods become stable. That is, Z in short time variations and in daily variations is well expressed as a linear function of X and Y, but Z transfer functions in the intermediate periods are variable.

Usually in the short period variations, Z components don't have so much origin external to the earth, but Z has a great amount of external origin in its daily variations. If there are linear relations among X, Y and Z, the errors of A and B become small. The same is found in the geoelectric fields at the Mito group.

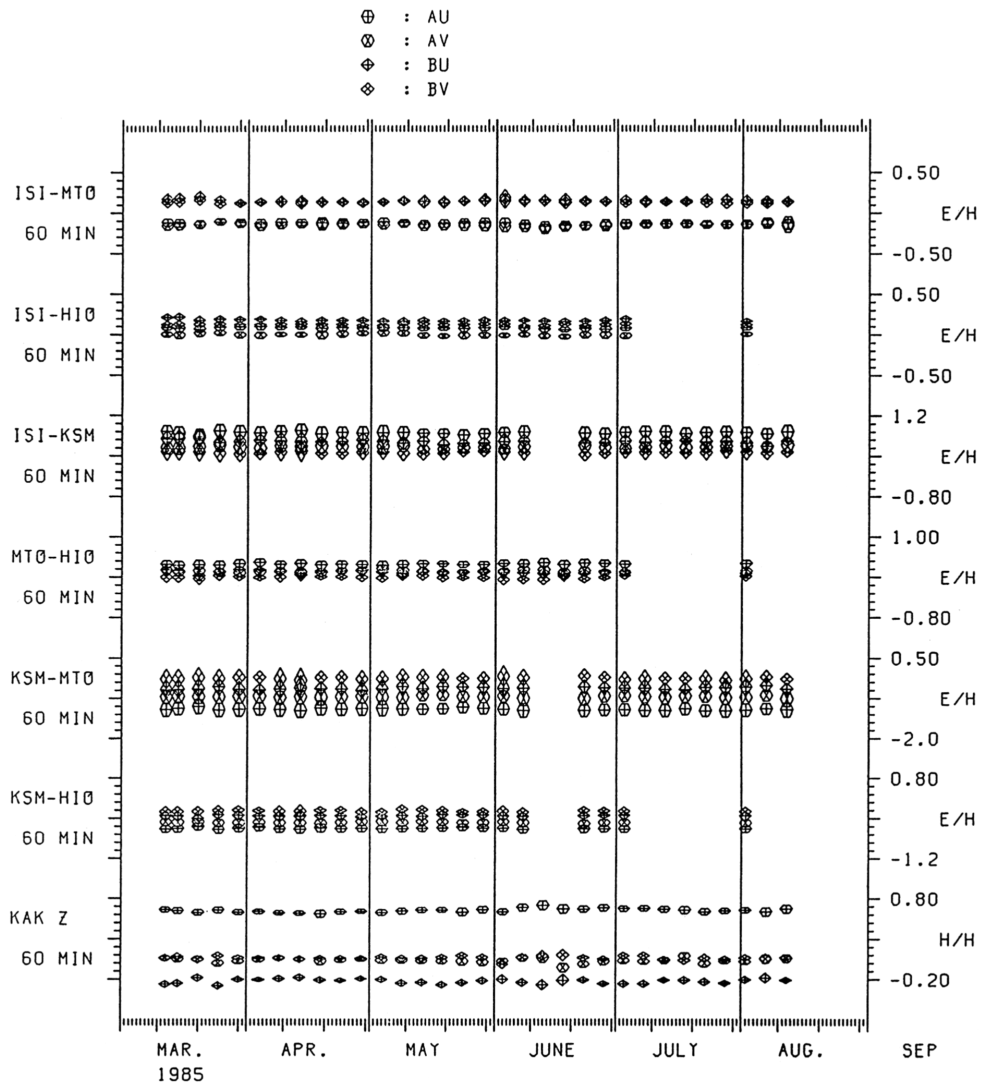

Fig. 6-1(a) Time variations of impedance tensors at the Mito group and transfer functions at KAK in a 60-minute period (T=60 m). Height of the mark represents the mean square error (±σ).

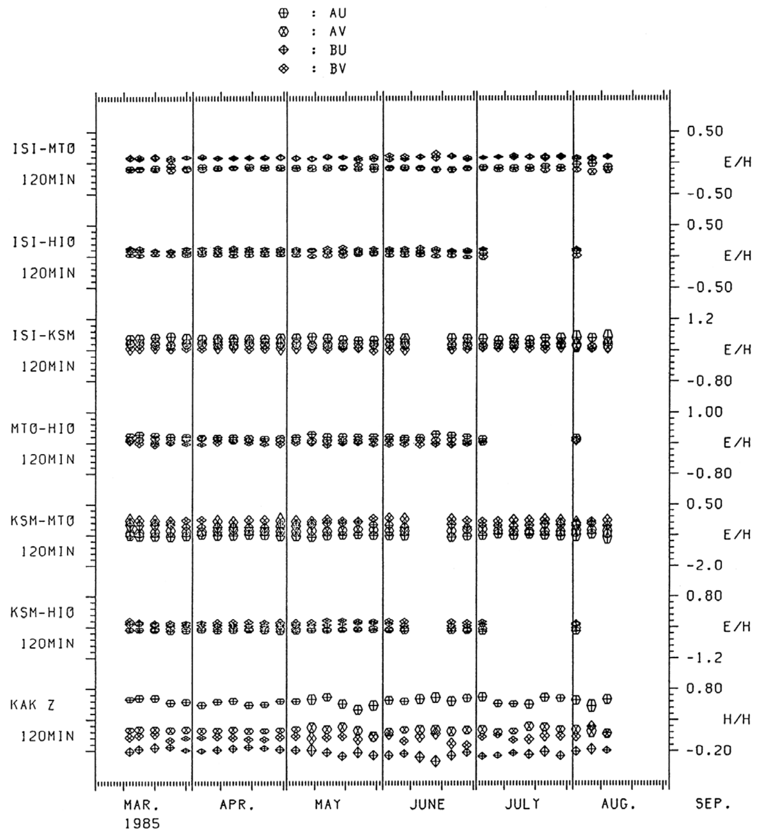

Fig. 6-1(b) Time variations of impedance tensors at the Mito group and transfer functions at KAK in a 120-minute period (T=120 m). Height of the mark represents the mean square error (±σ).

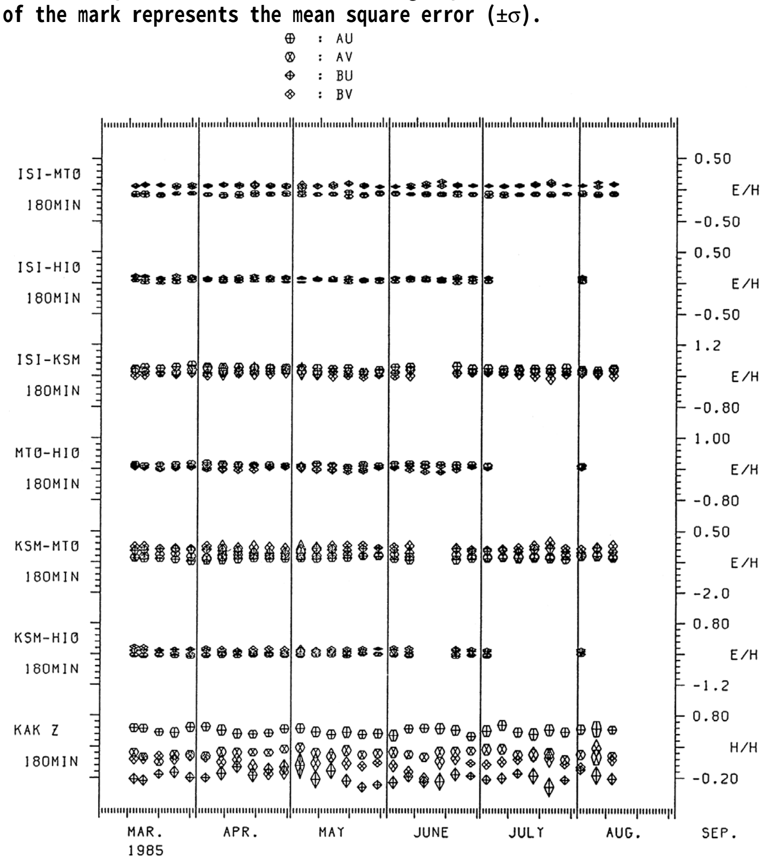

Fig. 6-1(c) Time variations of impedance tensors at the Mito group and transfer functions at KAK in a 180-minute period (T=180 m). Height of the mark represents the mean square error (±σ).

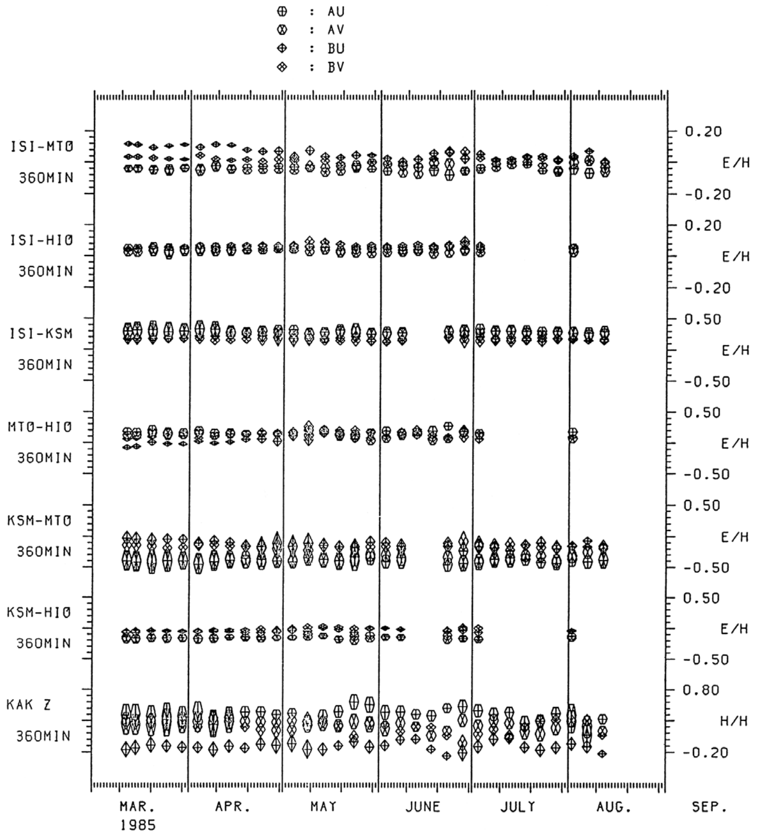

Fig. 6-1(d) Time variations of impedance tensors at the Mito group and transfer functions at KAK in a 360-minute period (T=360 m). Height of the mark represents the mean square error (±σ).

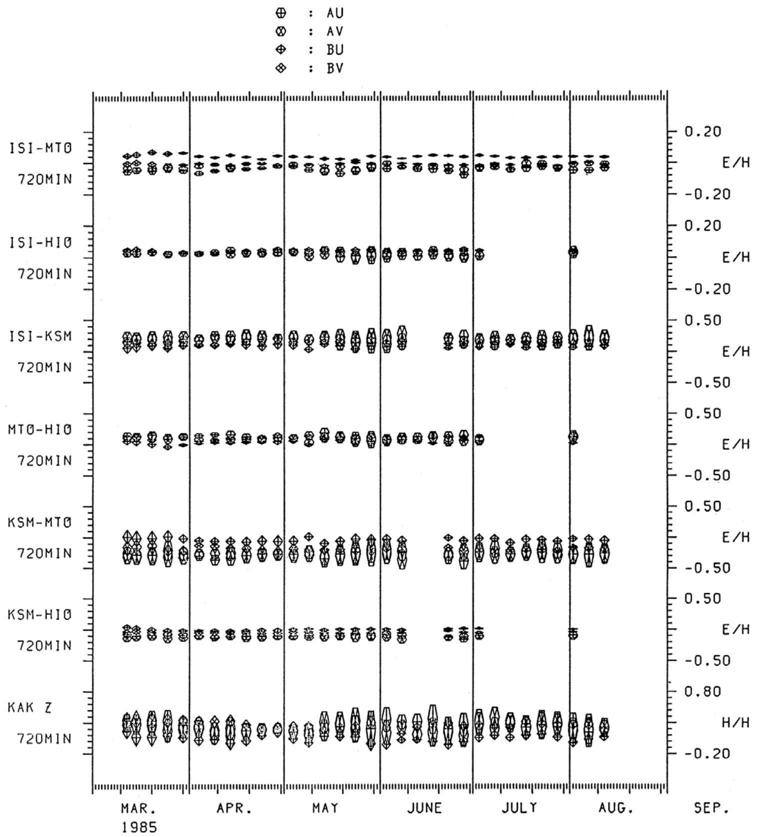

Fig. 6-1(e) Time variations of impedance tensors at the Mito group and transfer functions at KAK in a 720-minute period (T=720 m). Height of the mark represents the mean square error (±σ).

7. Elimination of the electrical fields induced by geomagnetic variations
- Detection of the anomalous earth potential -

The author aims to detect the precursors of earthquakes and volcanic eruptions in real time, and to mitigate from these calamities. On the contrast described in Section 6, if we assume that the electrical structures of the aboveground and/or underground of the earth are constant, the electrical fields induced by geomagnetic variations are noises for the detection of anomalous earth potential related to tectonic activities. As the induced electrical fields are affected by these structures, the method of calculating the induced fields from the structures is also considered. However, it is impossible to assume the structures completely. In this section, the method of detecting the anomalous changes by using the relation with the observed electrical and magnetic fields is developed further.

Using a stochastic difference equation, Mori (1987) and Takayama and Mori (1987) developed the method for subtracting the effect of magnetic changes such as magnetic storms and daily variations, which allows real-time detection of earth potential associated with tectonic activities. If we assume that the responses of the geoelectric changes to the geomagnetic changes at a certain time do not change with time, we can detect the anomalous changes from the observed geoelectric fields by means of calculating the induced electrical variations by geomagnetic variations. Though they analyzed using the data of geoelectric variations and the geomagnetic horizontal two components of hourly mean values for about five months, the author expands the analysis ranges.

7-1 Analysis method by a stochastic differential equation

We assume that the induced electrical variation E(t) at a certain time “t” is expressed as a finite linear combination of past, present and future values of the northward component X(t) and the eastward component Y(t) of the geomagnetic variation. That is, E(t) is assumed to be expressed with a stochastic differential equation:

$$E(t)=\sum_{m=-L}^{K}\{a(m)\cdot X(t-m)+b(m)\cdot Y(t-m)\}+\varepsilon(t) \qquad (7\text{-}1)$$

Where a(m) and b(m) are coefficients of the impulsive response for the geomagnetic variations, that is X(t - m) and Y(t - m), respectively. $\varepsilon(t)$ is an uncorrelated part of the geomagnetic variation. Parameters K and L are lag numbers, and coefficients a(m), b(m) (m = -L ~ K) are calculated so as to minimize the AIC (Akaike Information Criterion) (Akaike, 1973; Sakamoto et al., 1986) expressed as follows:

AIC=−2 log(maximum log likelihood of the model)
+2(number of free parameters of the model)

Here, the number of parameters estimated from data should be less than $2n^{1/2}$. If the difference of AIC values is larger than one or two, then the difference is considered to be significant (Sakamoto et al., 1986).

Henceforth in this paper, AIC will indicate the difference from minimum AIC.

7-2 For geoelectric fields between Kasama and Mito

Geoelectric variations at the Mito group have been analyzed by making use of static models in order to remove the induced variations. When we calculate the AIC values for observed geoelectric fields at KSM-MTO and geomagnetic X and Y components at KAK, then E(t) = KSM-MTO in equation (7-1) , and the result is denoted simply by

KSM-MTO(OBS) = (X, Y).

Here, OBS means observation values.

When using X, Y and Z as associated data, the stochastic differential equation is as follows:

$$E(t)=\sum_{m=-L}^{K}\{a(m)\cdot X(m)+b(m)\cdot Y(t-m)+c(m)\cdot Z(t\text{-}m)\}+\varepsilon(t) \qquad (7\text{-}2)$$

In this case, the result is represented simply by

KSM-MTO(OBS) = (X, Y, Z).

The analyses using hourly mean values of KSM-MTO and (X, Y) or (X, Y, Z) at KAK are done in the following intervals:

A : 1985/ 4/ 1 00:00 ～ 5/11 00:00
KSM-MTO(OBS) = (X, Y)
B : 1985/ 4/ 1 00:00 ～ 5/11 00:00
KSM-MTO(OBS) = (X, Y, Z)
C : 1985/11/20 00:00 ～ 12/30 00:00
KSM-MTO(OBS) = (X, Y)
D : 1985/11/20 00:00 ～ 12/30 00:00
KSM-MTO(OBS) = (X, Y, Z)

AIC.FORT(EC2D)

KSM-MTO(OBS)=(KAK X, KAK Y) AIC.DATA(KM2001)

1985 4M 1D 0H - 1985 5M 11D 0H (JST) INT=60MIN N= 961

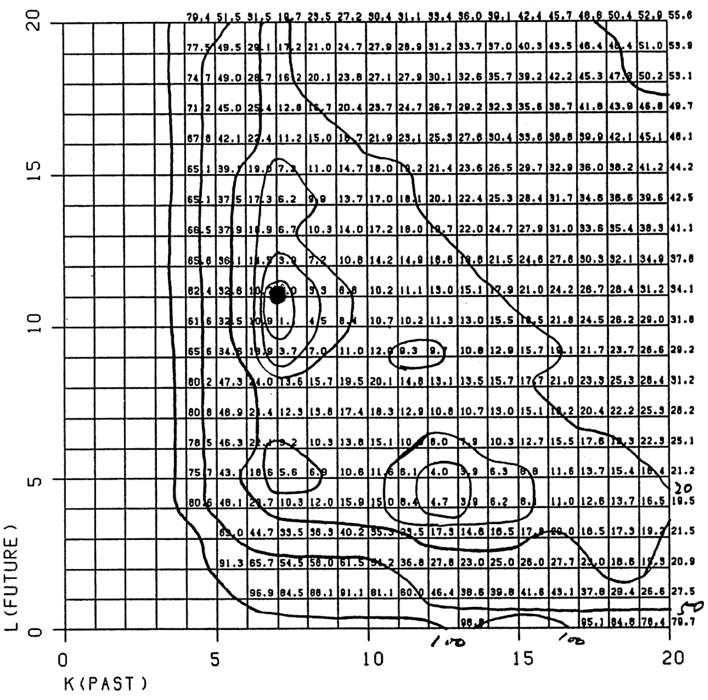

AIC.FORT(RESPON)

KSM-MTO(OBS)=(KAK X, KAK Y) AIC.DATA(KM2001)

1985 4M 1D 0H - 1985 5M 11D 0H (JST) INT=60MIN N= 961

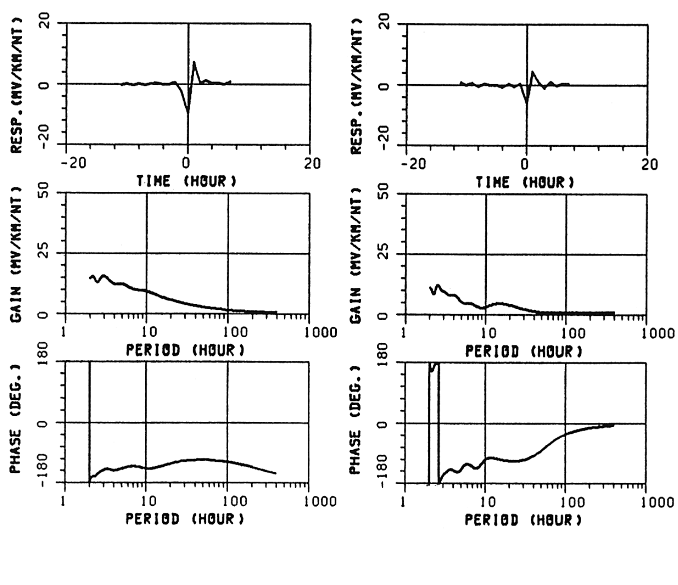

Fig. 7-1(a) The result analyzed using the stochastic difference equation for KSM-MTO in the case of A. The upper half of the figure shows the distribution of AIC values in terms of abscissa K(past) and ordinate L(future). The minimum value marker is shown by ●. The lower half shows the response function for minimum AIC. The impulsive response in the time domain, the amplitude and the phase of the response functions in the frequency domain are expressed sequentially from the top in the lower half of the figure.

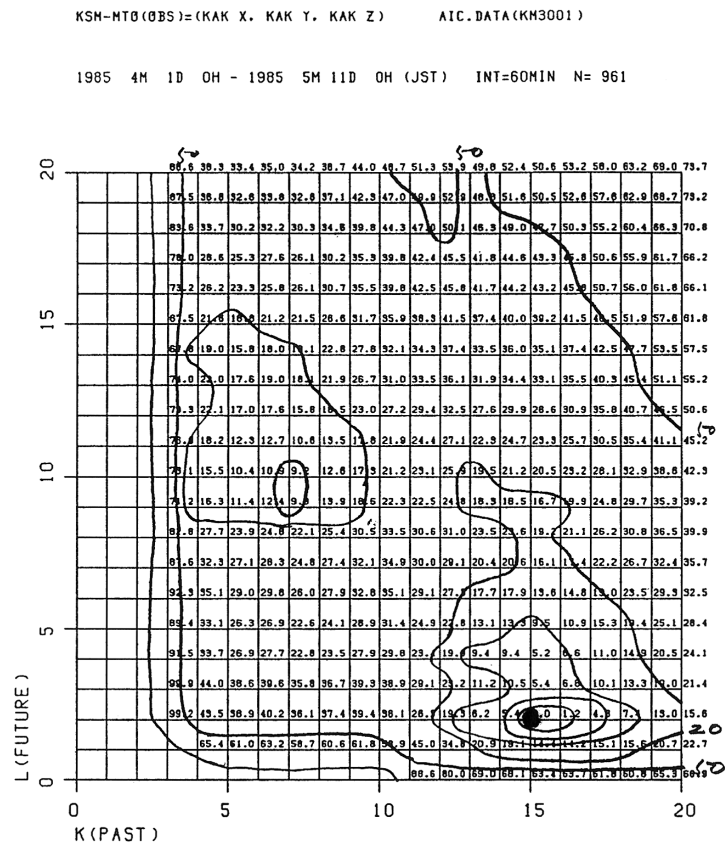

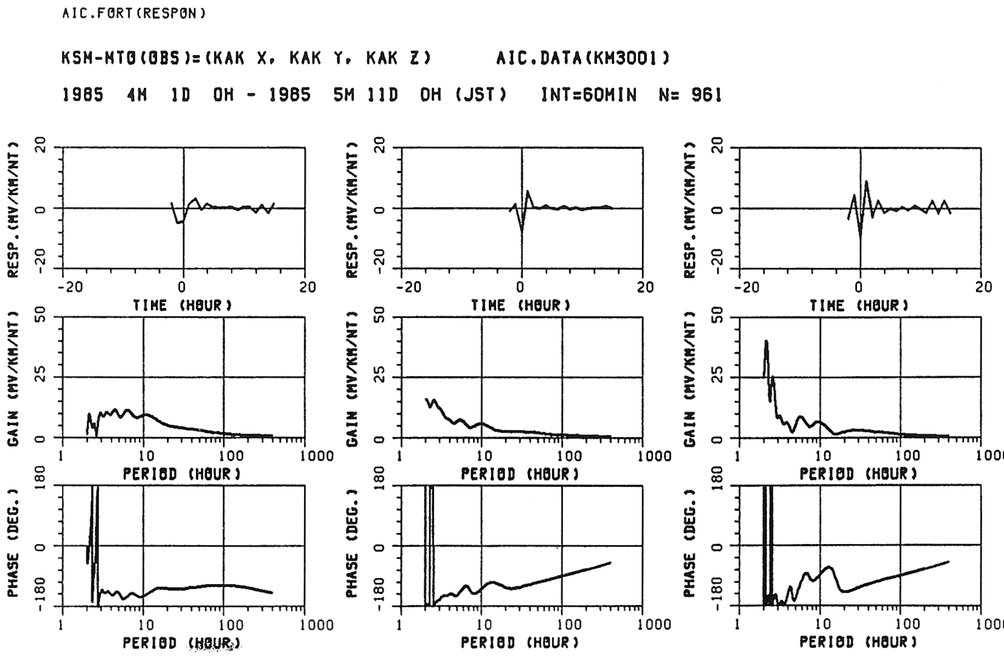

Fig. 7-1(b) The result analyzed using the stochastic difference equation for KSM-MTO in the case of B. The legends are the same as in figure 7-1(a).

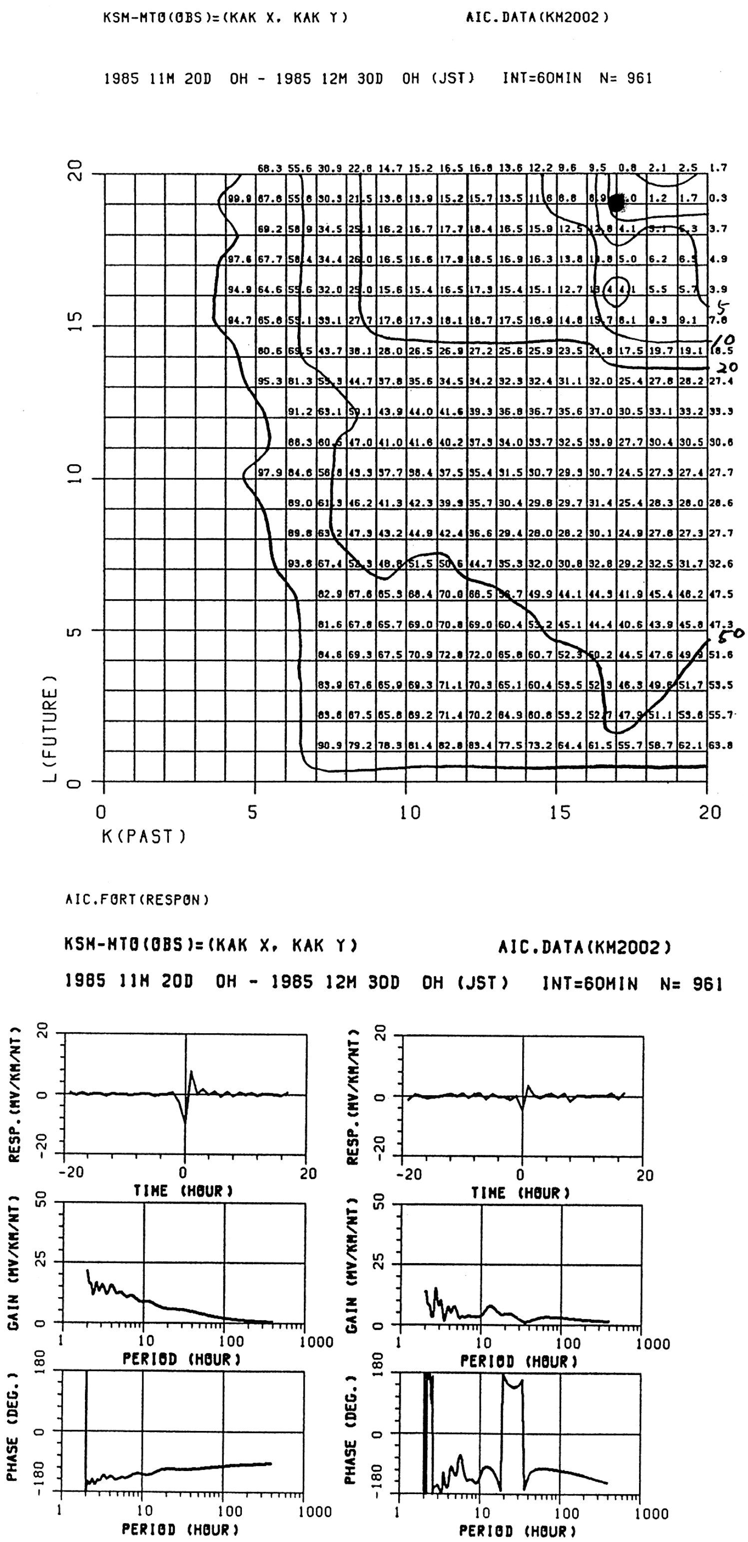

Fig. 7-1(c) The result analyzed using the stochastic difference equation for KSM-MTO in the case of C. The legends are the same as in figure 7-1(a).

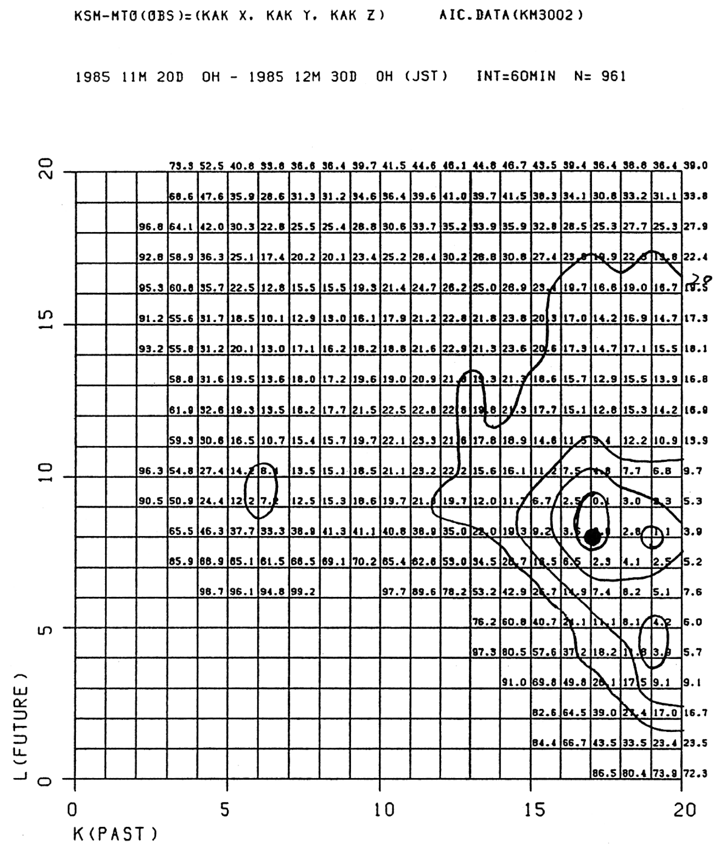

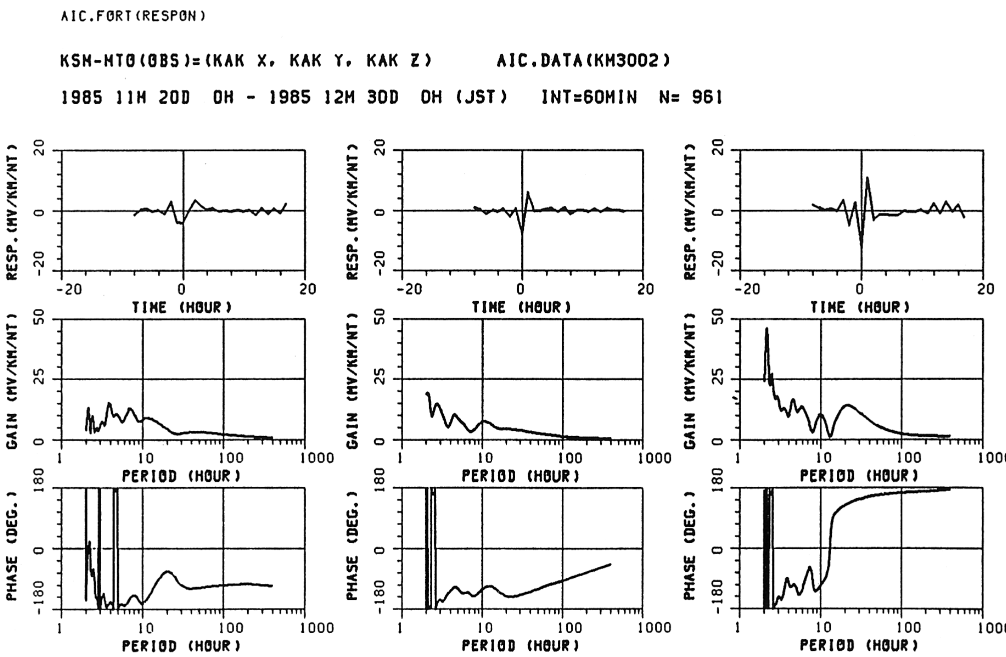

Fig. 7-1(d) The result analyzed using the stochastic difference equation for KSM-MTO in the case of D. The legends are the same as in figure 7-1(a).

In each case of A, B, C and D, the AIC distributions are shown in the upper half of Fig. 7-1 (a) ~ (d). The minimum value in each figure is marked by a closed circle (•), and the contour lines are drawn by the values of 2, 5, 10, 20, 50 and 100. We select a set of the parameters, K and L, so as to minimize the AIC value, and determine the coefficients, a(m), b(m) (and c(m)), corresponding to m = -L ~ K. The lower half of Fig. 7-1(a) ~ (d) shows the response functions for the minimum AIC.

In cases A, B, C and D, (K, -L) = (7, -11), (15, -2), (17, -19) and (17, -8), respectively, for the minimum AIC. For example, for model A, the electrical field at a certain time can be represented using the magnetic fields in the time range of K hours ago to L hours afterwards. In case B adding the Z component (Fig. 7-1(b)), the response for X is considerably different from case A (Fig. 7-1(a)), and the coefficients for large future values K do not become small. Ideal coefficients in a stochastic differential equation are larger for m = -1 ~ 1 than for other m's, and K and L are small values. But for B, the coefficients for Z become rather large values for K larger than 12. So the response function is not smooth in this case.

For C (Fig. 7-1(c)), (K, -L) = (17, -19), K and L are large values for the minimum AIC, and the parameter number p = 75. So it cannot be said that the model is effective by the reason that p is greater than $2n^{1/2}$ = 62, but the coefficients are used here. For D (Fig. 7-1(d)), the model is effective, but the coefficients for K and L are not small values for the larger K and L, and the gain and phase of the response are not as smooth as in case B.

Using the coefficients for A ~ D, the estimated (EST) electrical fields at KSM-MTO are calculated from the observed magnetic fields at KAK; furthermore the residual (RES) electrical fields are calculated by subtracting the estimated values from the observed electrical fields (OBS). That is, RES = OBS - EST. The results are shown in Fig. 7-2(a) ~ (d). In these figures, the coefficients obtained for A ~ D are also applied for another period.

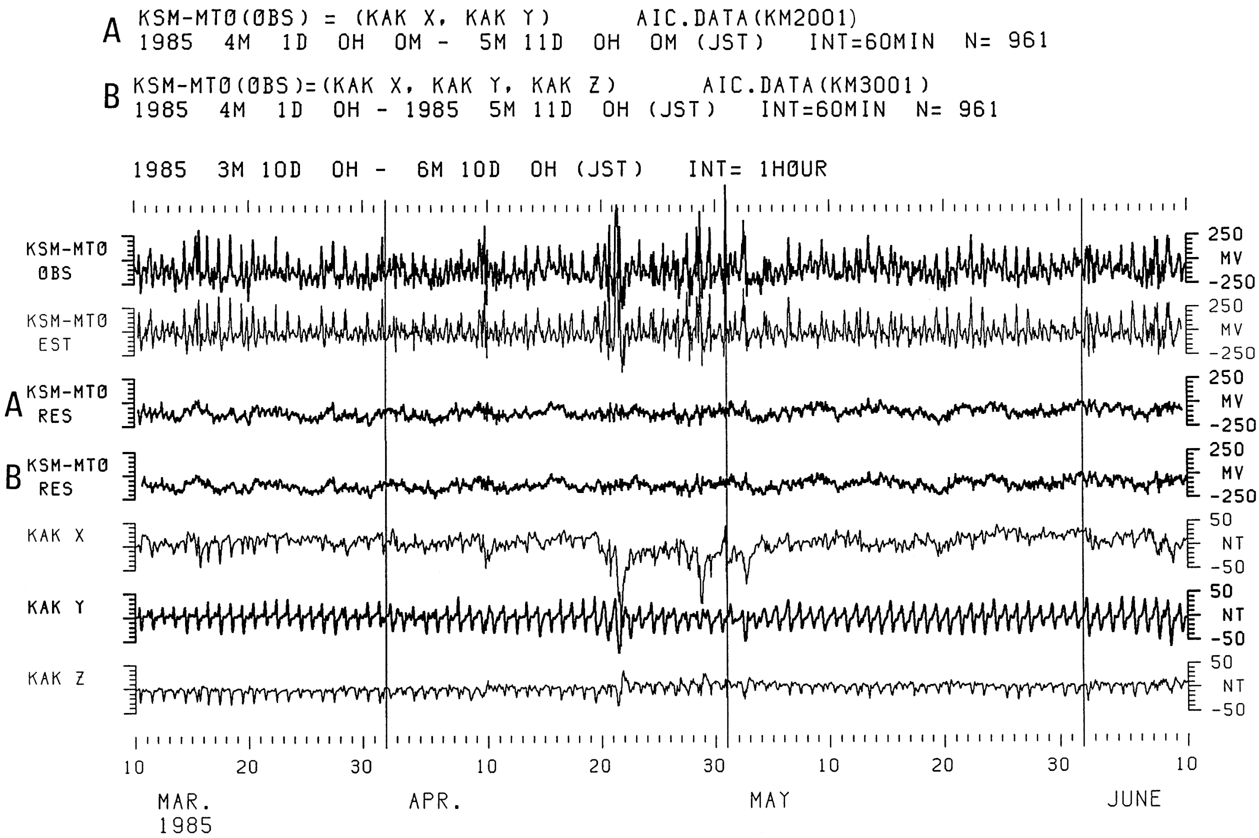

Fig. 7-2(a) Observed (OBS), estimated (EST) and residual (RES) electrical fields at KSM-MTO. Coefficients obtained for the case of A and B are applied for the period March 10 to June 10, 1985.

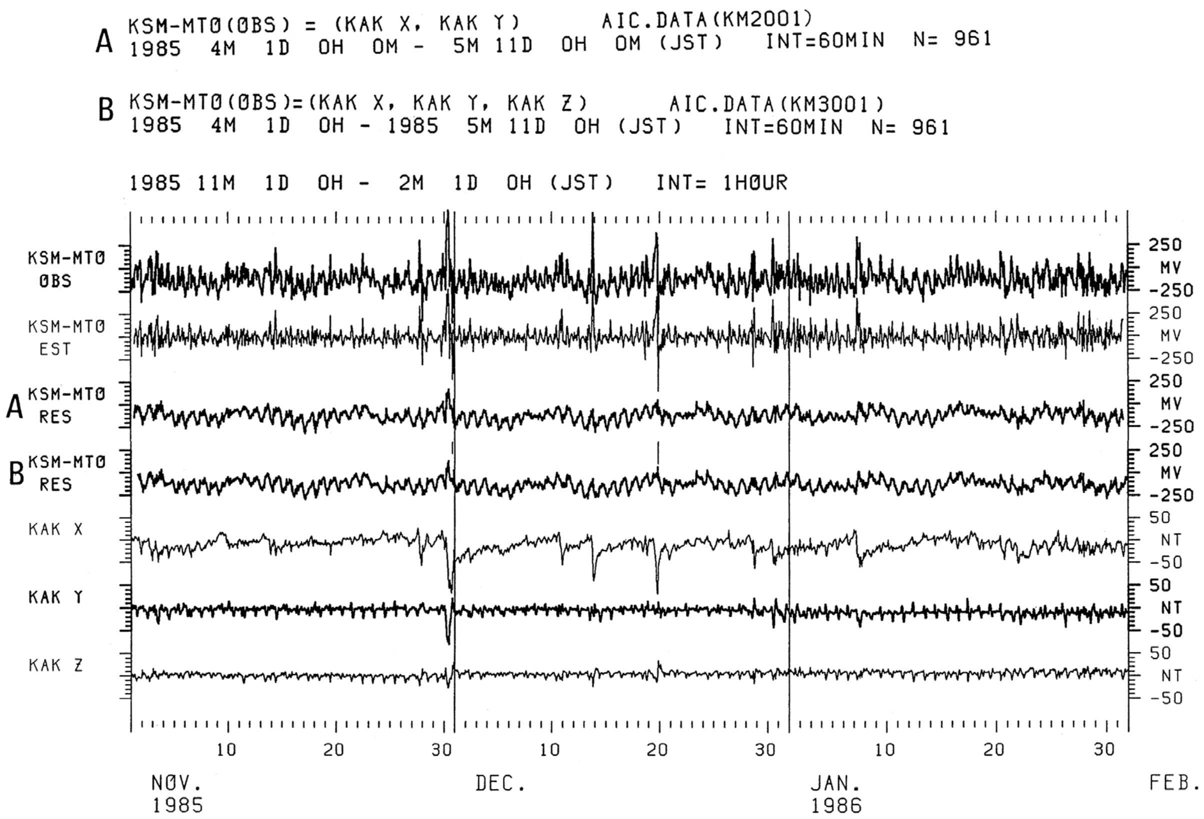

Fig. 7-2(b) Observed (OBS), estimated (EST) and residual (RES) electrical fields at KSM-MTO. Coefficients obtained for the case of A and B are applied for the period November 1, 1985, to February 1, 1986.

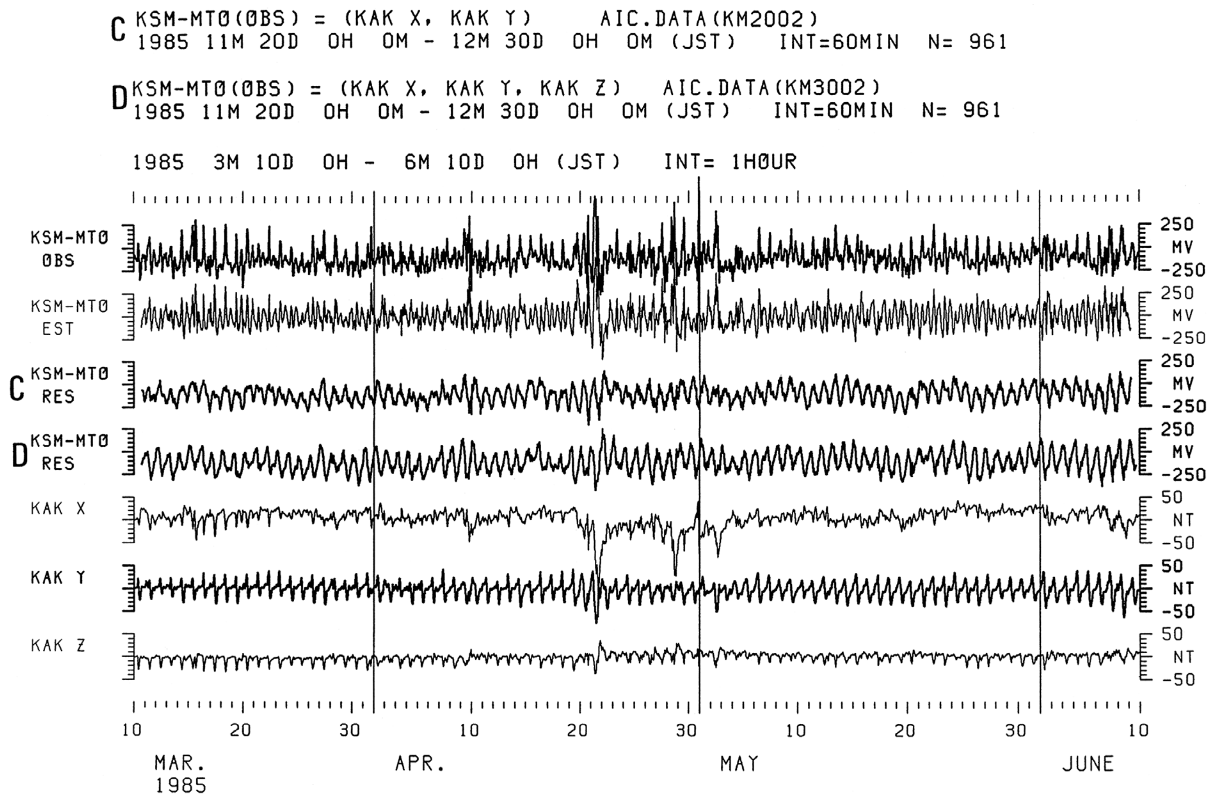

Fig. 7-2(c) Observed (OBS), estimated (EST) and residual (RES) electrical fields at KSM-MTO. Coefficients obtained for the case of C and D are applied for the period March 10 to June 10, 1985.

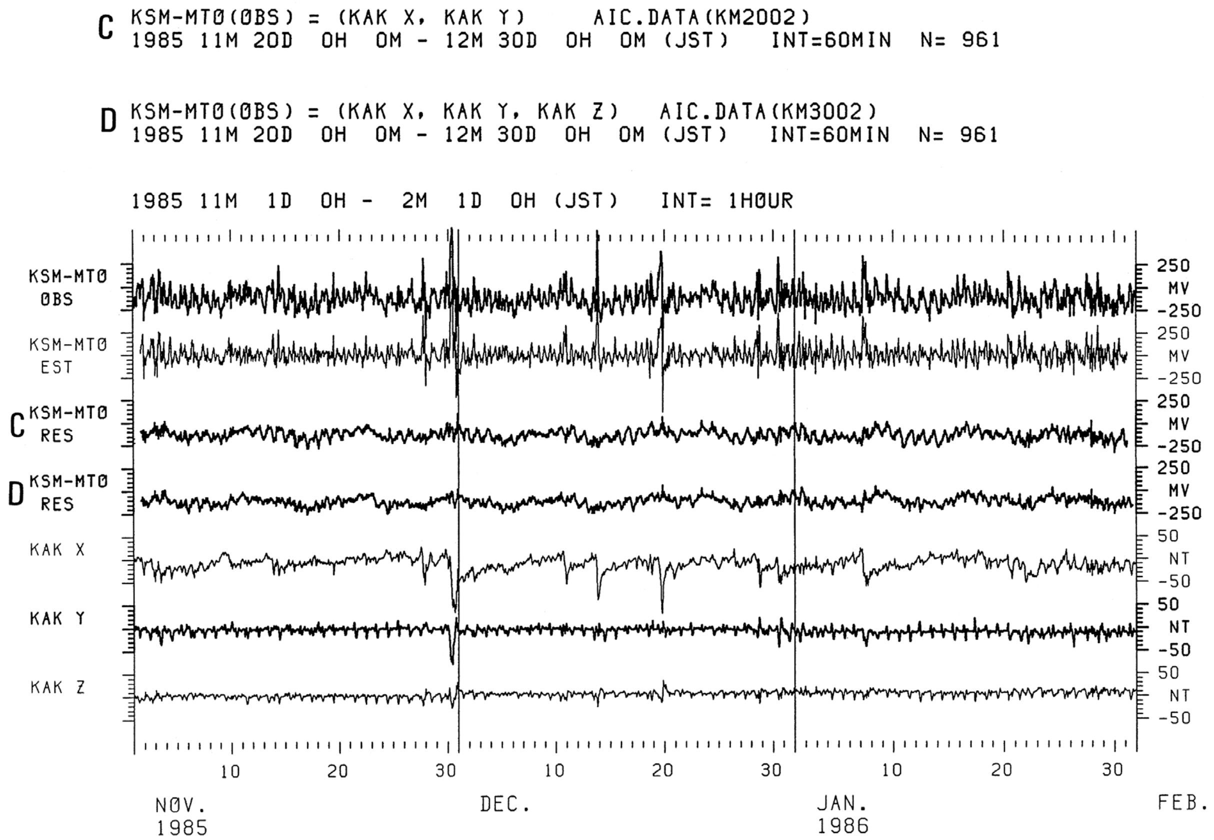

Fig. 7-2(d) Observed (OBS), estimated (EST) and residual (RES) electrical fields at KSM-MTO. Coefficients obtained for the case of C and D are applied for the period November 1, 1985, to February 1, 1986.

The results read from Fig. 7-2 (a) ~ (d) are made itemized statements.

(1) The residual fields for the period of A and B (Fig. 7-2(a)) are almost the same whether Z is considered or not, and the electrical fields induced by geomagnetic fields such as daily variations and magnetic storms are considerably separated from the original data. That is, the predominant induced components in the observed geoelectric variations are almost completely separated for KSM-MTO.

(2) When the coefficients resulted for A and B are applied for almost the same period from November, 1985, to January, 1986 (Fig. 7-2(b)), the electrical fields induced by short period magnetic variations are considerably separated, but those induced by daily variations are not so.

(3) When the coefficients resulting from C and D are applied for almost the same period from November, 1985, to January, 1986 (Fig. 7-2(d)), the result for D, in which Z is considered better than C, and the daily variations are considerably eliminated.

(4) When the coefficients resulting from C and D are applied for different periods from March to June, 1986 (Fig. 7-2(c)), it looks like that the daily variations in RES are greater than those in OBS.

(5) The results of (4) may be reflected that the determined minimum AIC is not significant because of a large K+L. Otherwise, it is considered that the data used for the period was not good, or that it was affected by the seasonal effect.

(6) The effect using Z as associated data appears well for the period including models C and D, but the effect does not appear for the period including models A and B.

As shown in Section 5, Z is experientially expressed as a linear function of X and Y for short period geomagnetic variations in the frequency domain. As shown in Fig. 6-1(a) of Section 6, Z transfer functions in the 60-minute period are fairly stable in time. Those in the 120- ~ 360-minute range become scattered, and those of 720-minute periods become stable. That is, Z in short time variations and in daily variations is well expressed as a linear function of X and Y, but the Z transfer function in the intermediate periods is variable. Adaptation to such a statistical model used in this section seems to induce a good result when X, Y and Z are mutually independent. In order that Z not be independent of X and/or Y, the effect of Z on electrical variations is larger than necessary, so the responses may become unnatural. So in the case using Z as associated data, the result is not so effective. It may be effective to remove the effect of Z from the residual variation using X and Y. It was not possible to make it progress there this time, so it remains a subject for future study.

7-3 Application to the data of electrical fields at the Mito group and Z at Kakioka

The coefficients so as to minimize AIC for geoelectric fields at all lines of the Mito group and the Z component of the geomagnetic field at KAK are calculated in the period around on May, 1986, in addition to the periods of A and B in the previous section.

On Z, a stochastic differential equation follows, the same as on E(t) of equation (7-1).

$$Z(t)=\sum_{m=-L}^{K}\{a(m)\cdot X(t-m)+b(m)\cdot Y(t-m)\}+\varepsilon(t) \tag{7-3}$$

Here, the analyzing intervals for calculating parameters are rewritten as follows:

A：1985/ 4/ 1 00:00 ～ 5/11 00:00
N = 961 (40 days)
B：1985/11/20 00:00 ～12/30 00:00
N = 961 (40 days)
C：1986/ 4/15 00:00 ～ 5/15 00:00
N = 721 (30 days)

The AIC values for K and L are calculated in the range K (and L) = 0 ～ 20.

The case of C at KSM-MTO is shown in Fig. 7-3. AIC takes on a minimum value when (K, -L) = (19, -2), and the response function curves for Y become considerably oscillating in the short periods. Fig. 7-4 ～ 7-8 shows typical examples in various combinations. The parameters (K, -L) for an adopted minimum AIC in each case are tabulated in Table 7-1. In the cases of ISI-MTO and MTO-HIO, K+L do not become small values. For ISI-HIO, as shown in Table 7-1, in all periods, values of K+L become small. For ISI-KSM (Fig. 7-6), values of K+L are small in A and B, and these responses are similar, but in C, K = 19, and the response is not smooth. Similar tendencies are seen for KSM-HIO and ISI-KSM.

Table 7-1 The minimum AIC (K, -L) in the periods of A (1985/4/1 - 5/11), B (1985/11/20 - 12/30) and C (1986/4/15 - 5/15)

	A	B	C
KSM-MTO	(7, -11)	(17, -19)	(19, -2)
ISI-MTO	(12, -11)	(7, -16)	(13, -11)
ISI-HIO	(4, -2)	(9, -1)	(6, -6)
ISI-KSM	(7, -1)	(14, -1)	(19, -1)
MTO-HIO	(16, -1)	(8, -15)	(17, -5)
KSM-HIO	(7, -5)	(5, -1)	(19, -6)
Z	(12, -6)	(8, -20)	(20, -8)

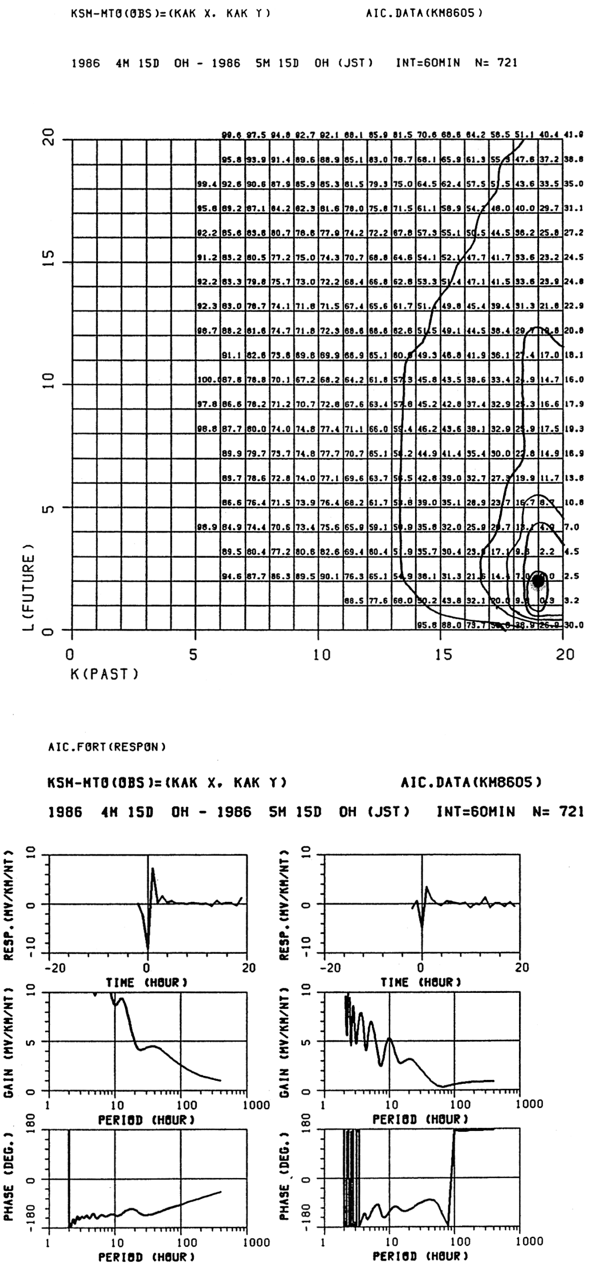

Fig. 7-3 AIC distribution at KSM-MTO in the interval C and response function in the case of minimum AIC.

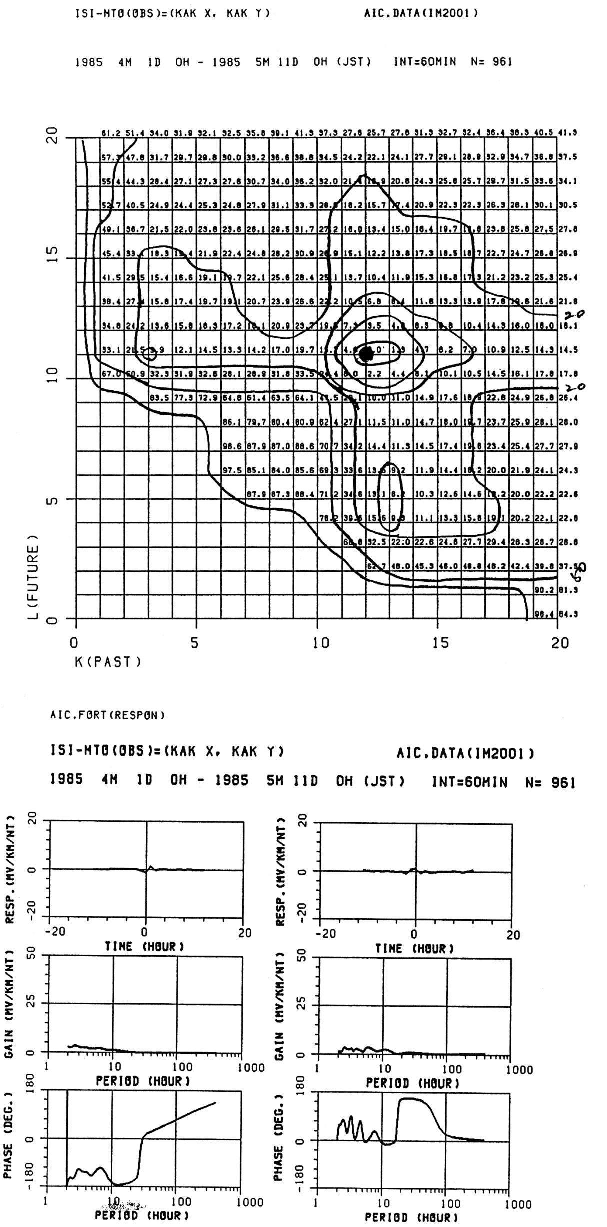

Fig. 7-4 AIC distribution at ISI-MTO in the interval A and response function in the case of minimum AIC.

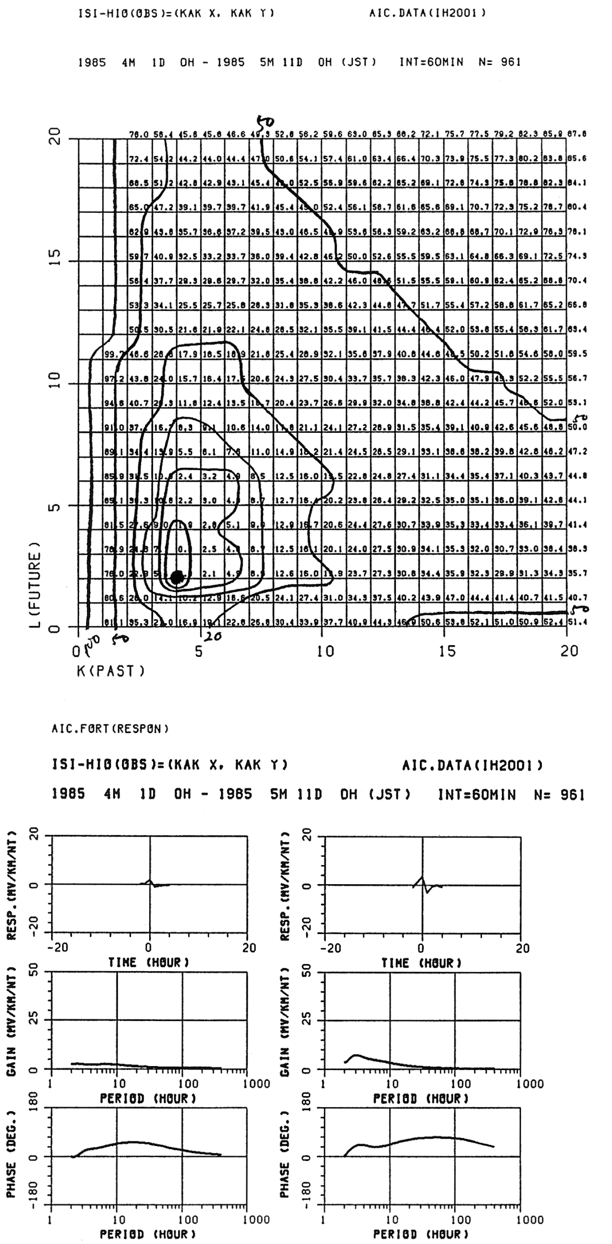

Fig. 7-5 AIC distribution at ISI-HIO in the interval A and response function in the case of minimum AIC.

The results on Z are shown in Fig. 7-9(a), (b), (b') and (c). In the cases of B (Fig. 7-9(b)) and C (Fig. 7-9(c)), the values of K+L in minimum AIC are large, that is, (K, L) = (8, -20) and (20, -9). However, AIC indicates a local minimum in (K, -L) = (8, -8) in both B and C. So (K, -L) = (8, -8) is adopted, and the responses are calculated. The bottom of Fig. 7-9(b') and Fig. 7-9(c) shows the responses.

The estimated values (EST) and residual value (RES = OBS - EST) at all the components at the Mito group and Z at KAK are calculated using the parameter in Table 7-1 and the geomagnetic X and Y variations at KAK. The results are shown in Fig. 7-10(a), (b) and (c). In each figure, RES-A, RES-B and RES-C represent the residual values for the parameters for the A, B and C periods, respectively.

RES-A and RES-C in Fig. 7-10(a) are almost the same, and daily and short period variations are considerably rejected. But in RES-B, daily variations are almost left behind, as they are still remaining. In the period B (Fig. 7-10(b)), the amplitudes in RES-B are smaller than those in RES-A and RES-C. The period C (Fig. 7-10(c)) is the same season one year after the period A, and the results have almost the same tendency to A. So it is said that the parameters at a certain season are usable in the season of another

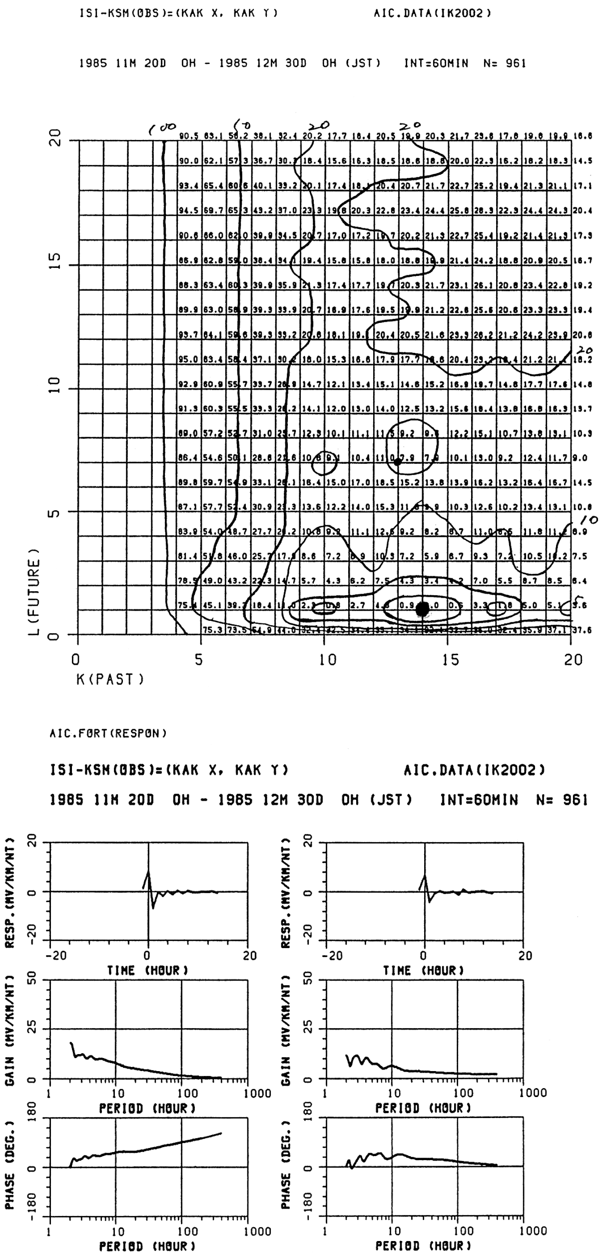

Fig. 7-6 AIC distribution at ISI-KSM in the interval B and response function in the case of minimum AIC.

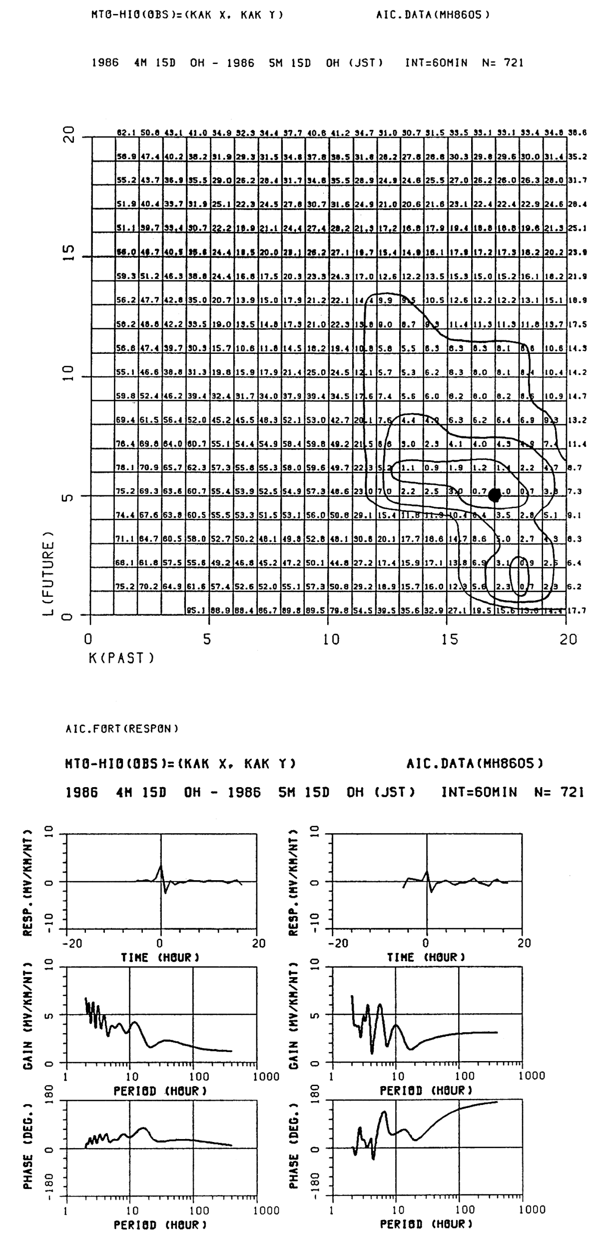

Fig. 7-7 AIC distribution at MTO-HIO in the interval C and response function in the case of minimum AIC.

year. Although the electromagnetic state of the earth does not understand how it is changing with seasons, it could be said that the same coefficient can be used at the same season. Although it asked for the relation between Z, and X and Y in order to hold the key which asks for how much influence it has comparatively from the earth's exterior, and from the inside of the earth, at the present stage, it is unknown.

The change of response of the earth's current to geomagnetic change is not necessarily based only on changes of the internal structure of the earth. The influence of the earth's exterior is also considered. The key of at what rate the influence of an earth exterior and underground structure is included is unknown at the present stage. It becomes a research subject whether one can ask for such a coefficient, since it is desirable to use the same coefficient through one year. On the contrary, studying seasonal changes of the electromagnetic state of the earth is also considered from the coefficient from which a season therefore changes.

7-4 Spectral analysis

Amplitude spectrums of the observed electrical and magnetic fields (OBS) and the residual electrical fields using the coefficients calculated with model A, B

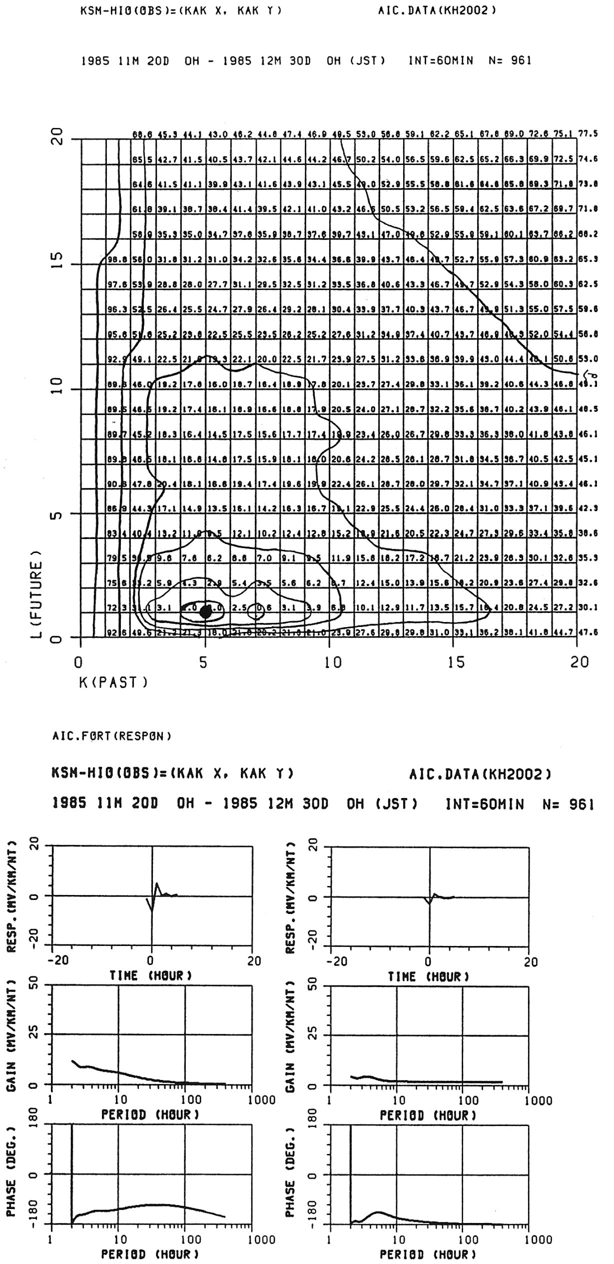

Fig. 7-8 AIC distribution at KSM-HIO in the interval B and response function in the case of minimum AIC.

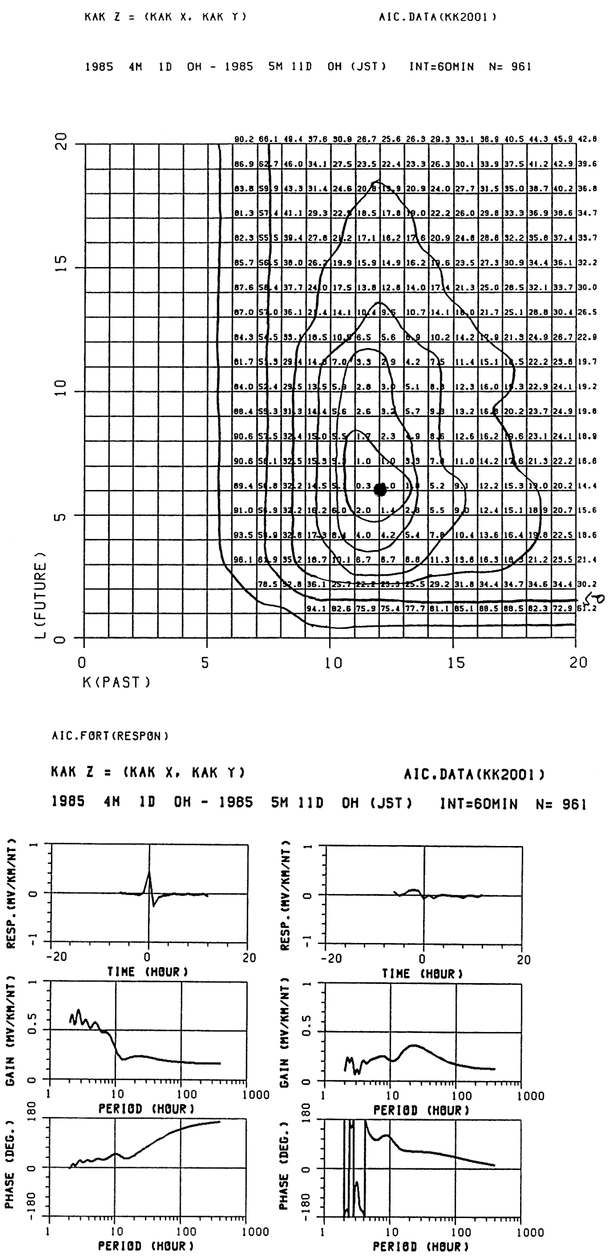

Fig. 7-9(a) AIC distribution at KAK Z in the interval A and response function in the case of minimum AIC.

and C in Section 7-3 (RES-A, RES-B and RES-C) are calculated. The period of the data used for analysis is as follows:

1: 1985/10/1 00:00 ~ 1986/10/ 5 00:00
T = 1h N = 8857 (369 days)
2: 1985/10/1 00:00 ~ 1986/4/26 00:00
T = 1h N = 4969 (207 days)
3: 1986/4/1 00:00 ~ 1986/10/25 00:00
T = 1h N = 4969 (207 days)

Here T is a data interval, and N is the number of data.

The following tidal constituents will be referred to in this paper.

2Q	28.0062 h	
Q_1	26.8684 h	Major lunar elliptic tide
O_1	25.8193 h	Principal lunar diurnal tide
M_1	24.8332 h	Minor lunar elliptic tide
P_1	24.0659 h	Principal solar diurnal tide
S_1	24.0000 h	Meteorological diurnal tide
K_1	23.9345 h	Luni-solar declinational diurnal tide
J_1	23.0985 h	Small lunar elliptic tide
N_2	12.6583 h	Major lunar elliptic tide
ν_2	12.6260 h	Major lunar evectional tide
M_2	12.4206 h	Principal lunar semidiurnal tide

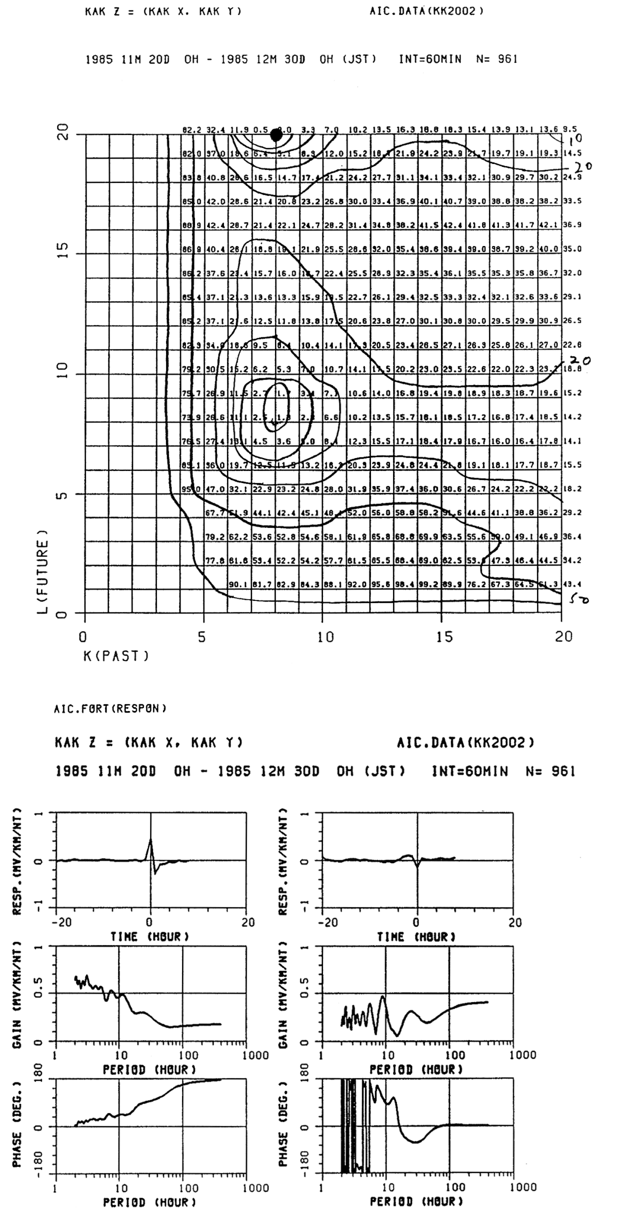

Fig. 7-9(b) AIC distribution at KAK Z in the interval B and response function in the case of minimum AIC.

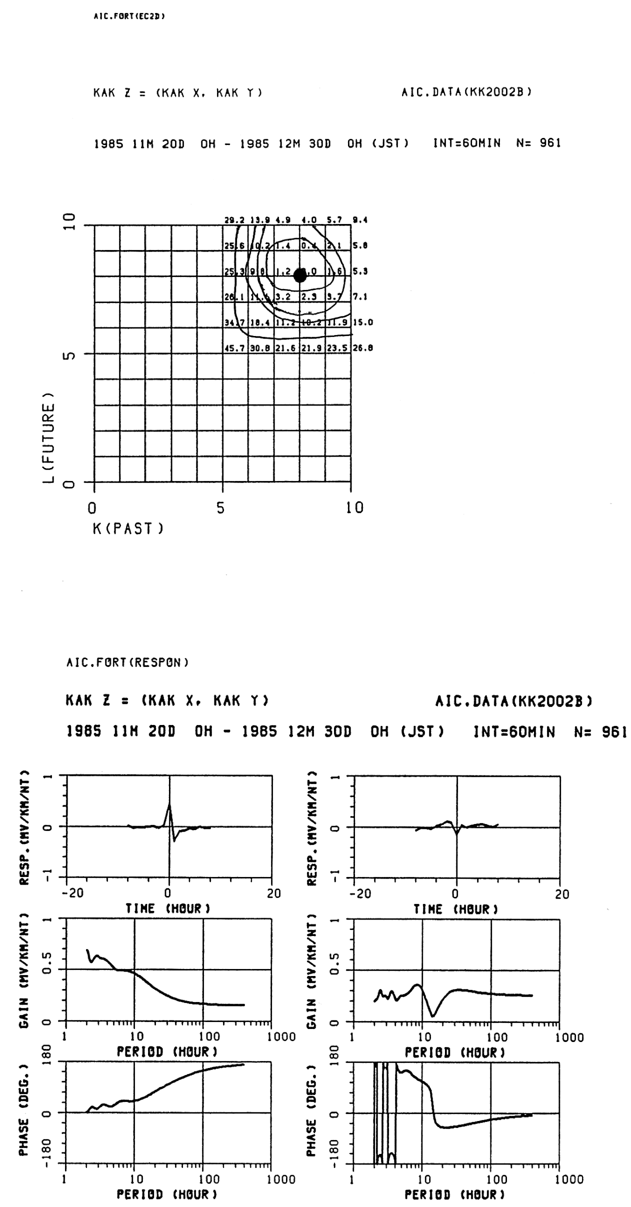

Fig. 7-9(b') AIC distribution at KAK Z in the interval B and in the range (K, L)=(10, -10) and response function in the case of minimum AIC.

S_2	12.0000 h	Principal solar semidiurnal tide
R_2	11.9836 h	Minor solar elliptic tide
K_2	11.9672 h	Luni-solar declinational semidiurnal tide

Fig. 7-11(a) ~ (c) represent the amplitude spectra for the various components in the range of 3 ~ 1000 hours for the period "1," and they are calculated by means of the least square method. In all of these figures, conspicuous constituents of 10 or fewer hours are the higher harmonics of the diurnal variation (S_n (n = 3 ~ 6)). The amplitude spectra of 10 ~ 30 hours are shown in Fig. 7-12(a) ~ (h) rearranged for every ingredient. In these figures, "1," "2" and "3" on the upper part denote the period, "O" on the left side denotes the amplitude spectrum of the observed field, and "A," "B" and "C" on the left side denote those of the residual fields in the cases of model A, B and C respectively. Predominant peaks for the tidal harmonics are noted in these figures.

Fig. 7-13 shows the amplitude spectra of X, Y and Z at KAK, tide at Ooarai (OOARAI TIDE) and atmospheric pressure at Youkaichiba (YOUKA PRESS), using hourly mean values from September 8, 1985, to August 23, 1986. The spectra of X, Y, Z and PRESS show large peaks for the tidal constituents of the solar diurnal and its higher harmonics (S_1, S_2, S_3, S_4, S_5 and S_6). For TIDE, the tidal constituents of O_1, K_1, M_2, S_2, Q_1, ν_2 and R_2 are predominant.

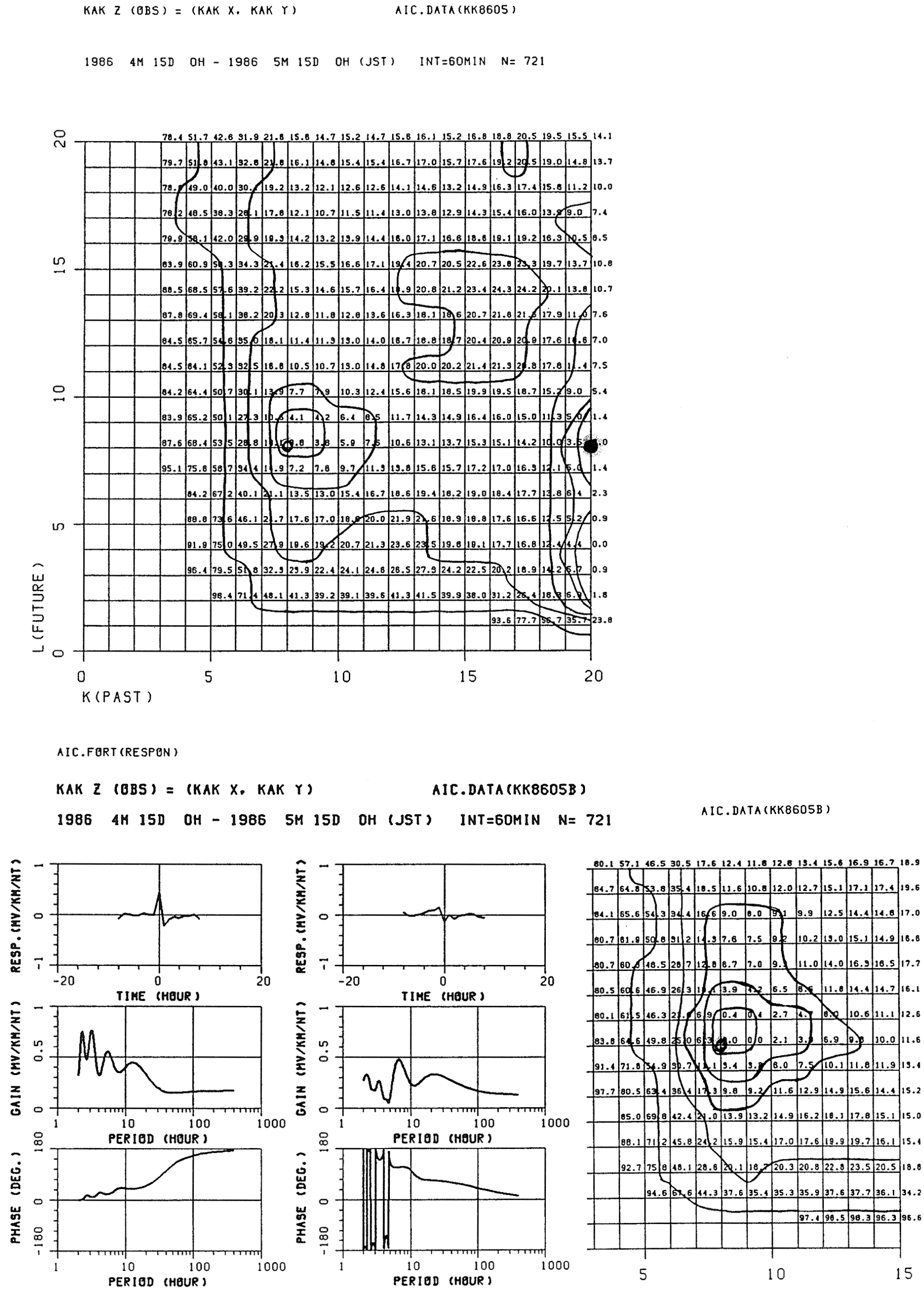

Fig. 7-9(c) AIC distribution at KAK Z in the interval C and response function in the case of minimum AIC (top). The bottom right shows the AIC distribution in the range (K, L)=(15, -15)

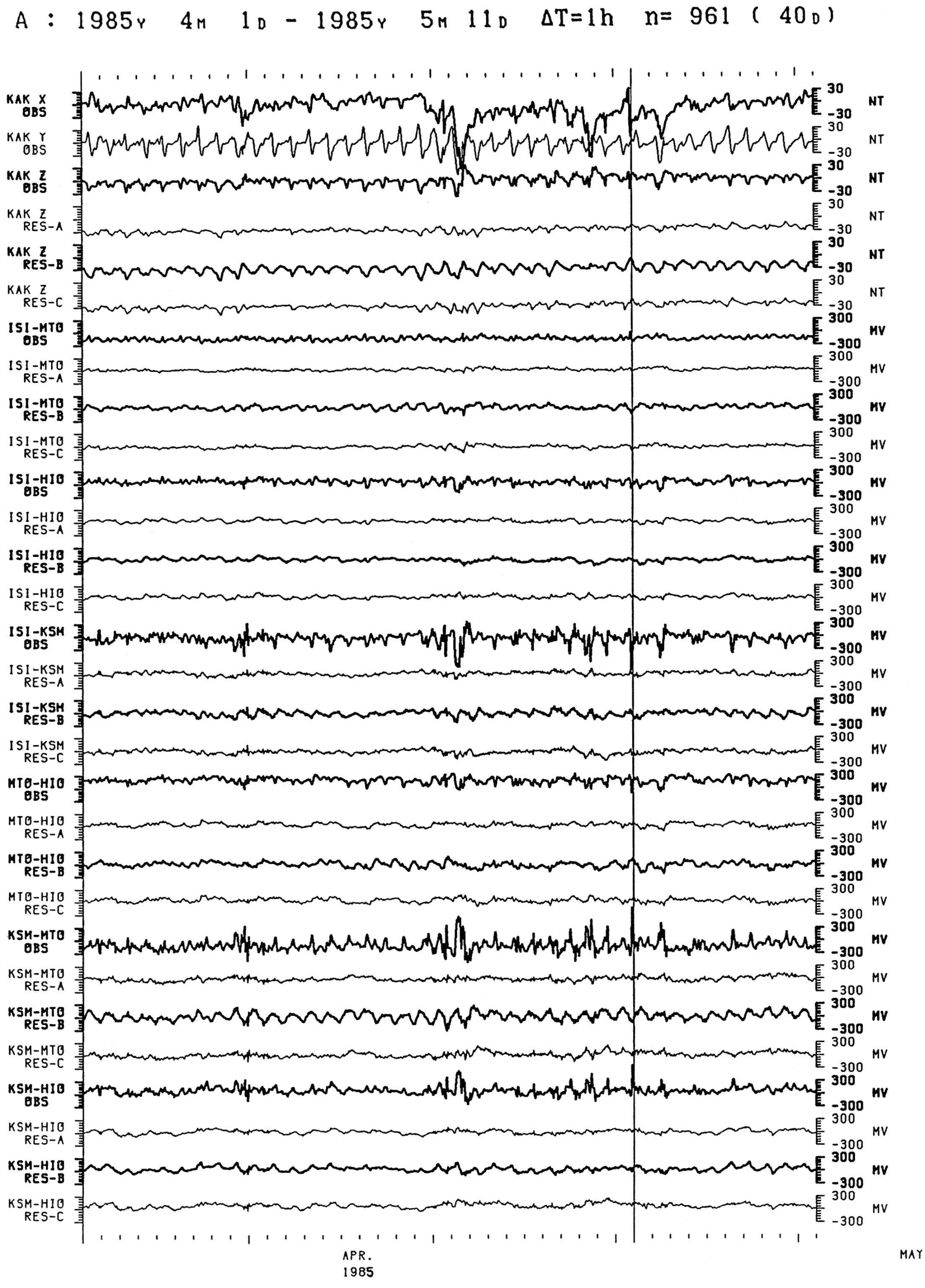

Fig. 7-10(a) Observed geomagnetic variations at KAK and geoelectric variations at the Mito group, and the residual variations from April 1 to May 11, 1985. OBS represents the observed variation, and RES-A, RES-B and RES-C represent the residual variations in the case of the parameters in the case of A, B and C periods, respectively.

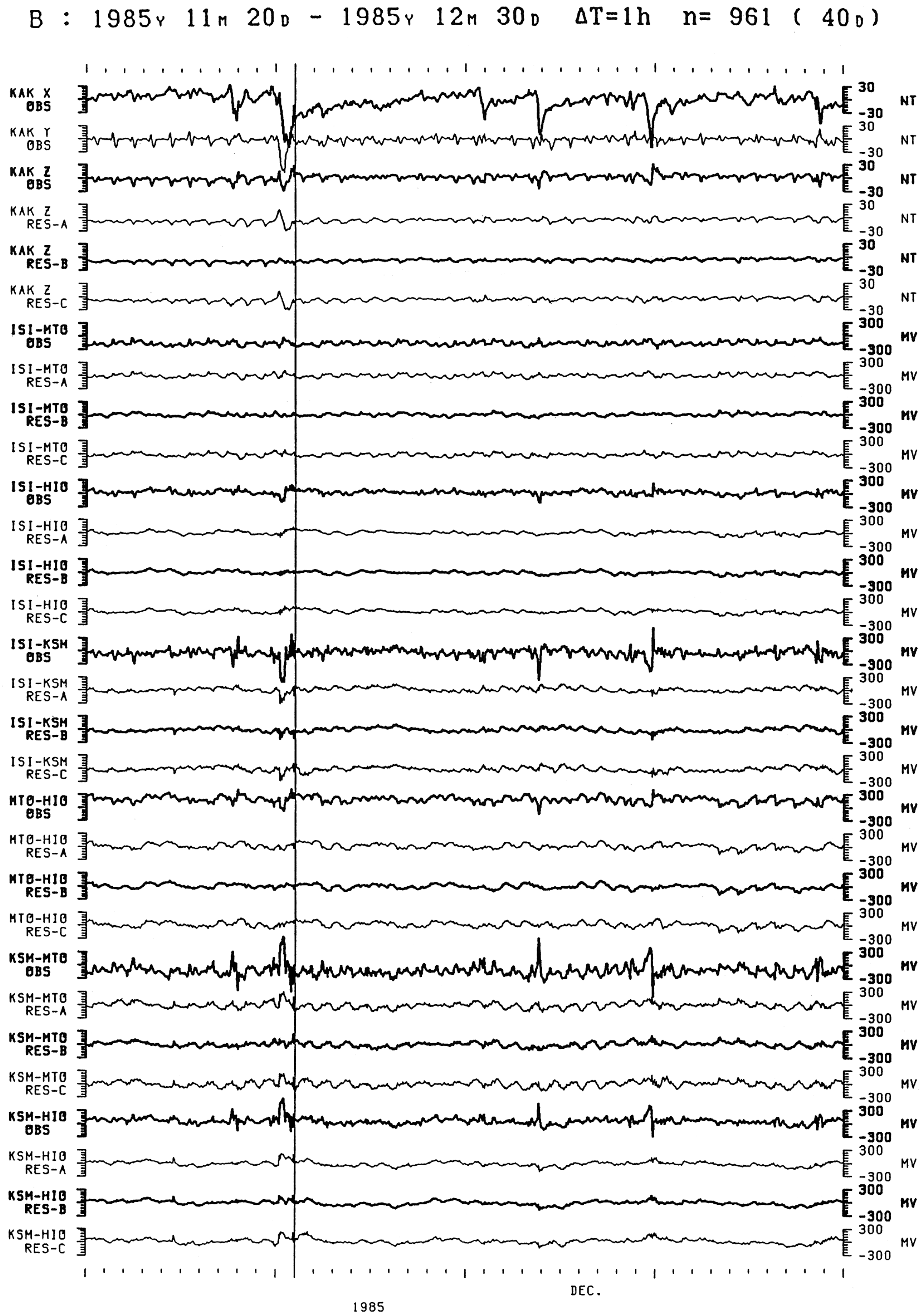

Fig. 7-10(b) Observed geomagnetic variations at KAK and geoelectric variations at the Mito group, and the residual variations from November 20 to December 30, 1985. The legends are the same as in figure 7-10(a).

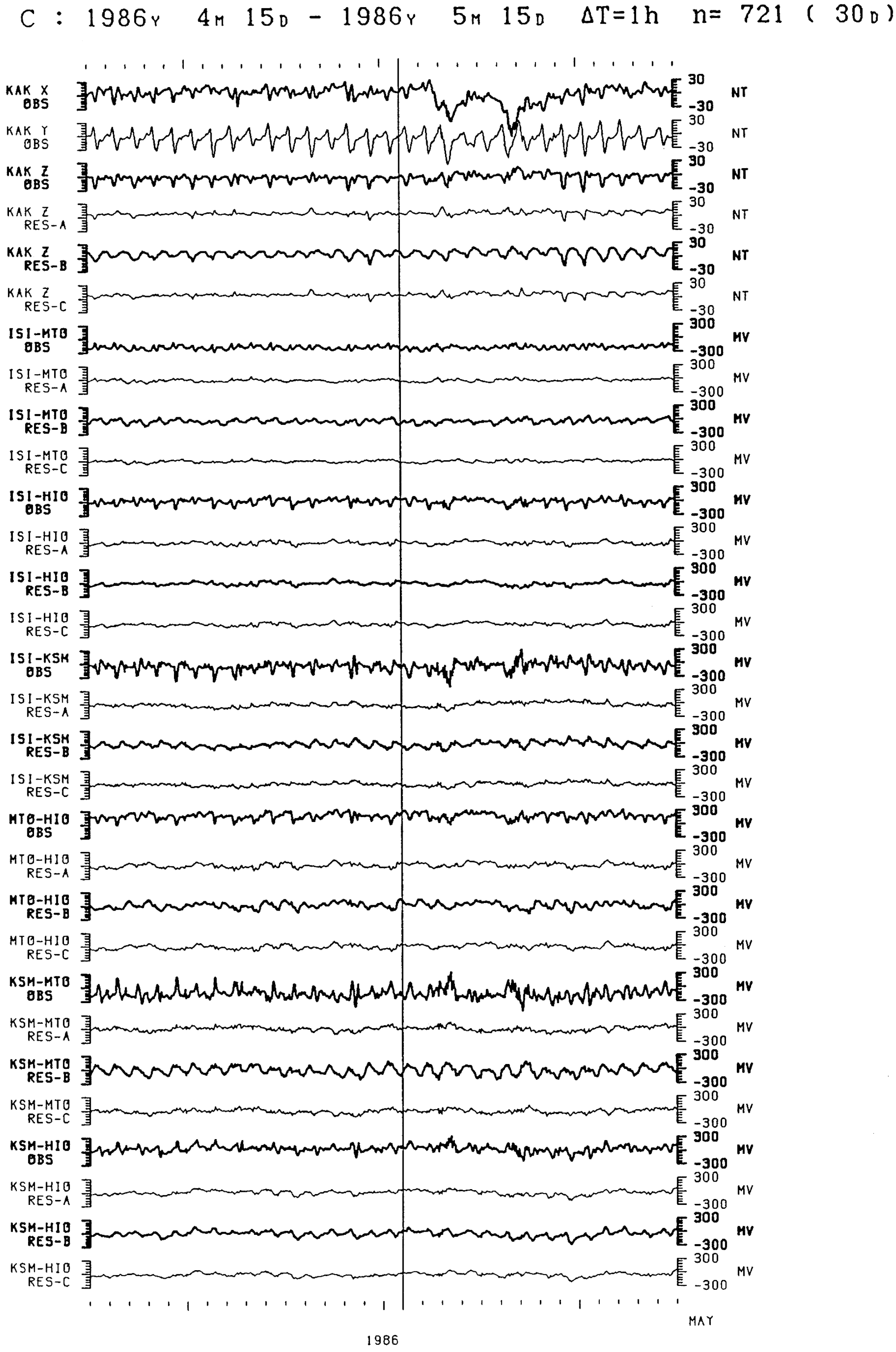

Fig. 7-10(c) Observed geomagnetic variations at KAK and geoelectric variations at the Mito group, and the residual variations from April 15 to May 15, 1986. The legends are the same as in figure 7-10(a).

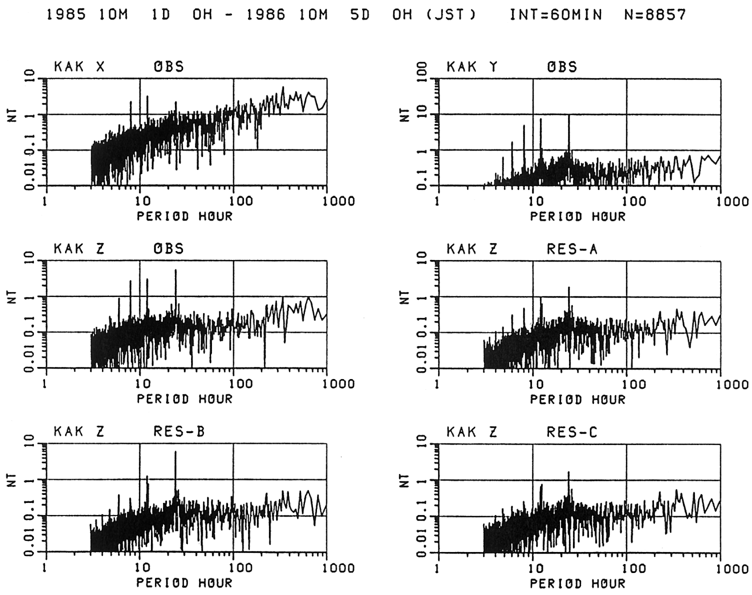

Fig. 7-11(a) Amplitude spectra for the observed (OBS) and the residual (RES-A, RES-B, RES-C) fields of X, Y and Z at KAK in the range of 3-1000 hours for the period "1" (from October 1, 1985, to October 5, 1986).

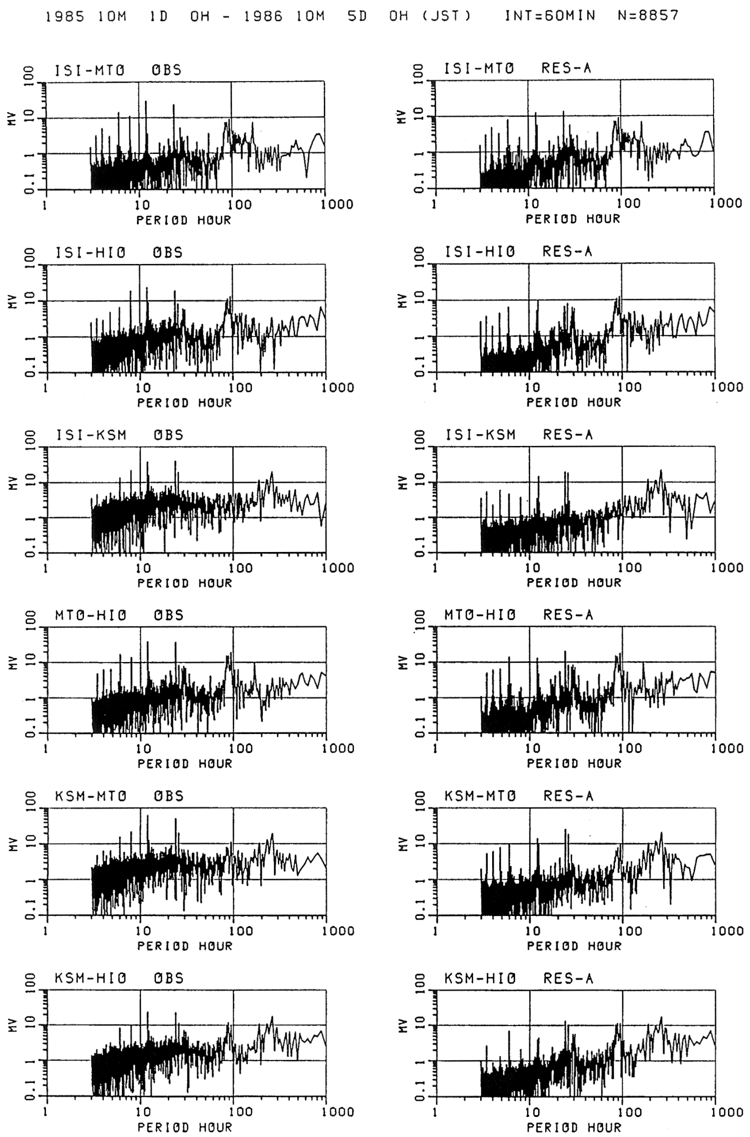

Fig. 7-11(b) Amplitude spectra for the observed (OBS) and the residual (RES-A) fields of the geoelectric variations at the Mito group in the range of 3-1000 hours for the period "1" (from October 1, 1985, to October 5, 1986).

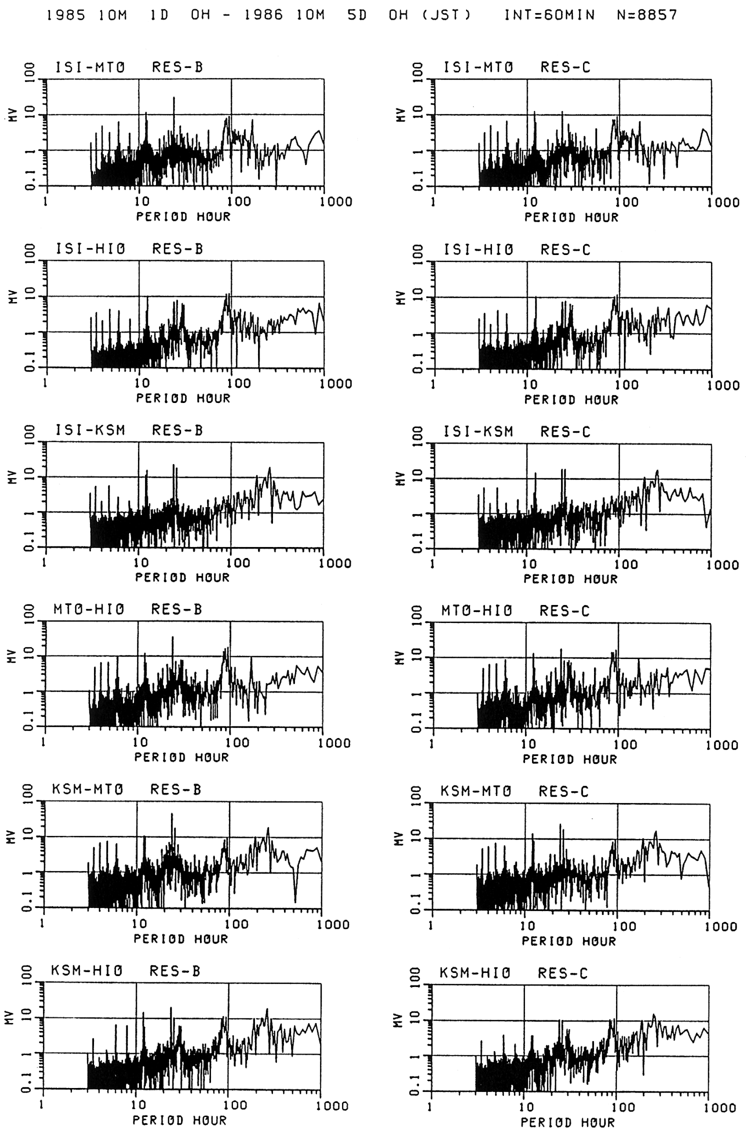

Fig. 7-11(c) Amplitude spectra for the residual (RES-B, RES-C) fields of the geoelectric variations at the Mito group in the range of 3-1000 hours for the period "1" (from October 1, 1985, to October 5, 1986).

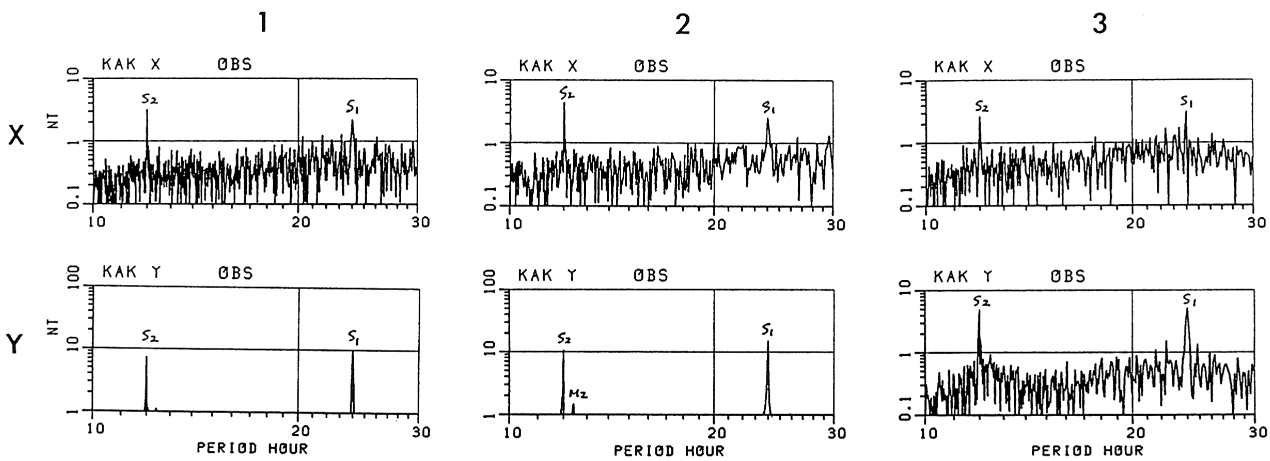

Fig. 7-12(a) Amplitude spectra for the observed (OBS) fields of X and Y at KAK in the range of 10-30 hours for the period "1," "2" and "3."

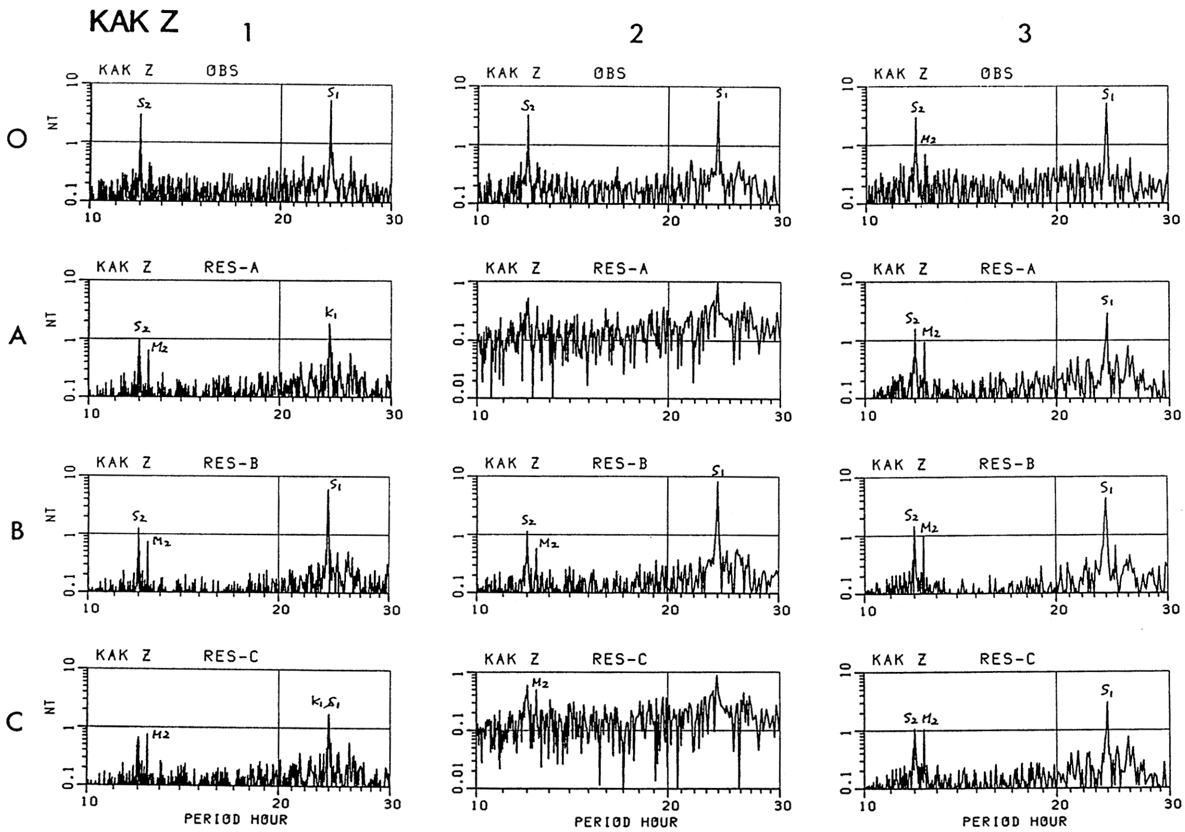

Fig. 7-12(b) Amplitude spectra for the observed “O” and residual “A,” “B” and “C” fields of Z at KAK in the range of 10-30 hours for the period “1,” “2” and “3.”

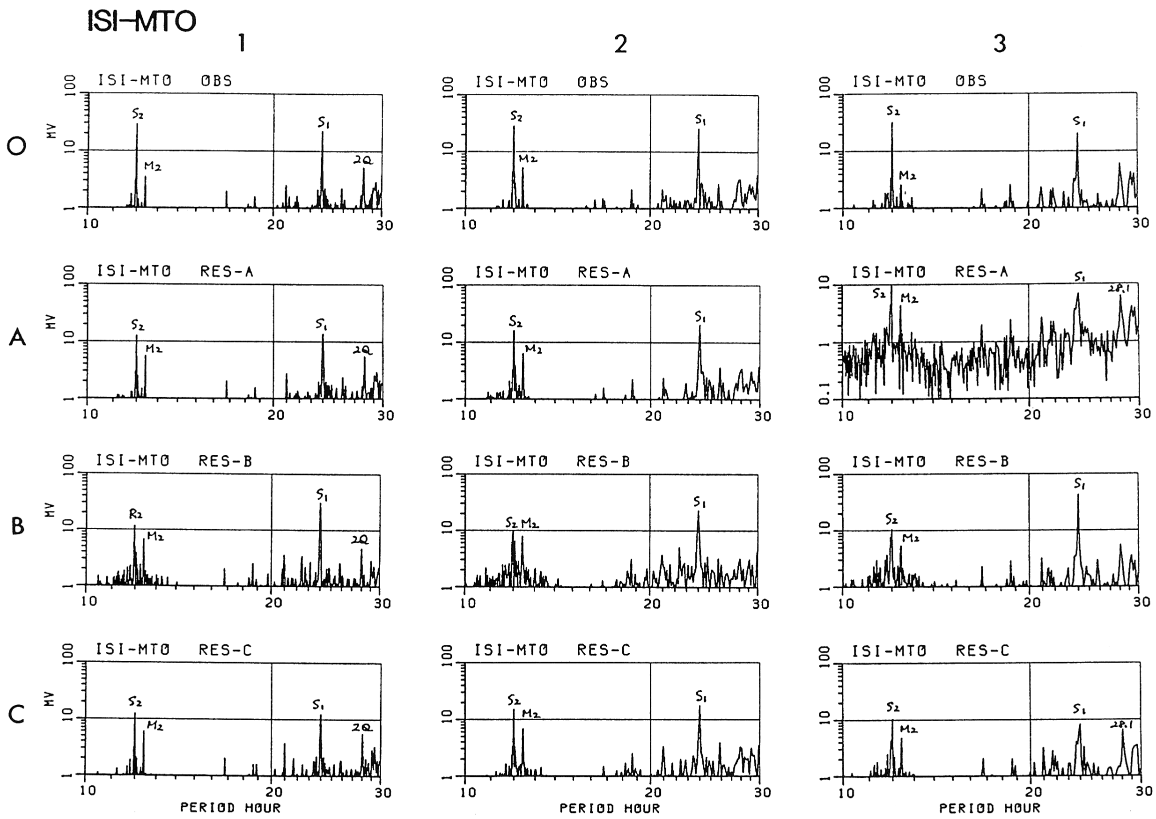

Fig. 7-12(c) Amplitude spectra for the observed “O” and residual “A,” “B” and “C” fields of the geoelectric variations at ISI-MTO in the range of 10-30 hours for the period “1,” “2” and “3.”

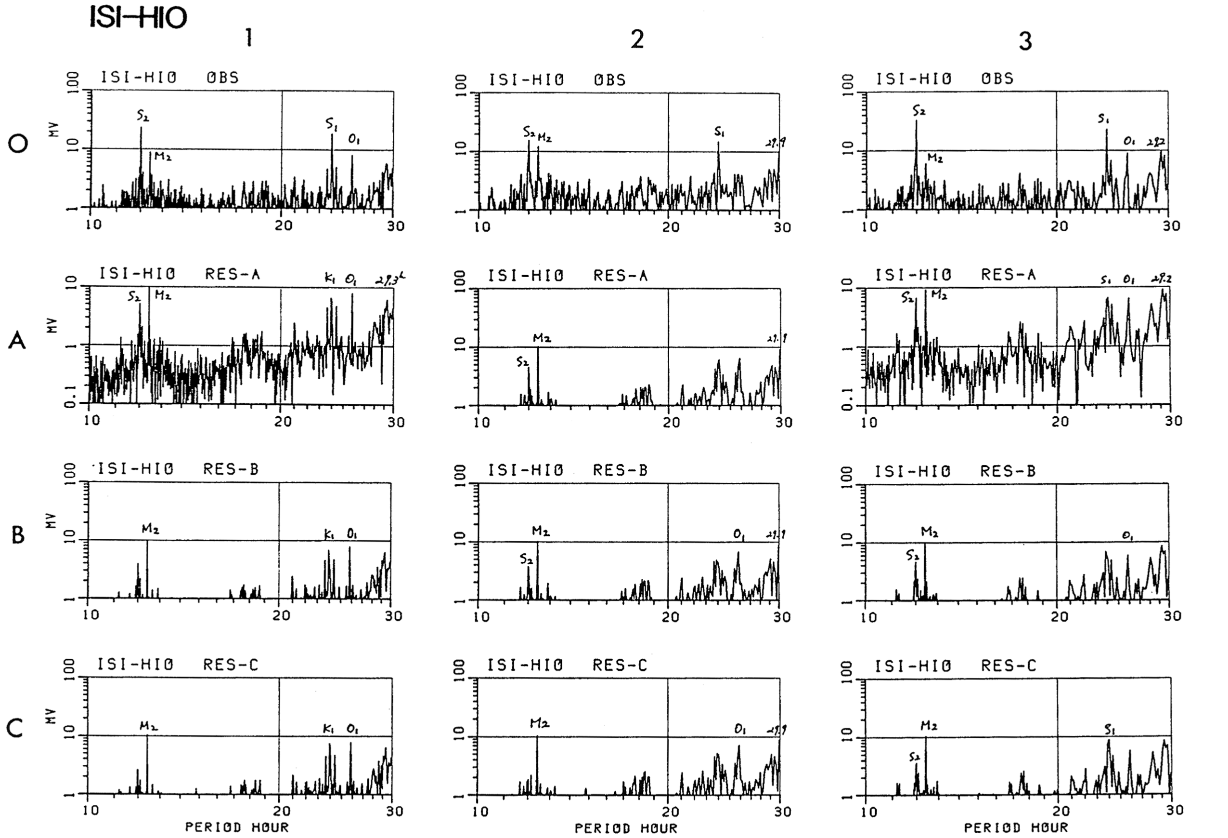

Fig. 7-12(d) Amplitude spectra for the observed "O" and residual "A," "B" and "C" fields of the geoelectric variations at ISI-HIO in the range of 10-30 hours for the period "1," "2" and "3."

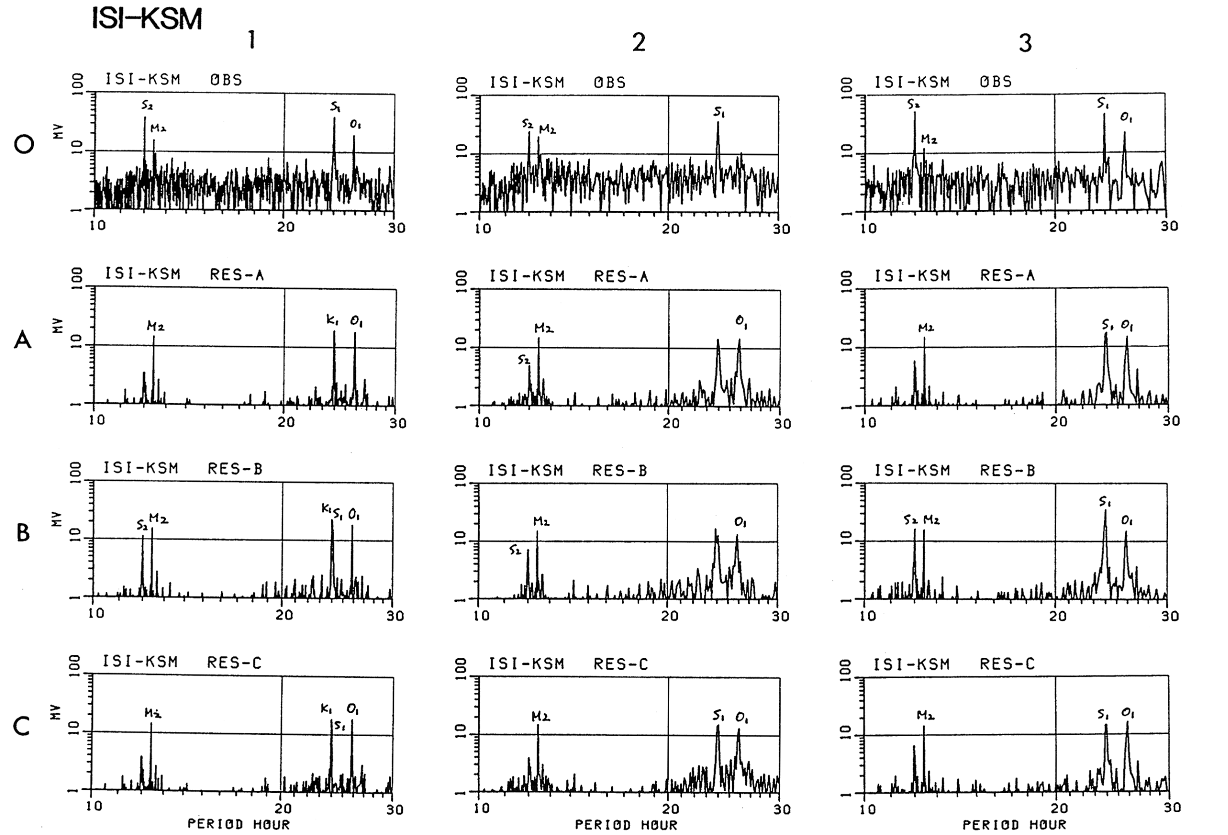

Fig. 7-12(e) Amplitude spectra for the observed "O" and residual "A," "B" and "C" fields of the geoelectric variations at ISI-KSM in the range of 10-30 hours for the period "1," "2" and "3."

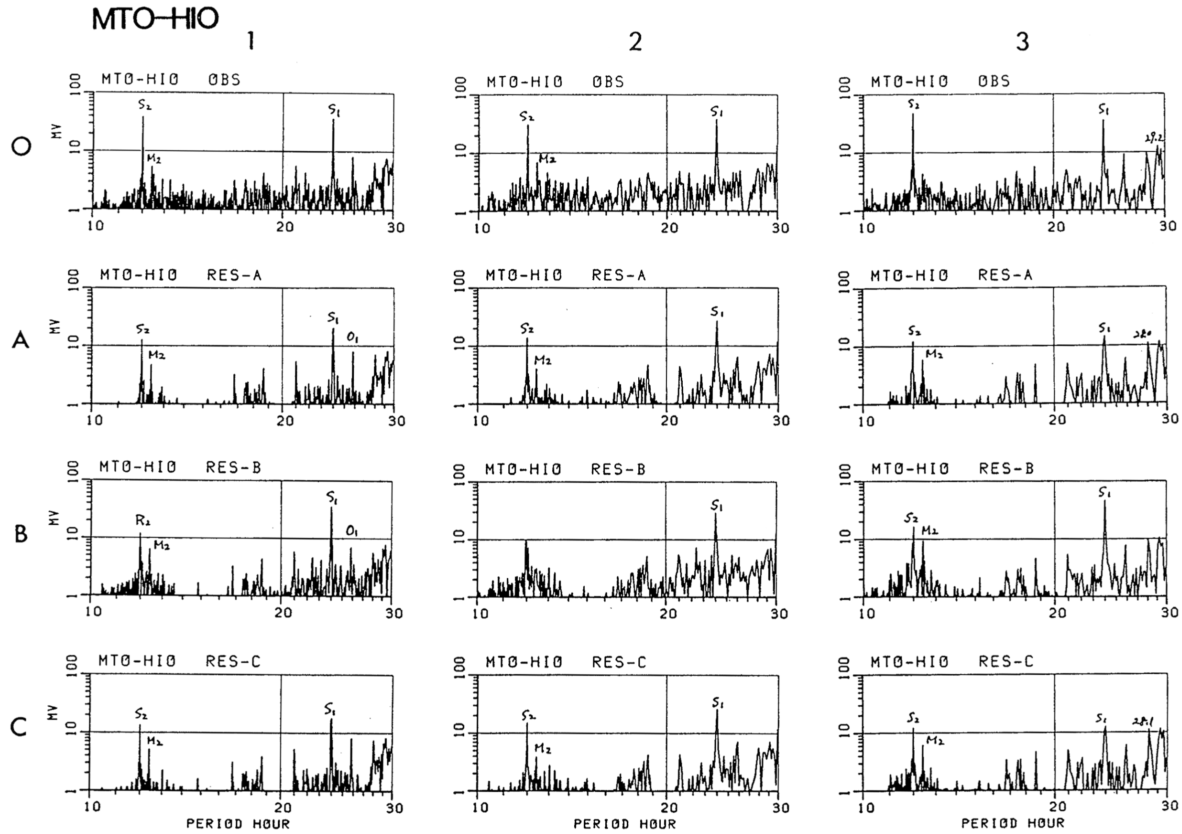

Fig. 7-12(f) Amplitude spectra for the observed "O" and residual "A," "B" and "C" fields of the geoelectric variations at MTO-HIO in the range of 10-30 hours for the period "1," "2" and "3."

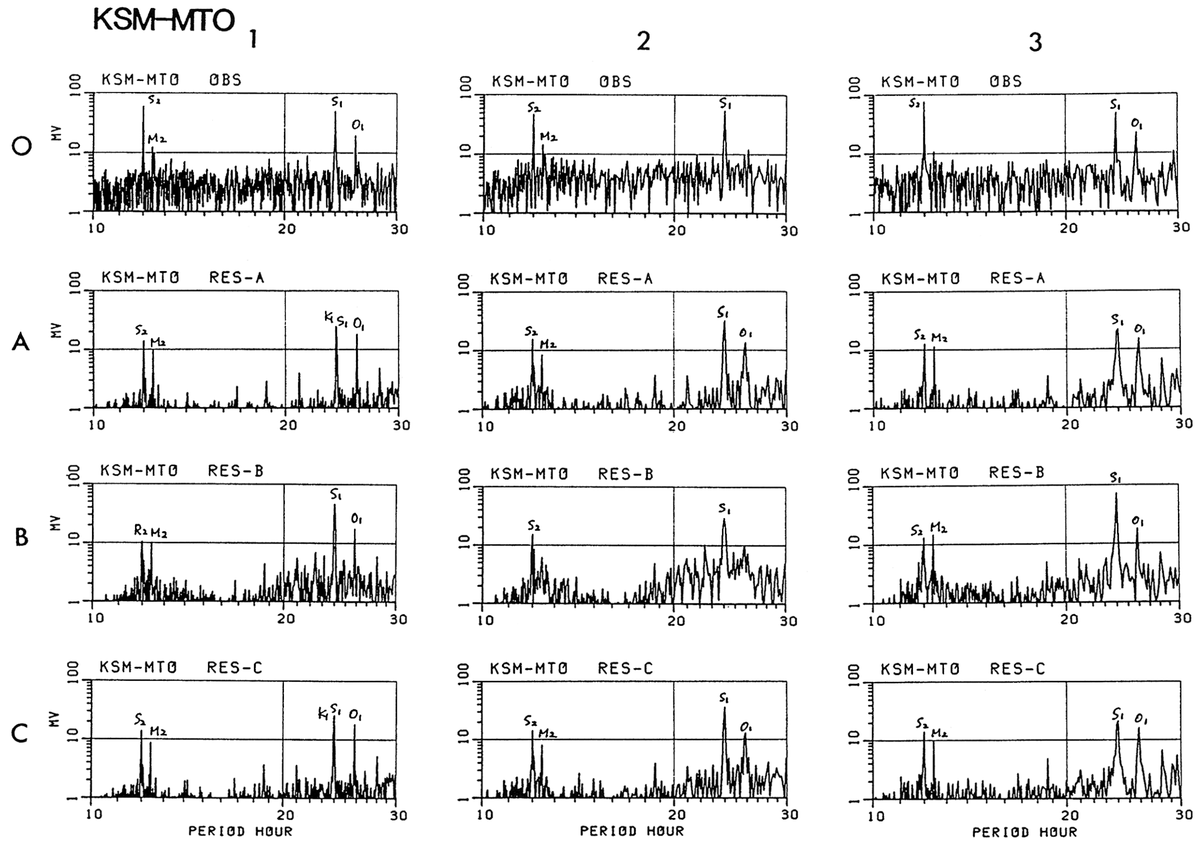

Fig. 7-12(g) Amplitude spectra for the observed "O" and residual "A," "B" and "C" fields of the geoelectric variations at KSM-MTO in the range of 10-30 hours for the period "1," "2" and "3."

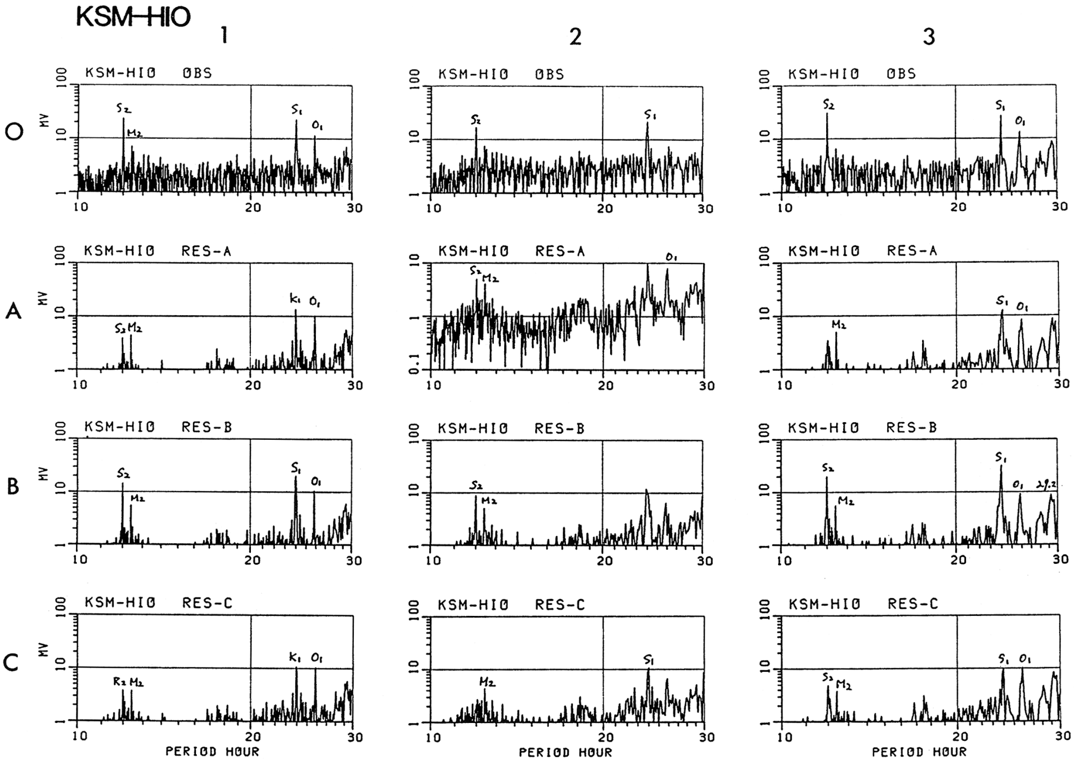

Fig. 7-12(h) Amplitude spectra for the observed "O" and residual "A," "B" and "C" fields of the geoelectric variations at KSM-HIO in the range of 10-30 hours for the period "1," "2" and "3."

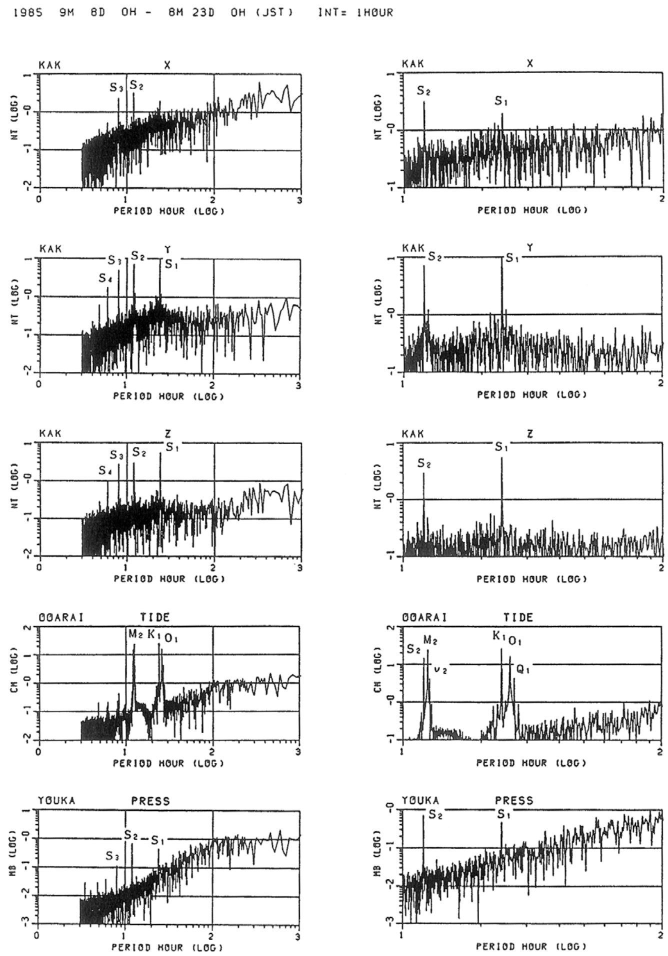

Fig. 7-13 Amplitude spectra of X, Y and Z at KAK, tide at Ooarai (OOARAI TIDE) and atmospheric pressure at Youkaichiba (YOUKA PRESS) using hourly mean values from September 8, 1985, to August 23, 1986.

Fig. 7-14 shows the amplitude spectra of SEF (electrical field on the sea floor off Tokai), PRESS (sea level off Tokai), TIDE (coastal sea level at Omaezaki), H (geomagnetic horizontal component at KAK), Z (geomagnetic vertical component at KAK), D (geomagnetic declination at KAK) and F (geomagnetic total force at KAK) from January 1 to December 31, 1980 (Mori, 1987). The amplitude spectra of the SEF show large peaks for the tidal constituents of O_1, P_1, S_1, K_1, N_2, M_2, S_2, R_2 and K_2.

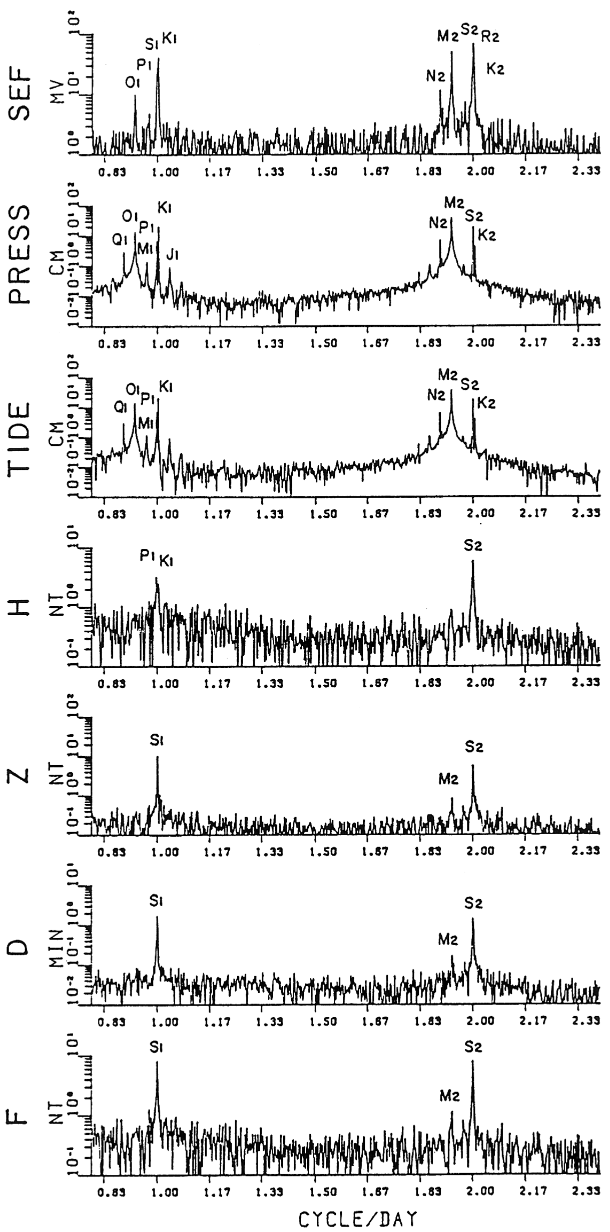

Fig. 7-14 Amplitude spectra of SEF (electrical field on the sea floor off Tokai), PRESS (sea level off Tokai), TIDE (coastal sea level at Omaezaki), H (geomagnetic horizontal component at KAK), Z (geomagnetic vertical component at KAK), D (geomagnetic declination at KAK) and F (geomagnetic total force at KAK) from January 1 to December 31, 1980, after Mori (1987).

Fig. 7-12(a) ~ (h) lead to the following results:

(a) As shown in Fig. 7-12(a), X and Y are dominated by the diurnal and semidiurnal harmonics (S_1 and S_2), and Y has the weak peak of M_2.

(b) As shown in Fig. 7-12(b), S_1, S_2 are conspicuous at the observed field of Z, and M_2 is conspicuous for a while only in period "3." S_1 and S_2 of the residual fields of Z are almost removed in some cases, and not in some cases. The amplitudes of M_2 are almost the same in all of the cases. It cannot be understood that the K_1 constituent that differs slightly from S_1 is conspicuous.

(c) As shown in Fig. 7-12(c), S_1 remains without decreasing at all during the periods in the cases of B at ISI-MTO. In the cases of A and C at period "3," the amplitude of S_1 and S_2 decrease, and the daily variations are almost removed. M_2 is conspicuous in all of the cases, and 2Q (28.1h) are conspicuous during the periods "1" and "3."

(d) As shown in Fig. 7-12(d), S_1, S_2, O_1 and M_2 are conspicuous for "O" at ISI-HIO at the periods "1" and "3." In the residual fields, the diurnal variations such as S_1 and S_2 are fairly well removed. So, O_1 and M_2 which are seldom contained in geomagnetic changes become conspicuous, and also K_1 becomes conspicuous.

(e) The spectra of ISI-KSM (Fig. 7-12(e)) are almost the same as those of ISI-HIO.

(f) For MTO-HIO in Fig. 7-12(f), S_1 and S_2 are not removed in all of the cases.

(g) For KSM-MTO in Fig. 7-12(g), the removal of S_1 and S_2 does not work the same as MTO-HIO.

(h) For KSM-HIO in Fig. 7-12(h), removal of S_1 and S_2 work except in the case of B.

It can be read in the residual electrical fields that the changes correspond to the constituents which geomagnetic changes have removed in many cases. It is one of the subjects that the constituents such as M_2, O_1, Q_1 and 2Q, etc., seen in the residual electrical fields, depend on the earth tide or the ocean tide.

There are large amplitudes of the 3.5-4 days' periodic changes in the observed electrical fields at ISI-MTO and HIO-MTO. These periodic changes are also seen in Fig. 4-1; furthermore at KSM-MTO, 7-10 days' periodic changes are seen. Those excellence cycles are not seen in the geomagnetic fields at KAK, the electrical field on the sea floor off Tokai and the tidal change at Omaezaki (Fig. 7-4(a)). It is also a subject of future research to pursue what these changes mean.

The constituents of S_2, S_1, M_2, O_1, Q_1 and 2Q are calculated using the hourly mean values of geomagnetic horizontal components at KAK and geoelectric fields at the Mito group from 00:00 on March 8 to 17:00 on July 2, 1985. Fig. 7-15 shows the orbits of these constituents. The number of data used for calculation of each constituent is the multiple numbers of the constituent period. That is, the numbers for S_2, S_1, M_2, O_1, Q_1 and 2Q are 2641, 2641, 2485, 2583, 2688 and 2802. The top of the figure shows the orbit of the constituent of the observed geomagnetic variations. From the 2nd step to the bottom of the figure shows the orbits of the constituent of the geoelectric changes in the various three combinations among base lines at the Mito group. OBS in the figure means the observed field, and RES is the residual field using the model A in Section 7-2. The height and width of the cross in the figure show the scale values, ones at S_2 and S_1 are 4nT in the geomagnetic fields, and those at other constituents are 2nT in the geomagnetic fields and 2 mV/km in the geoelectric fields.

The amplitudes and the predominant directions of the electrical field among ISI, MTO and KSM (ISI-MTO-KSM) and among HIO-MTO-KSM bring generally the same results. These predominant directions are almost the same as those in the short period variations of geoelectric fields resulted by Takayama and Mori (1987). It can be read that S_2 and S_1 in the residual field are quite small as compared with those in the observed field.

The predominant direction of geoelectric variations are largely affected by underground conductivity structure, as will be described in Section 11.

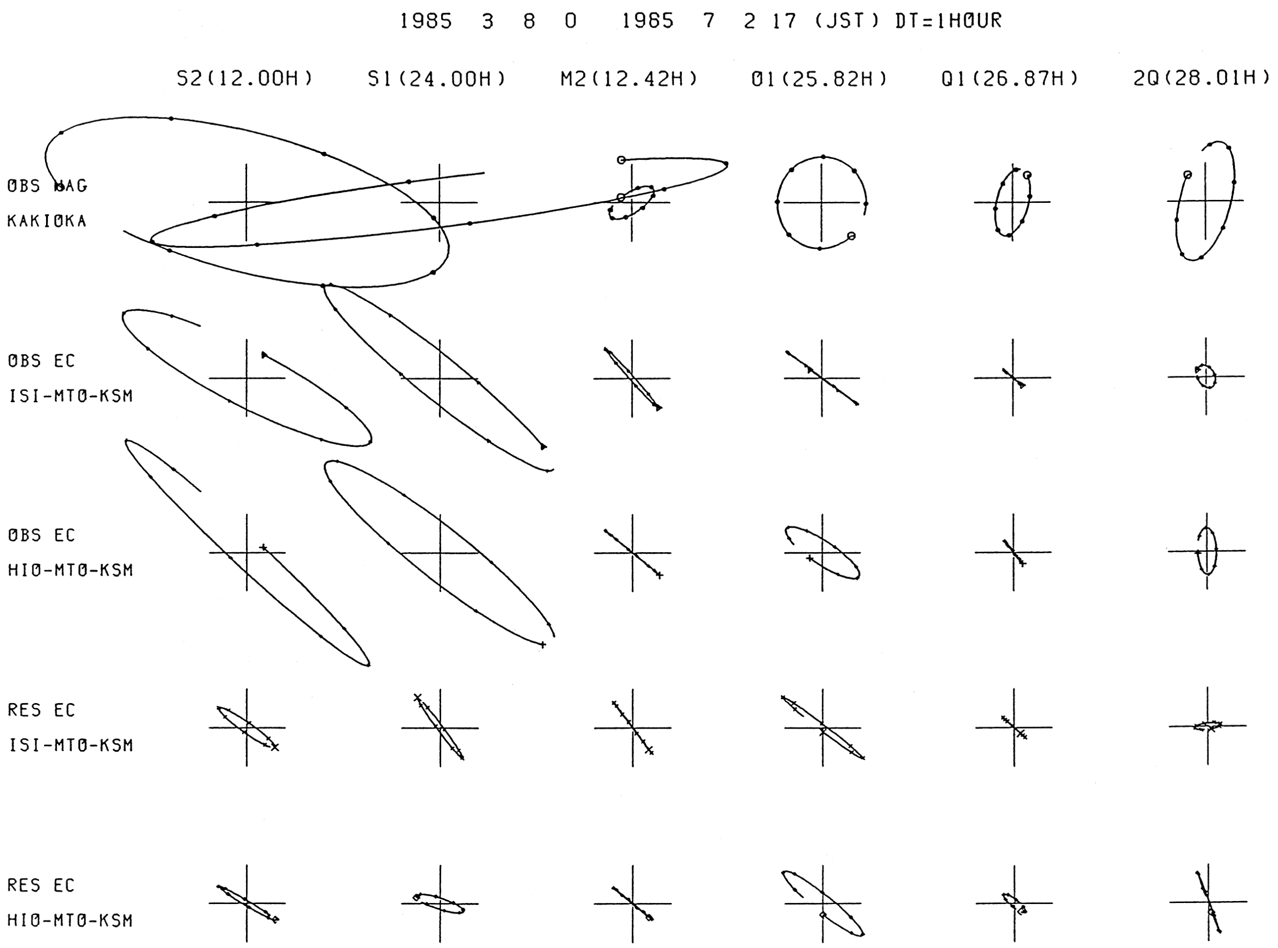

Fig. 7-15 Polar diagrams of S_2, S_1, M_2, O_1, Q_1 and 2Q constituents in geomagnetic fields at KAK and geoelectric fields at the Mito group. The data from 00:00 on March 8 to 17:00 on July 2, 1985, are used.

7-5 When using per-minute data

Unusual electromagnetic phenomenon reported to be the sign of an earthquake are found throughout the cycle and continuation time. Although the analysis used hourly values in Section 7-2 to 7-4, if it is possible to analyze using 1-minute values, the abnormalities of a wide cycle are detectable. Therefore, analyses using values per minute are tried here.

Fig. 7-16 shows geoelectric variations at the Mito group and geomagnetic variations at KAK by average values for 1 minute from 05:00 on February 20 to 07:00 on February 21, 1987. Using these data, AIC values are calculated for KSM-MTO(OBS) = (X, Y) in the range (K, -L) = (20, -15). The distributions of the AIC are shown in the top of Fig. 7-19. However, the value which shows the minimum AIC cannot be found in the range. The cause is considered to be that the geoelectric responses for geomagnetic variations do not become small if the cycle does not become lengthened to 24 hours or more, that is, the response of a long cycle cannot be expressed with a per-minute value. Then, the data are passed through a high-pass filter with the cut-off period of 180 minutes, as shown in Fig. 7-17. Fig. 7-18 shows the geoelectric and geomagnetic variations which let the filter of Fig. 17 pass to the data Fig. 7-16. The filter was designed referring to Ashida and Saito (1970).

The AIC distribution is calculated about the case which lets the filter pass to the observation value at ISI-MTO, and shown in the bottom of Fig. 7-19. Fig. 7-20 shows the response in this case. The minimum value of AIC is set to K = 19, but the value of K+L does not become small.

It may be necessary to shorten the filter cycle to a slight degree. Or, a better result with it may be obtainable to let a filter pass at only one of the two observation values. The reason for that is considered to be that it is better to have lost the coherency between the two fields in a longer period than a certain period. It is also considered that it is better to seek a relationship so that both should be like that and to seek for a coefficient.

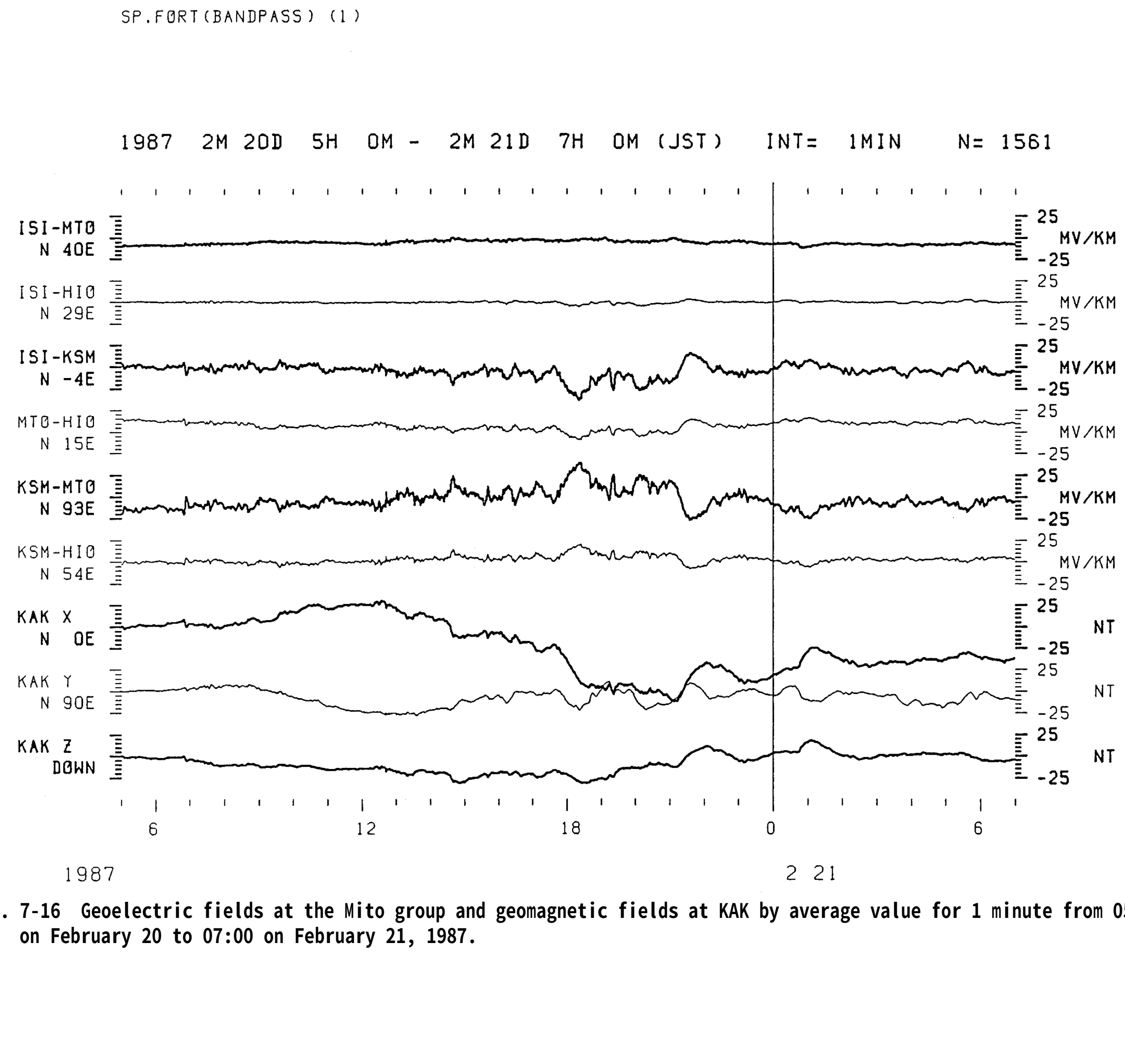

Fig. 7-16 Geoelectric fields at the Mito group and geomagnetic fields at KAK by average value for 1 minute from 05:00 on February 20 to 07:00 on February 21, 1987.

SP.FØRT(BANDCHA)

FILTER.DATA(HP180)
HIGH-PASS FILTER CHEBYSHEF N=5
PERIØD= 60.0 60.0 180.0 300.0

N	0	1	2	3	4	5
A(1,N)	1.0000000000	0.0	0.0	0.0	0.0	0.0
B(1,N)	1.0000000000	0.0	0.0	0.0	0.0	0.0
A(2,N)	0.9644613000	-4.8223065001	9.6446130001	-9.6446130001	4.8223065001	-0.9644613000
B(2,N)	1.0000000000	-4.9276313570	9.7131370520	-9.5735643290	4.7182437601	-0.9301851195

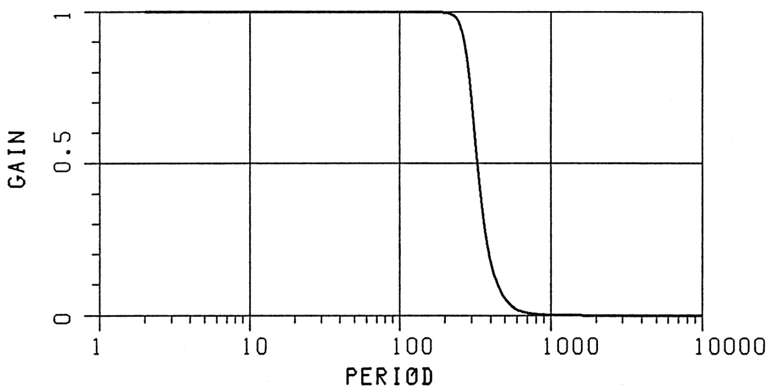

Fig. 7-17 Characteristics of high-pass filter.

SP.FØRT(BANDPASS) (2)

FILTER.DATA(HP180)
HIGH-PASS FILTER CHEBYSHEF N=5
1987 2M 20D 5H 0M - 2M 21D 7H 0M (JST) INT= 1MIN N= 1561

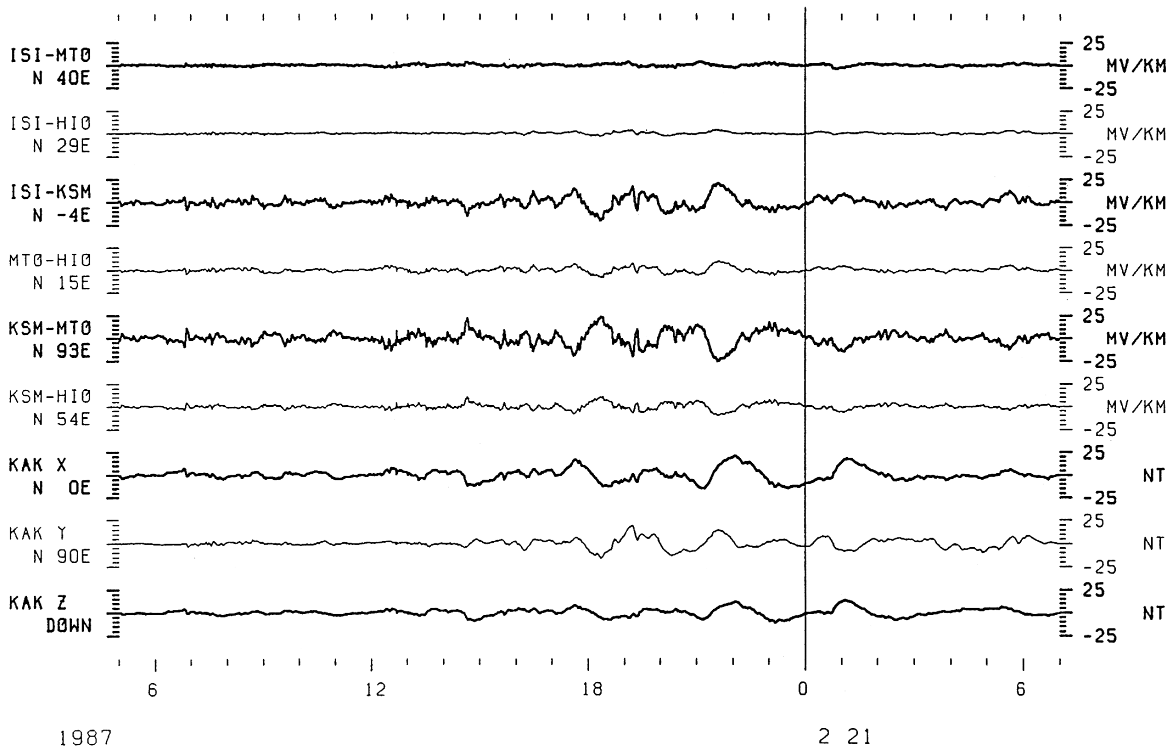

Fig. 7-18 The geoelectric and geomagnetic variations which let the filter pass shown in Fig. 7-17 to the data in Fig. 7-16.

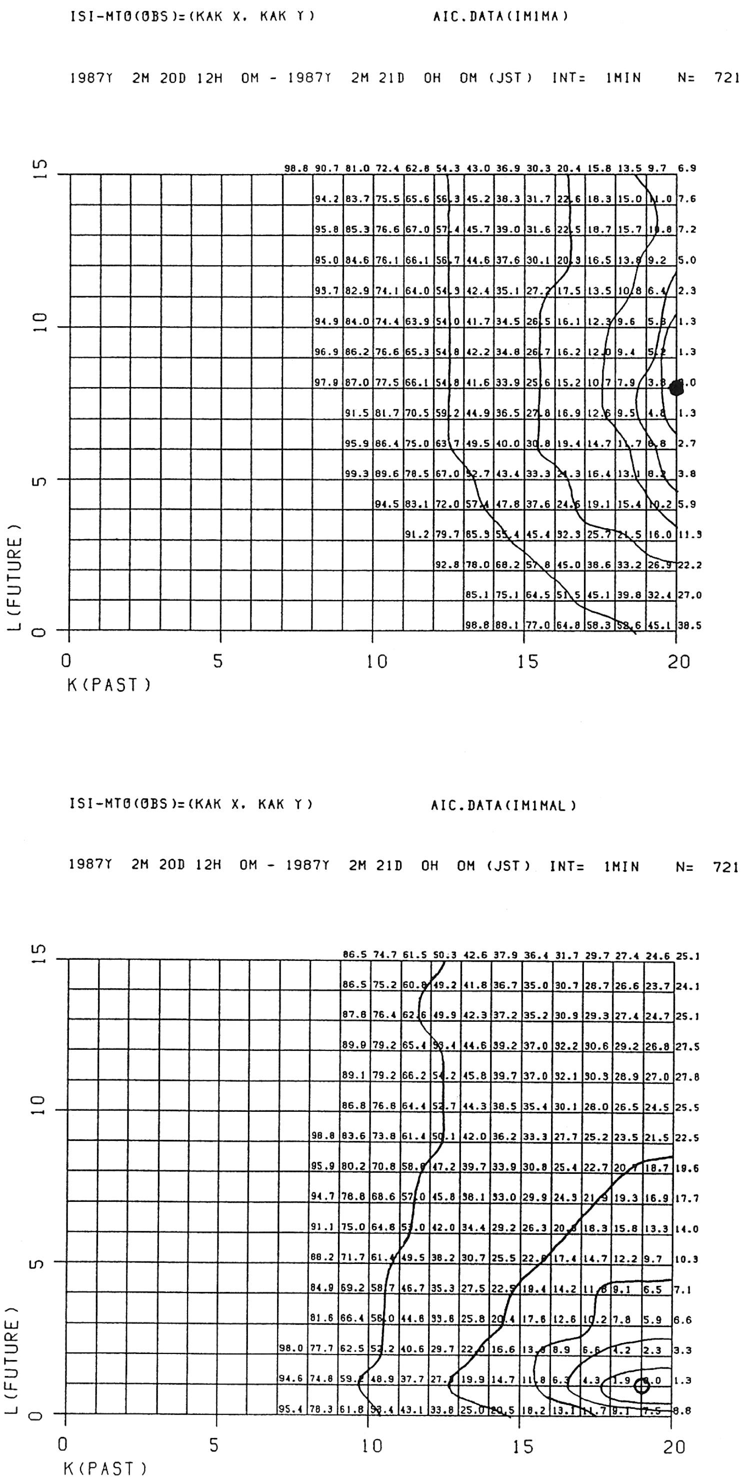

Fig. 7-19 The distribution of AIC by the per-minute value data of ISI-MTO from 05:00 on February 20 to 07:00 on February 21, 1987. The top shows the case which does not let a filter pass, and the bottom the case which lets the filter pass.

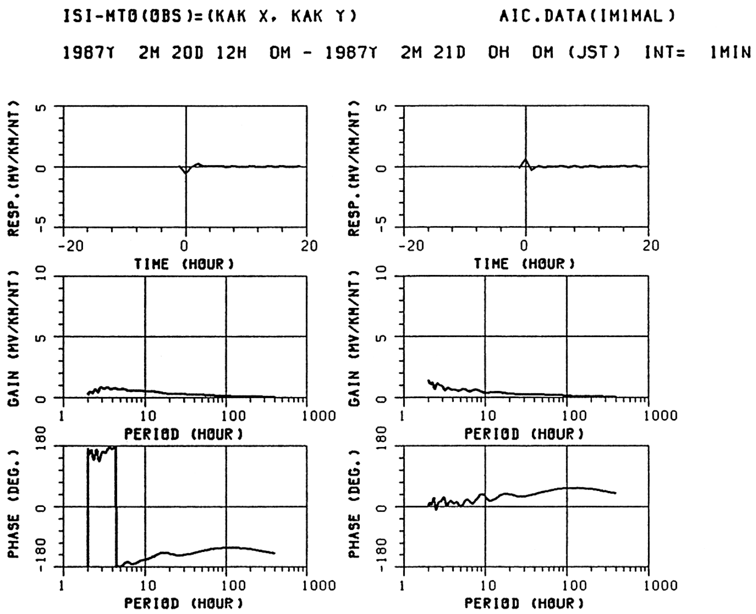

Fig. 7-20 The response function on (K, -L)=(19, -1) in the bottom of Fig. 7-19.

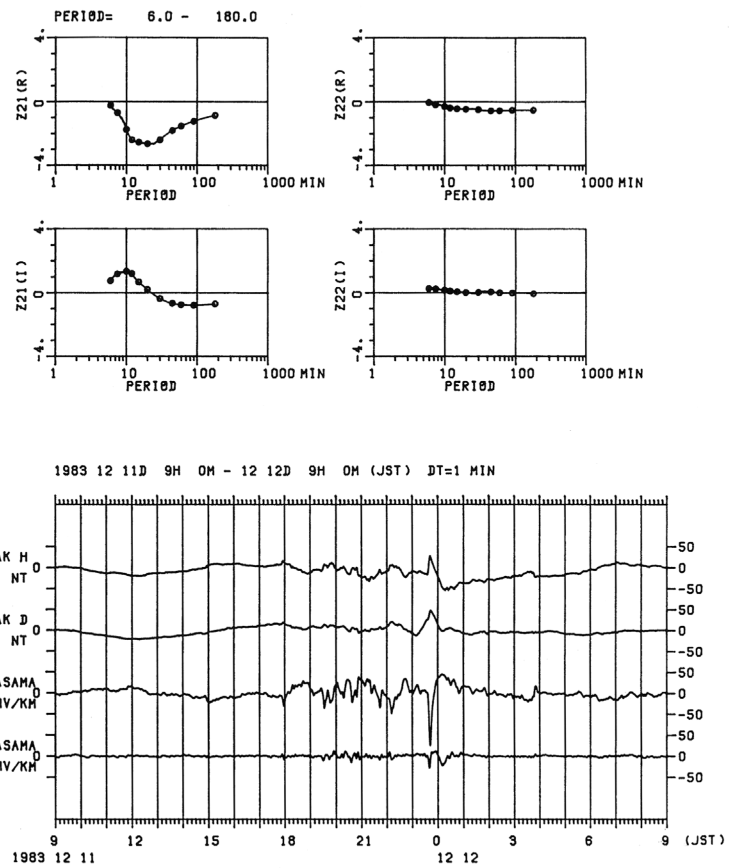

Fig. 7-21 The top shows the impedance tensors at SMO-KSM in the range from 6 to 200 minutes which read and plotted the average curve from Fig. 5-2. In the bottom, the H and D components of the geomagnetic fields at KAK, the observed geoelectric field at SMO-KSM (KASAMA) and the residual geoelectric field which deducted the calculated value from the observed one are expressed sequentially from the top.

7-6 Use of the transfer function and impedance tensor

Methods of removing change induced by geomagnetic variations from observed geoelectric and geomagnetic variations are tried using the impedance tensor and transfer function. It may be difficult to detect an unusual phenomenon in real time in this case.

As an example, the case of geoelectric fields at SMO-KSM (KASAMA) is shown in Fig. 7-21. The impedance tensors which read and plotted the average curve from Fig. 5-2 are shown in the upper part of Fig. 7-21. Fourier transforms of the H and D components of geomagnetic fields at KAK and of geoelectric field at SMO-KSM are carried out, and the impedance tensors read from curves are applied to each cycle, and the results of the induced electrical fields are obtained by Fourier reverse conversion. Here, impedance tensors in the range from 6 to 200 minutes are used. In Fig. 7-21, the 3rd curve expresses the observed geoelectric field, and the 4th curve the residual field which deducted the calculation value from the observation value.

Fig. 7-22 shows the transfer function at KAK and impedance tensors at the Mito group which read and plotted the average curve from Fig. 5-5 and Fig. 5-6(a)-(f). Fig. 7-23 shows the geomagnetic variations at KAK and the geoelectric variations at the Mito group from 00:00 on May 18 to 00:00 on May 23, 1985, which are passed through a low-pass filter of 50 minutes, and the residual fields are shown in Fig. 7-24. Here, the impedance tensors in the range from 20 to 200 minutes are used. It can read that the daily variations except Z are considerably removed from the figure.

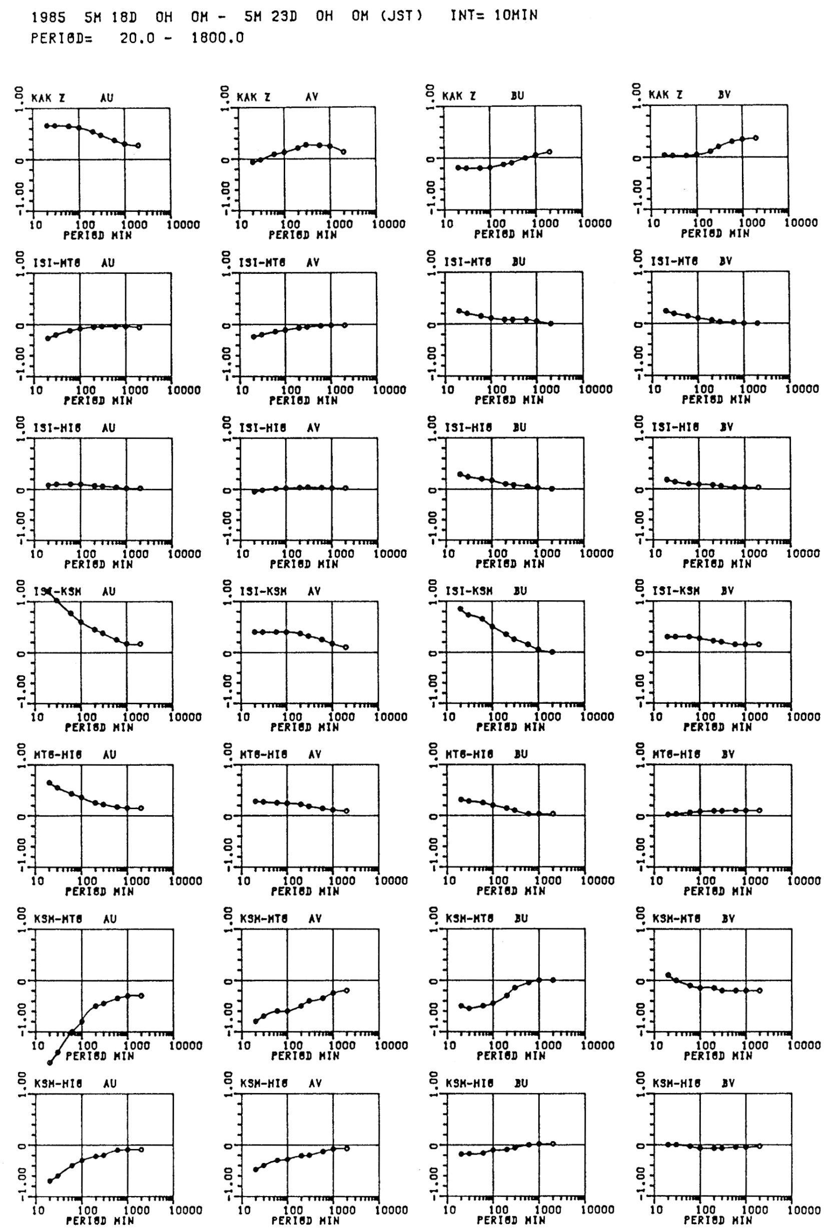

Fig. 7-22 Transfer function at KAK and impedance tensors at the Mito group which are read and plotted the average curves from Fig. 5-5 and Fig. 5-6(a)-(f).

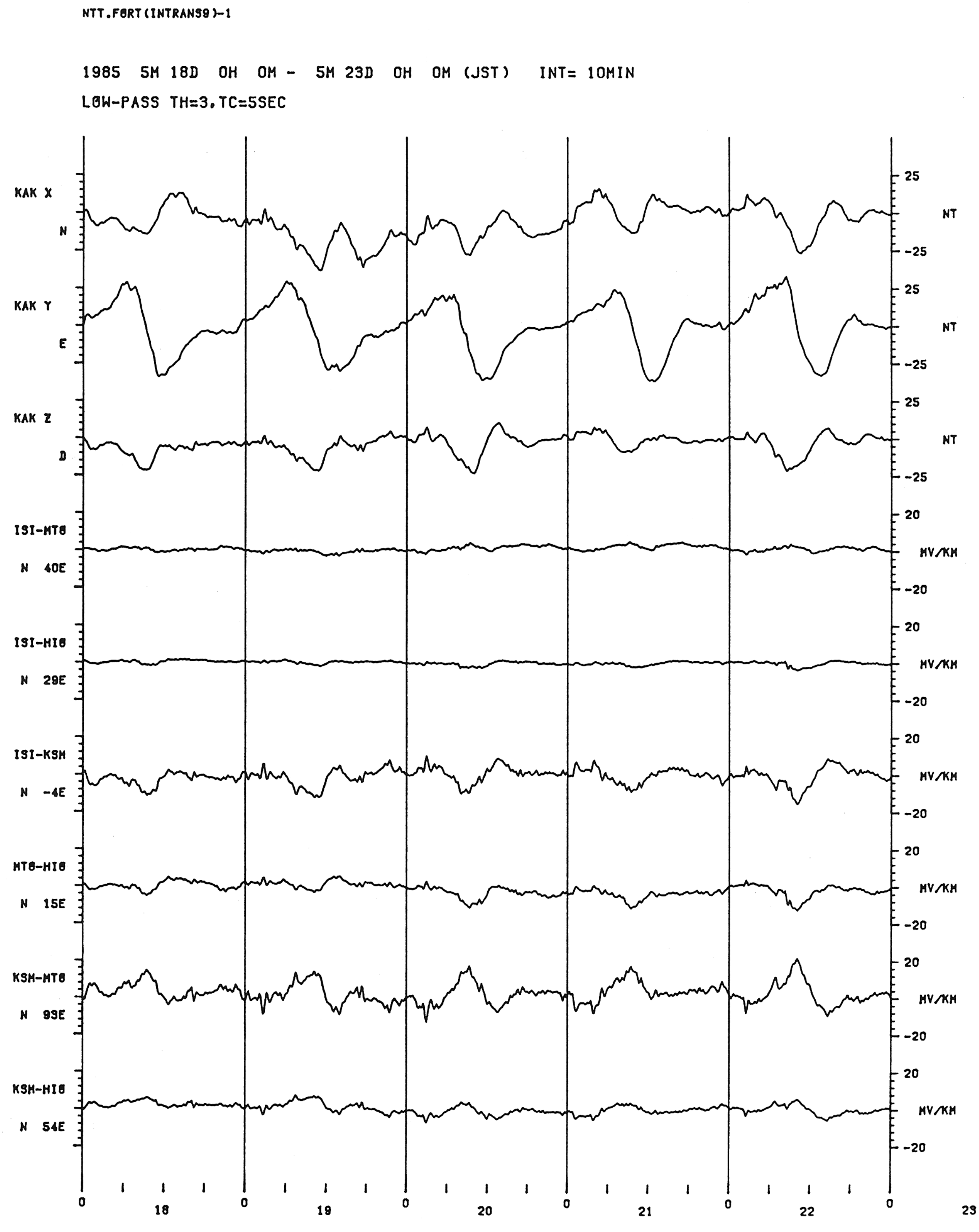

Fig. 7-23 Geomagnetic variations at KAK and geoelectric variations at the Mito group which are passed through a low-pass filter of 50 minutes to the 10-minute data from 00:00 on May 18 to 00:00 on May 23, 1985.

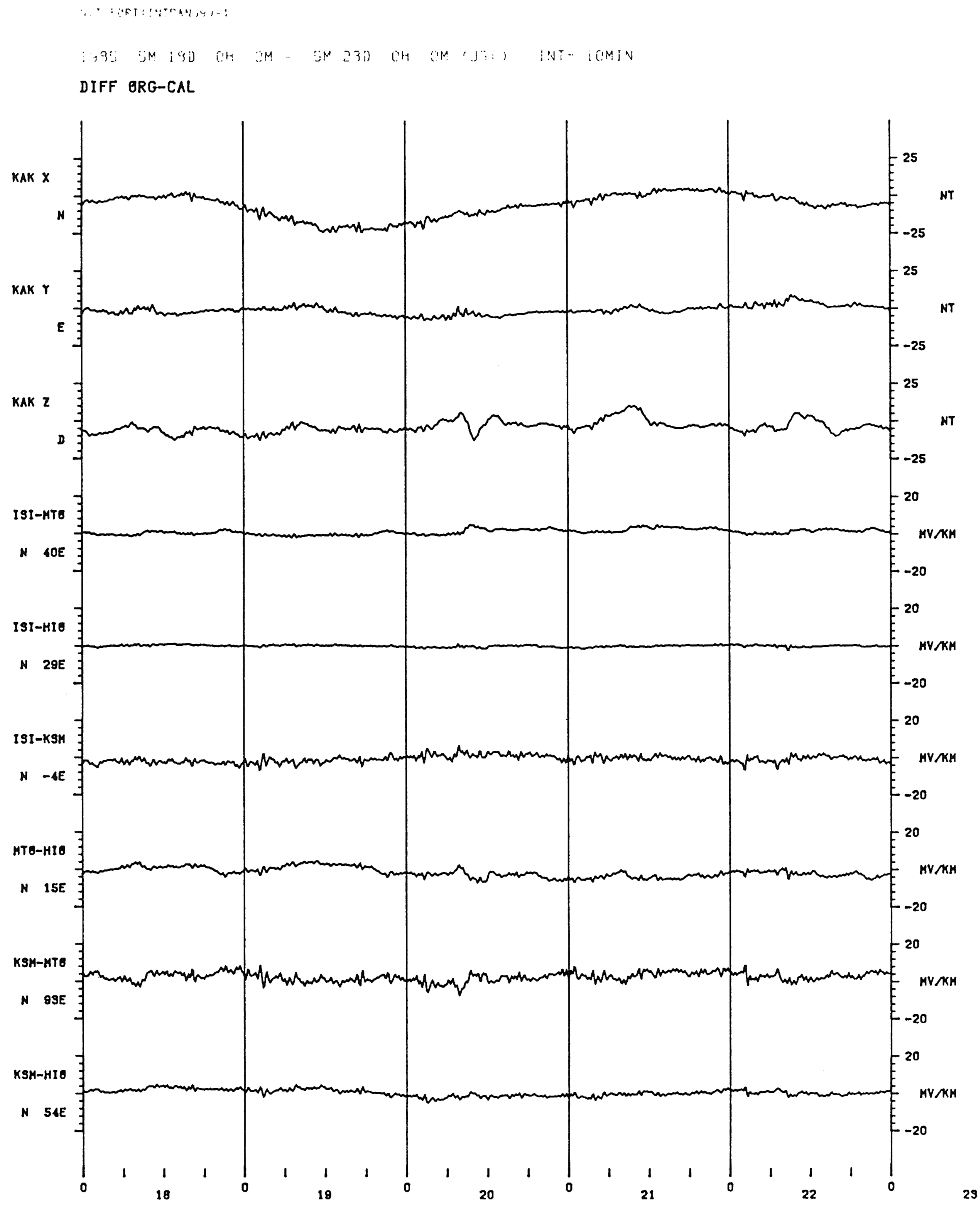

Fig. 7-24 The residual Z at KAK and the electrical fields at the Mito group which removed induced change from the variations of Fig. 7-23, here, the transfer function and the impedance tensors in the range from 20 to 200 minutes are used. The two curves of the upper part of the figure show the geomagnetic X and Y variations, which removed the change of the cycle of 20 to 2000 minutes.

8. Relation to tectonic activities

One of the great characteristics of the geoelectric observations using NTT facilities is long time stability as described in Section 4. Daily means of geoelectric and geomagnetic variations from March 1985 to July 1987 are shown in Fig. 8-1. Vertical and horizontal bars with Arabic numbers indicate the times when the main earthquakes and earthquake swarms took place near the observation networks. Their locations and lists are shown in Fig. 8-2. The horizontal bar in November 1986 indicates the volcanic eruption of the Izu-Oshima volcano. Some anomalous changes in the geoelectric fields at the Numazu group which appear to relate to tectonic activities were recognized, while there is no anomalous change in the Mito group.

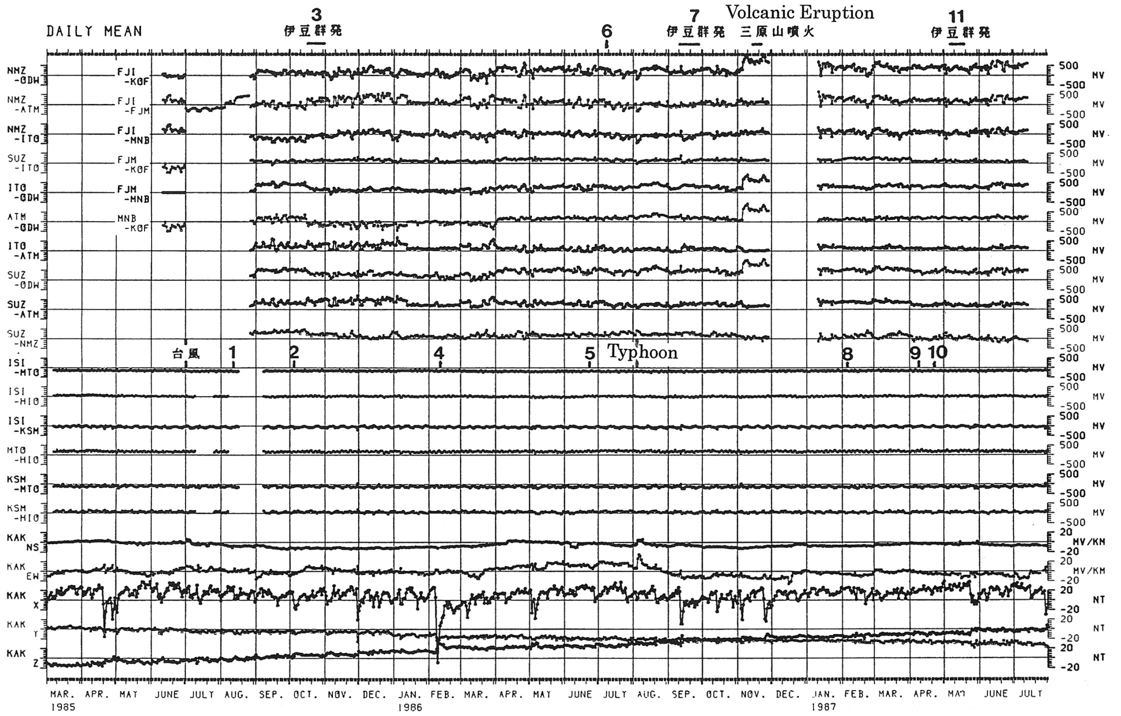

Fig. 8-1 Daily values of geoelectric and geomagnetic variations from March, 1985, to July, 1987. Vertical and horizontal bars with Arabic numerals indicate the times when main earthquakes and earthquake swarms took place near the observation networks, respectively. The locations and the lists of earthquakes and earthquake swarms are shown in Fig. 8-2. The horizontal bar on November, 1986, indicates the period of volcanic eruption of the Izu-Oshima volcano.

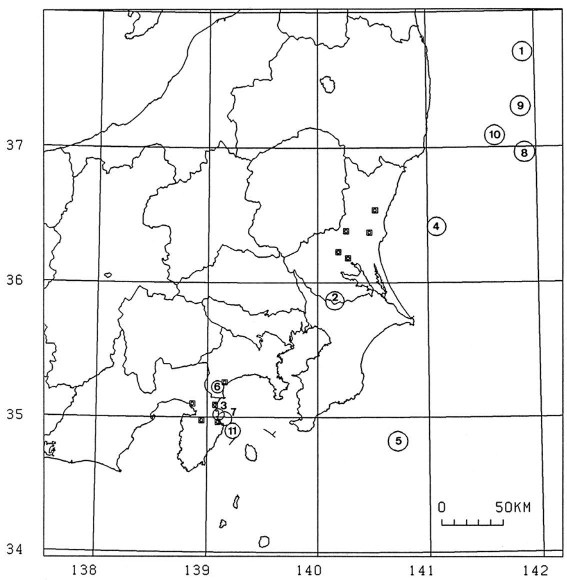

Fig. 8-2 List of earthquakes and earthquake swarms near the observation networks. The number 3, 7 and 11 are earthquake swarms.

No.	Date	Magnitude	Depth (km)
1	1985/8/12	6.4	52
2	1985/10/4	6.1	78
3	1985/10/13 ~ 11/10		
4	1986/2/12	6.1	44
5	1986/6/24	6.5	73
6	1986/7/9	4.1	15
7	1986/10/10 ~ 10/29		
8	1987/2/6	6.7	35
9	1987/4/7	6.6	44
10	1987/4/23	6.5	47
11	1987/5/6 ~ 6/4		

8-1 Relation to the earthquake swarms off the east coast of the Izu Peninsula

An earthquake swarm, which is indicated by number 3 in Fig. 8-1 and Fig. 8-2, occurred off the east coast of the Izu Peninsula from October 13 to November 10, 1985. The largest earthquake with magnitude of 3.8 occurred on October 29. As shown in Fig. 8-1, the electrical field at ATM-ODW decreased around October 15, 1985, for example. It is estimated that the geoelectric potentials at ATM, ITO and SUZ decreased by 300, 100 and 100 mV in the middle of October, respectively. As shown in Fig. 8-3, the volume strain meter at Higashi-Izu (HIGASHI), which distant is 15 km southward from Ito, shows a gradual compression during the same period. Changes of the volume strain meters seen in June to July in Fig. 8-3 are the influence of rain. The geoelectric potential and the volume strain are independent of each other, and only the geoelectric potential of these NTT observation stations near the epicenters and the volume strain meter at Higashi-Izu began to change just at the beginning of the earthquake swarm. If we presume from these facts, the anomalous changes in geoelectric potential seem to relate to the earthquake swarm. Fig. 8-4 shows hourly values of geoelectric and geomagnetic variations around October 1985. Only the geoelectric field at ATM-ODW in Fig. 8-4 shows a clear change, but others are not so clear. Also, it is not considered that patterns of the daily variations are changed.

In the past ten years, earthquake swarms have repeatedly occurred off the east coast of the Izu Peninsula, and earthquake swarms occurred in October 1986 and in May 1987 (Japan Meteorological Agency, 1987). When the earthquake swarms which are indicated by number 7 and 11 in Fig. 8-1 and Fig. 8-2 occurred, the volume strain meter at Higashi-Izu showed gradual compressions at the same time, but there were no anomalous changes in the geoelectric variations at either time. This is possibly due to the fact that the magnitude of the earthquake swarm was smaller and that the location was somewhat different from the previous swarm.

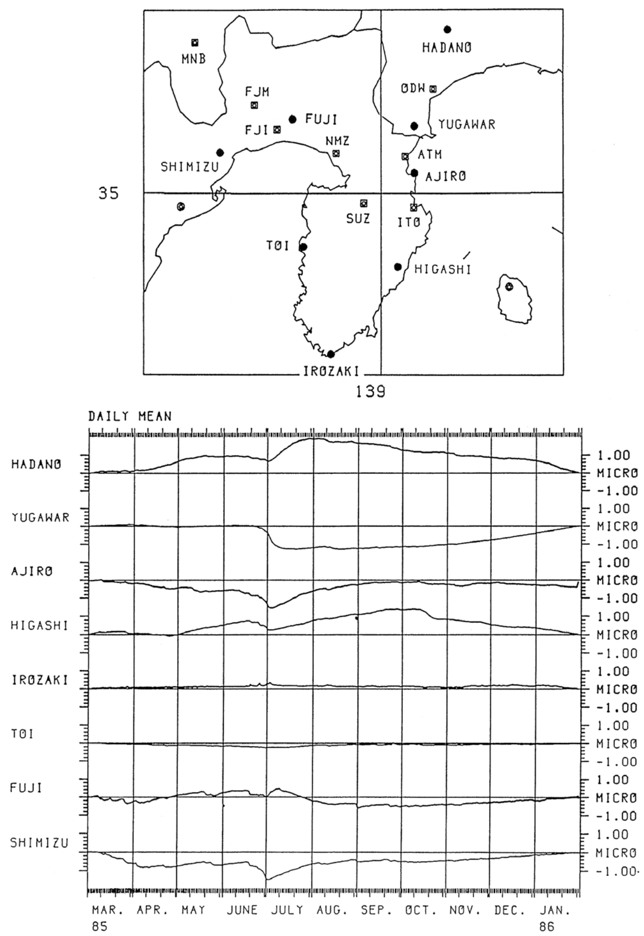

Fig. 8-3 Top: Volume strain meter (●) by JMA and geoelectric observation stations (□) of NTT. Bottom: Variations of volume strain meters during March, 1985, to January, 1986.

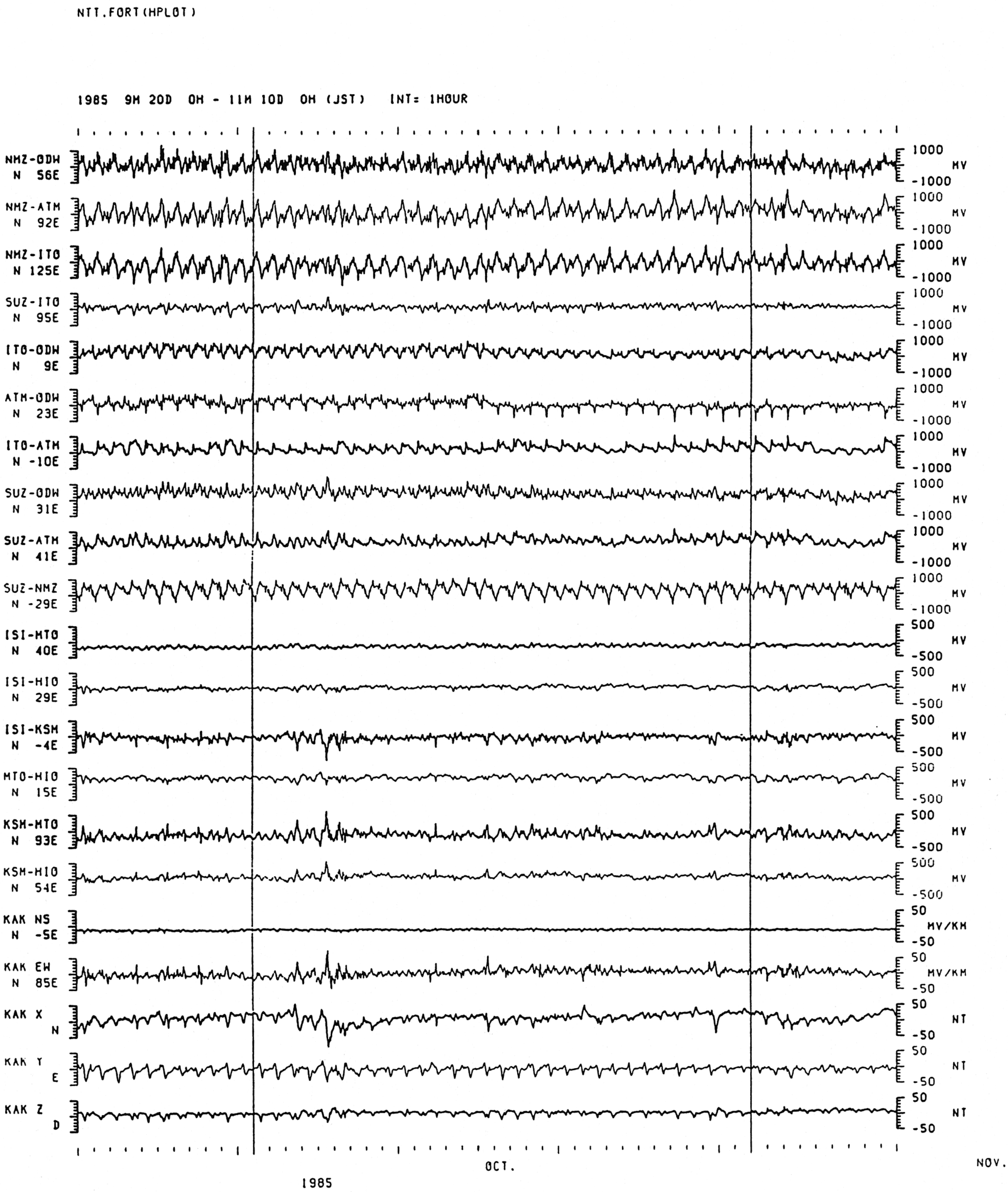

Fig. 8-4 Electrical variations in hourly mean values at NTT stations and electrical and magnetic variations at Kakioka around October 1985.

8-2 Relation to eruptions of Izu-Oshima volcano

The Izu-Oshima volcano violently erupted on November 15, 1986. There are abnormal changes in the electrical variations at NMZ-ODW, ITO-ODW, ATM-ODW, and SUZ-ODW at the beginning of October 1986 in Fig. 8-1. Fig. 8-5 shows the geoelectric variations at the Numazu group from September to November, 1986, as an elongated part of Fig. 8-1. The electrical potential at ODW began to decrease on November 6, and reached the minimum value of -800 mV around November 9. At other points of the Numazu group, however, the electrical potential at ATM could be seen to increase a little bit, but not so clearly. Since the geoelectric data of the Numazu group from November 29, 1986, to January 10, 1987, are missing because of trouble with the recording system, it is not clear how the geoelectric potentials at ODW recovered. Although the power supply was shut off in order to move the position of the recorder in NTT Numazu station late in December, since it reset when a wall socket was put in, it is thought that it began to write double records.

Hourly mean values of the electrical fields at the Numazu group are shown in Fig. 8-6 in October and November, 1986. The amplitudes of the daily variations are large, and these seem to be due almost completely to artificial noises. The patterns of the daily variations and the mean value of the electrical potential at ODW had been changed since November 6 00:00 or November 5 22:00, 1986. Abnormal changes on November 4 are electrical changes induced by a geomagnetic storm that occurred with ssc (sudden storm commencement) at 08:54 on November 4.

ODW is located at the extension of the Suruga Trough, and on the boundary of the Eurasia Plate and the Philippine Sea Plate. The flow of underground water, which is caused by a change of stress acting on the boundary, may possibly cause changes in the streaming potential and/or electrical conductivity. However, there is a possibility of a fortuitous change in the geoelectric potential at ODW.

The electrical potential at ODW relative to NMZ input in the fourth channel of the digital recorder as described in Section 2. It cannot be somehow that the circuit of only the fourth channels breaks down on the 1 time target, but there is a very little possibility, judging from order of the records.

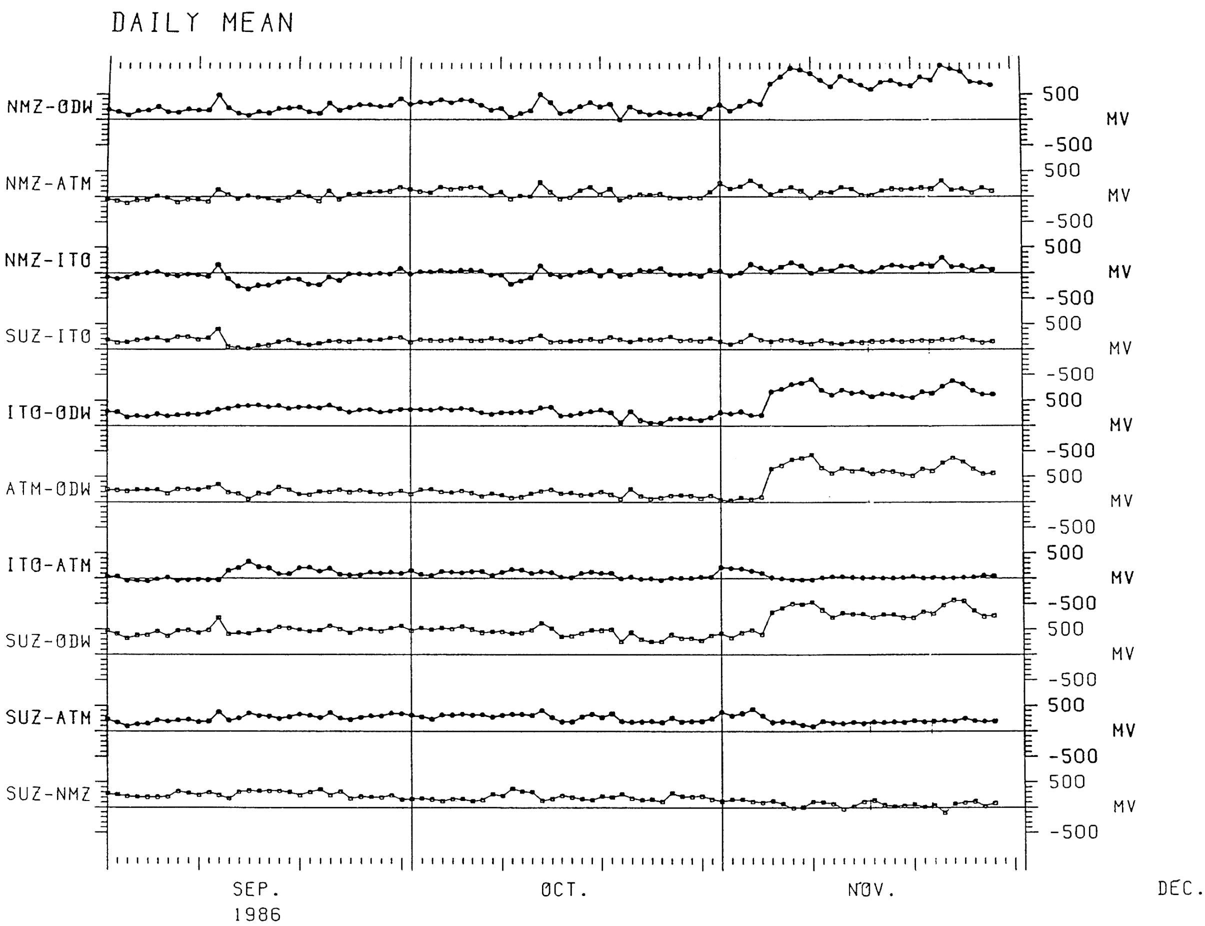

Fig. 8-5 Electrical variations in daily means at the Numazu group from September to November, 1986.

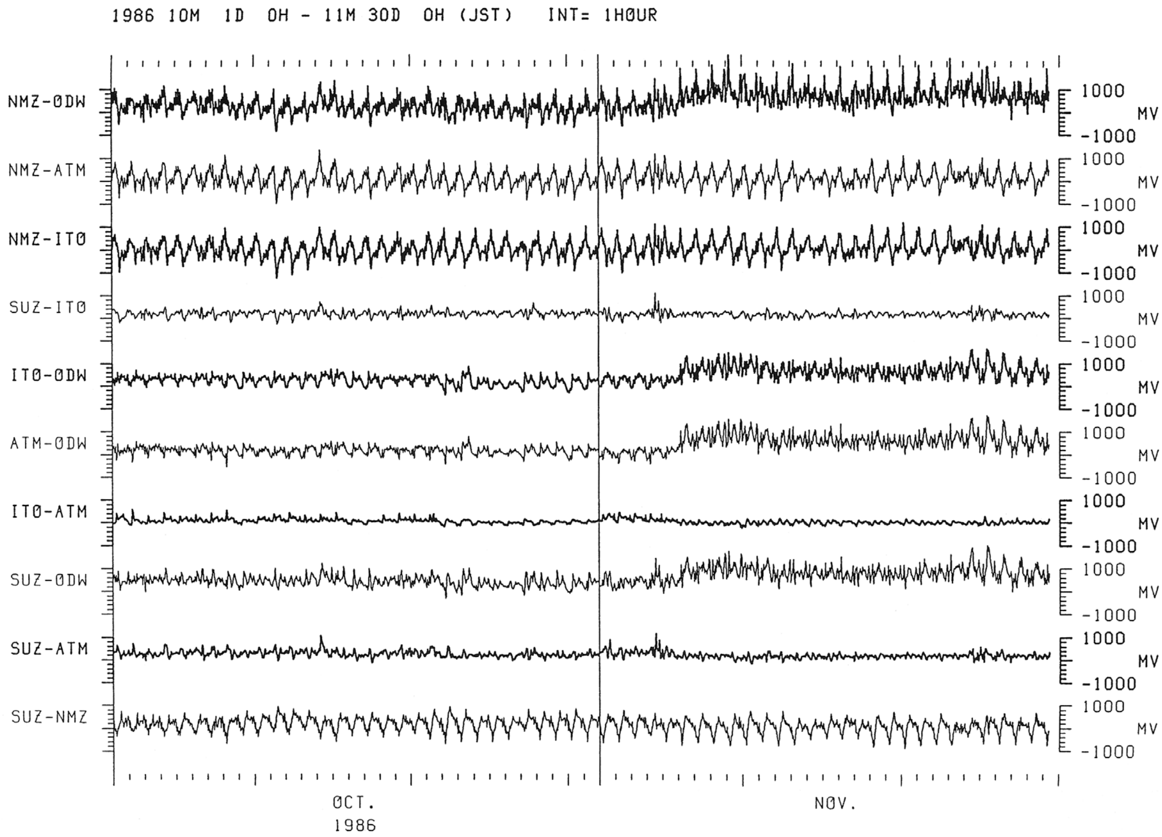

Fig. 8-6 Electrical variations in hourly means at the Numazu group during October to November, 1986.

8-3 Other changes

(1) Fujinomiya group

The electrical field at FJI-FJM (second line from the top of Fig. 4-1 and Fig. 8-1) became low from early in July to the middle of August. The NTT underground cable from FJM to KOF via MNB was inundated by heavy rain by the typhoon on June 30, 1985; after that observations were stopped. Continuous observation in the electrical resistivity of the Fujikawa fault showed the decreasing of the underground electrical resistivity generally at the same time (Earthquake Research Institute, University of Tokyo, 1987). So the decreasing of the electrical field at FJI-FJM may be reflecting the changes of the underground electrical conditions in a wide area.

(2) Numazu group

There is a bay-shaped change of -500 mV in the electrical potential graph at NMZ from the end of December 1985 to the beginning of January 1986 in Fig. 4-1 and Fig. 8-1. Also, there is the change of a volume strain meter at Fuji near NMZ during almost the same period in Fig. 8-3. Although the similar changes of the volume strain meter at Fuji changed several times in the past, it seems that the changes of electrical field and volume strain meter overlapped by chance.

The electrical fields at the Numazu group appear considerably changeable during March, 1986, and these seem to relate to oceanic tide. This will be described in the next chapter.

9. Relation to tide, atmospheric pressure and others

As mentioned in the introduction, it is considered that geoelectric variations are relative to various phenomena such as geomagnetic variations, motion of the sea water, earth tide, conditions of the earth's interior, atmospheric condition and so on.

Fig. 9-1 gives the daily mean values of the electrical field on the sea floor off Tokai (SEF), sea level by tsunami-meter off Tokai, coastal sea levels, atmospheric pressures and temperatures. The long time variations of SEF are affected by the pass of Kuroshio, which is a strong ocean current off the southwestern coast of Japan. The pass is highly changeable off Tokai district, and also relative to geomagnetic field changes at the Tokai area (Mori, 1987).

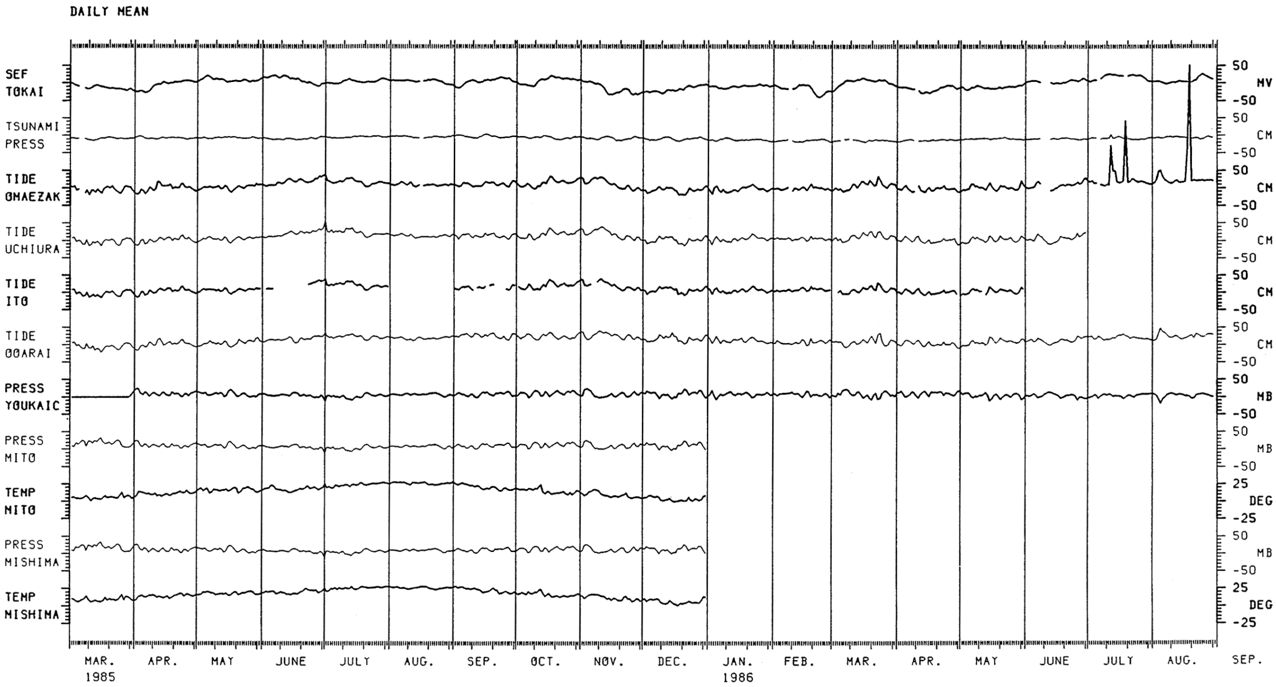

Fig. 9-1 Daily mean values of the electrical field on the sea floor off Tokai, sea levels, atmospheric pressures and temperatures during March, 1985, to August, 1986. From top to bottom, electrical field on the sea floor off Tokai (SEF : TOKAI), sea level by tsunami-meter off Tokai (TSUNAMI : PRESS), coastal sea level at Omaezaki (TIDE : OMAEZAKI), coastal sea level at Uchiura (TIDE : UCHIURA), coastal sea level at Ito (TIDE : ITO), coastal sea level at Ooarai (TIDE : OOARAI), atmospheric pressure at Youkaichiba (PRESS : YOUKAIC), atmospheric pressure at Mito (PRESS : MITO), temperature at Mito (TEMP : MITO), atmospheric pressure at Mishima (PERSS : MISHIMA) and temperature at Mishima (TEMP : MISHIMA).

As seen in Fig. 8-1 and Fig. 9-1, there are remarkable long period changes of the geoelectric fields at the Numazu group and sea levels and also atmospheric pressures around March 1986. In this section, coherencies between these various data are studied.

Fig. 9-2 ~ 9-4 show the coherencies, which are the ratio of the correlated power to total power, between various pairs. The coherency between components and the data periods are shown in the upper part of each figure, as for example, “KAK X : KSM-MTO(OBS)” and “1985 4M 1D 0H.” Coherencies are calculated for the first-stage trial, and deep consideration has not been carried out. What we can say at present is in the following memorandums.

(1) Coherency of KSM-MTO for X is high with a cycle shorter than 3 or 4 days ((a) of Fig. 9-2), and one for Y is high with a cycle shorter than one day ((b) of Fig. 9-2). It may be depend on how small the amplitude is of variations of Y with a cycle longer than one day. Coherencies for X are low at the period of O_1 (25.82h) and M_2 (12.42h) constituents. The cause is that the induced electrical fields by geomagnetic variations have small powers at the period of O_1 and M_2.

(2) Coherency of sea level (TIDE) for atmospheric pressure (PRESS) is very high with a cycle longer than 3 and /or 4 days ((c) of Fig. 9-3).

(3) The coherency of KSM-MTO for TIDE at Ooarai is high at the cycle of M_2 and around 24.5h ((c) of Fig. 9-2). The cycle of 24.5h may be the mean of the K_1(23.93h) and O_1(25.82h) constituents.

(4) The coherency of KSM-MTO for PRESS at Youkaichiba is small, and there is no particular correlation with the long cycle ((d) of Fig. 9-2). It is said that the periodic variations of 3 to 10 days in the geoelectric fields at the Mito group have no relation to the atmospheric pressure and ocean tide.

(5) The coherency of SUZ-ITO for TIDE at Ooarai is also high with the cycle of 5.5 days ((b) of Fig. 9-3).

(6) The coherency of ODW-NMZ for TIDE at Uchiura is high with a long cycle ((b) of Fig. 9-4). Both the electrical potential at the Numazu group of Fig. 8-1 and the tidal level of Fig. 9-1 were changed sharply in March, 1986. It is thought that the coherency is reflecting this.

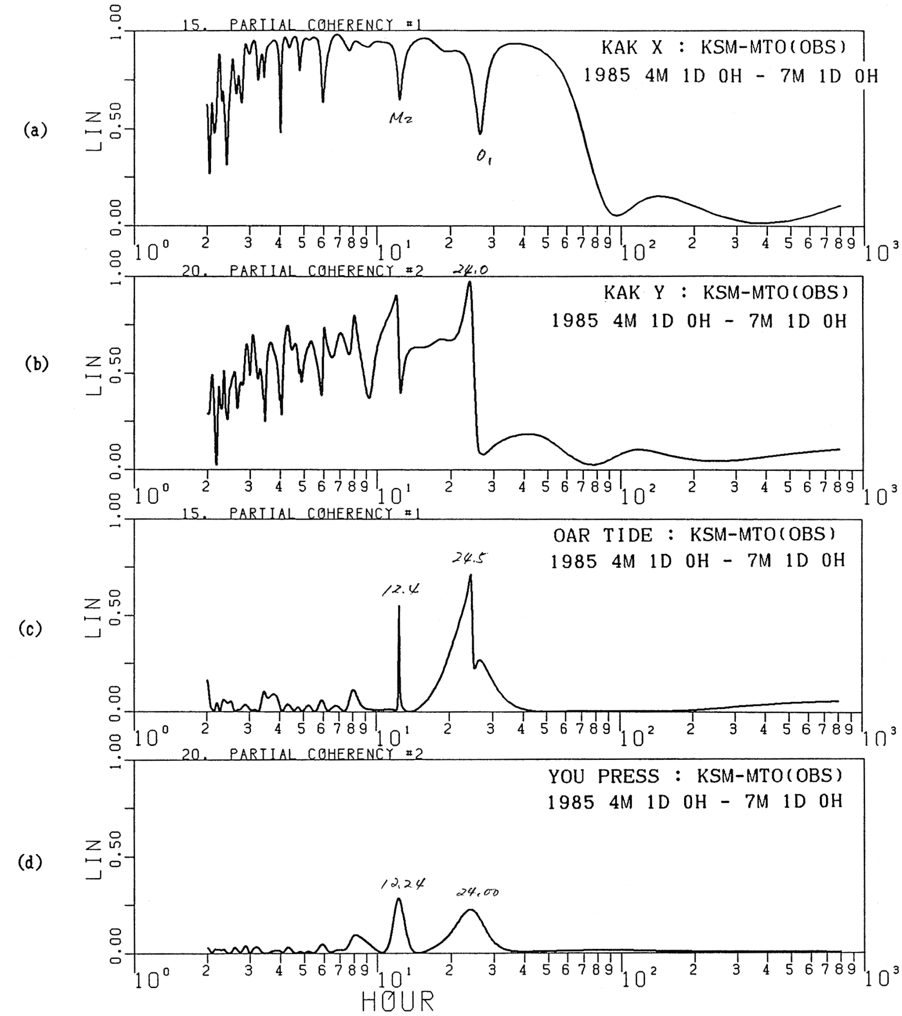

Fig. 9-2 Coherencies of KSM-MTO(OBS) for KAK X (a), KAK Y (b), TIDE at Ooarai (c) and PRESS at Youkaichiba (d).

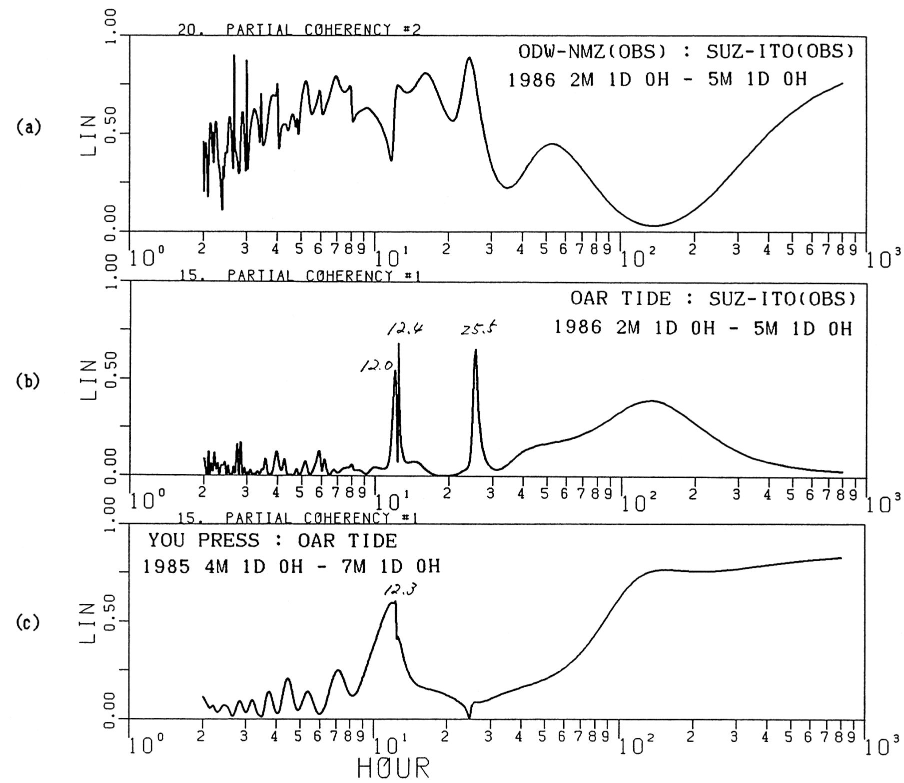

Fig. 9-3 Coherencies of SUZ-ITO(OBS) for ODW-NMZ(OBS) (a) and TIDE at Ooarai (b), and of TIDE at Ooarai for PRESS at Youkaichiba (c).

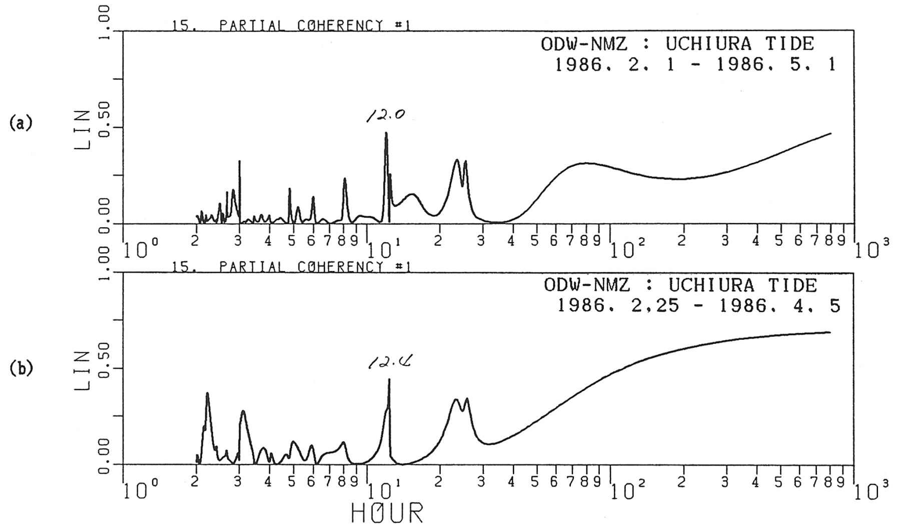

Fig. 9-4 Coherencies of TIDE at Uchiura for ODW-NMZ in two duration times.

10. Application for research of fault structure

On the research of earth resistivity by the direct current method, electrical currents of several to several tens amperes flow in the earth. The relation between the waveform of the current flowing in the earth and the waveform of the voltage which is received can be sought for information on the structure. The waveform can be distorted if there is a discontinuous layer. The presence of such a thing is confirmed in the active faults, such as the Senya fault (Ono and Uchida, 1982), Yamasaki fault (Electromagnetic Research Group for the Active Fault, 1982) and Kushibiki fault (Mori, et. al., 1983).

In this section, the application to fault research using artificial noise is tried instead of passing known current to the underground. Moreover, there is also a following purpose in exploring the possibility of detection of change of the electrical character relevant to tectonic activity. Honkura (1976) has calculated how much the amplitude and directions change, when the electrical conductivity changes. Even if the electrical noise by the direct-current train, etc., changes in time, it is possible that the response between points is fixed. It is also one of the subjects how much a response changes in time.

As shown in the records of the observed electrical fields at the Fujinomiya and Numazu group, the great portion of the observed electrical variations is an artificial noise in industrial regions and the places where a direct-current train runs. Since a direct-current train passes several 100 A current in the earth, we consider the current to be dispatch current and try fault research. It is thought that noises are observed in the wide area from the result of the observation of the electrical fields at the Fujinomiya and Numazu group. So, as the observation areas, the Iriyama fault near Fujinomiya and the Tanna fault near the center of the Numazu observation network are chosen. Moreover, there is also expectation that the position of the source of the artificial noises might be able to be presumed. Although the observation in the Fujikawa fault does not come to mind, since it performs the similar technique, it is introduced here.

10-1 Iriyama fault

Iriyama fault is located on the west side of the Fuji River as shown in Fig. 10-1, and is an active fault. Here, the observation was performed with 2 two-pen recorders in a tentative way on June 12, 1985. A pen recorder is set in the schoolyard of Yui-Kita elementary school as the base station. Since 1 Hz of telephone noises was observed there, there was concern because 1 Hz was due to be investigated also in regard to the noise waveform, but it was not recognized at other points.

Electrodes have been arranged along an L-character pattern of a 20 m baseline length, and the copper-copper sulfate electrodes are used. Fig. 10-2 shows the electrical variations at three points around the Iriyama fault and at the Fujinomiya group. The recorded papers are cut at the temporary points and then lined up together so that a vertical axis through all the papers may indicate the same time. The rectangular wave-noises are selected for about 30 seconds

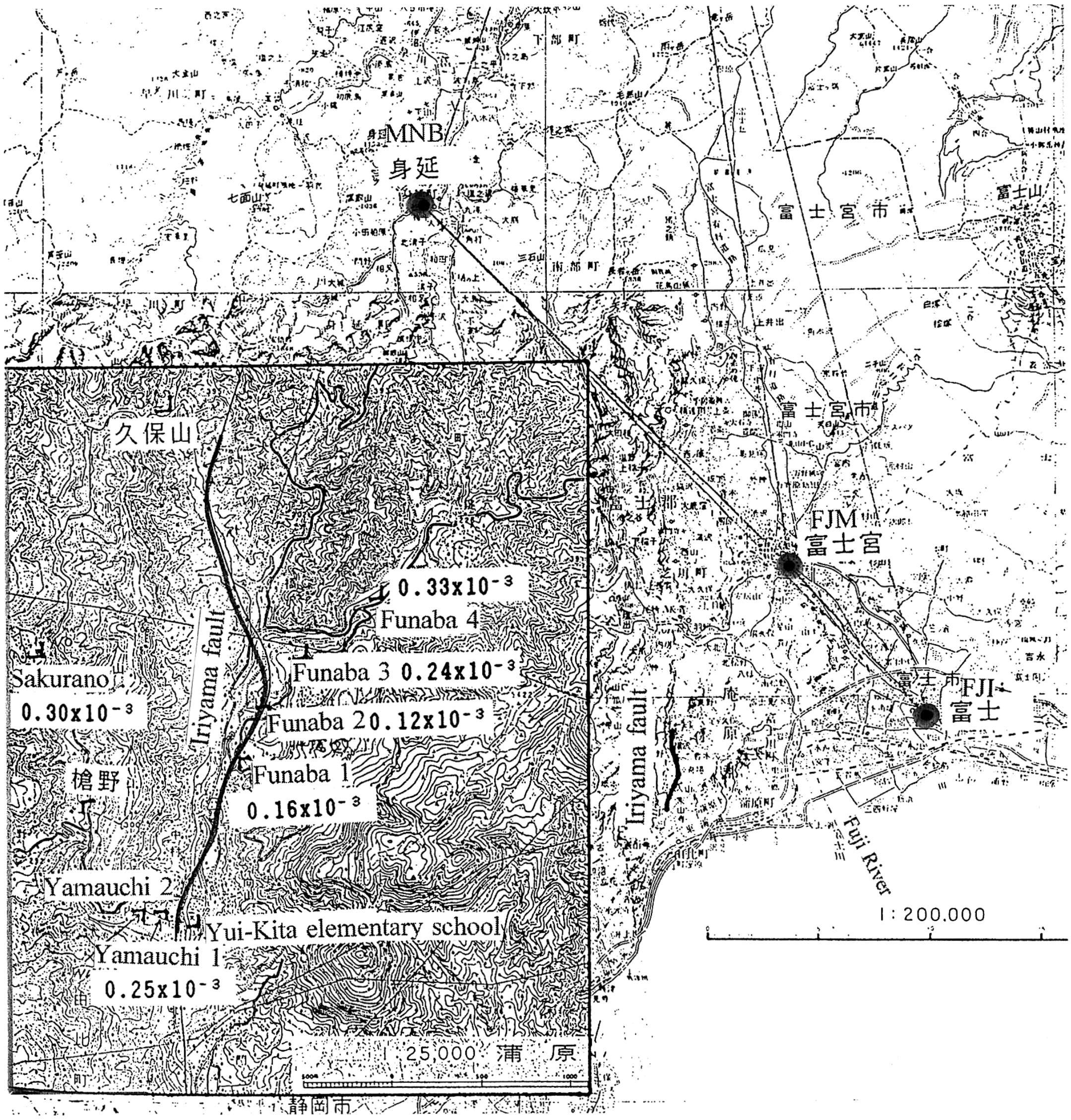

Fig. 10-1 Temporal electrical observation points and the amplitudes of the electrical noises around the Iriyama fault.

before and after 16:00 and 11:20 (arrows in Fig. 10-2), and the amplitude at each observation point is read on the basis of the potential difference between Fuji and Fujinomiya. The values are written down in Fig. 10-1. In Funaba-1 and Funaba-2, as compared with other points, the amplitudes are small, therefore these points are located in a low resistivity area, and are in agreement with the position of a fault. Although most directions of change of current are north and south, depending on the place, the direction of east and west also becomes large.

10-2 Tanna fault

Tanna fault also moved at the time of the Kita-Izu earthquake (M = 7.0) on November, 26, 1930, and a 2.5-3.5 m left gap level change was shown (Matsuda, 1972). The observation was carried out in the Tanna basin shown in Fig. 10-3 and near the center of the Numazu observation network. This place is located in a convenient position, although the observed noise judges whether it is a broader-based noise. Since the Tanna basin is covered by a deposition layer, even if a dislocation arises at such a place, not being detected at all electrically is also considered. However, when the electrical field is observed in a place of intense ups and downs, even if the change of the amplitude and/or the direction are actually observed, it is also considered that it becomes difficult to judge whether they are only a thing relevant to geographical feature in whether they are observed as a thing relevant to a dislocation. Therefore, this observation is performed by choosing flat grounds, also including an experimental meaning.

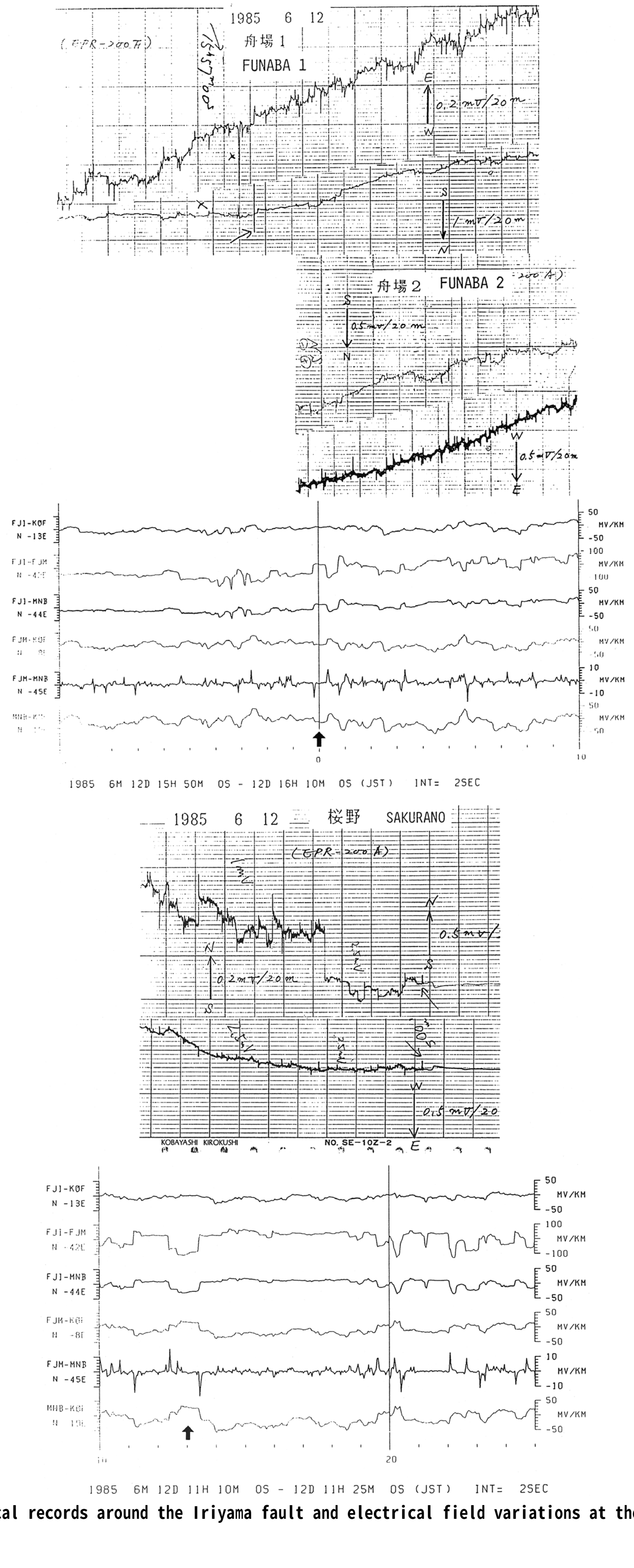

Fig. 10-2 Electrical records around the Iriyama fault and electrical field variations at the Fujinomiya group.

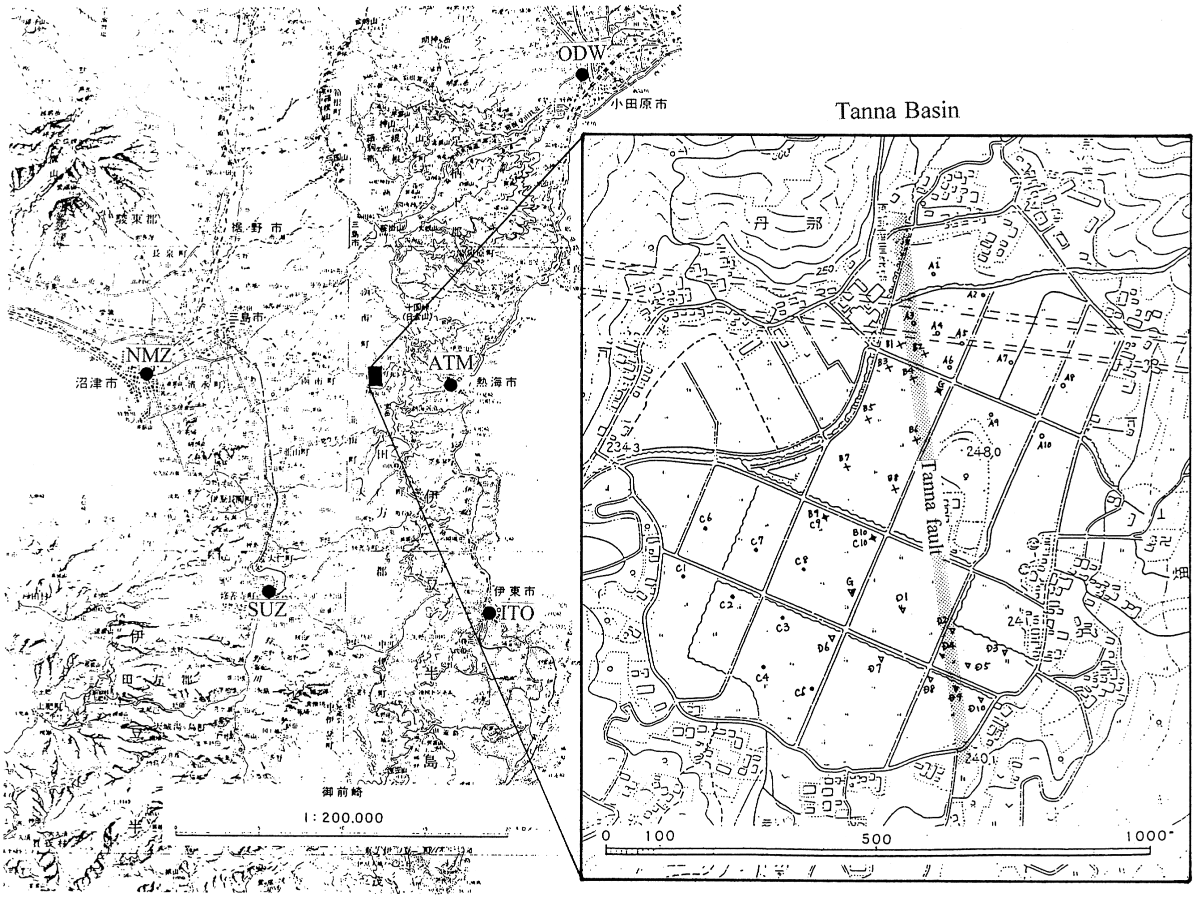

Fig. 10-3 Location of the Tanna fault and arrangement of temporal electrical observation points. Closed circles (●) show the NTT stations of the Numazu group.

The observations were conducted on March 12 and 13, 1986. The number of observing points is 40, and observation was carried out at intervals of 50 m or 100 m as shown in Fig. 10-3. Observation was conducted simultaneously with two digital recorders, which used a common ground, and 20 observation points were divided for measurements on two days, and two points were carried out in common among those. The sampling interval is 1 second, and electrical fields at the Numazu group are recorded also at 1-second intervals.

Fig. 10-5 shows the electrical records at the A and B observation groups for 20 minutes in the Tanna basin, and Fig. 10-4 shows the simultaneous record in the Numazu group. It is thought that the square wave for 20 seconds where the arrows are placed has a source of a noise near Numazu, and the same change is observed also around the Tanna fault. The similar square wave for 25 seconds at the C and D observation groups are also selected. Their orbits are drawn in Fig. 10-6. The Tanna tunnels are under the A observation group, and the dashed lines of the north and the south side show the positions of the tunnels of the JR Shinkansen railway and of the JR Tokaido railway, respectively. Although the trains of the Shinkansen are driven by alternating current and those of the Tokaido Line by direct current, an electrical noise shows an unusual change on the tunnel of Tokaido Line. It is not clear whether it is because there is something by which this unusual behavior reflected the structure of the tunnel itself, and a place from which current tends to leak to some tunnels. We do not yet have a conclusion about whether other things must be considered.

If the abnormalities near a tunnel are disregarded and we look at the whole, the amplitudes are large in the direction of north and east. This will be because the base of high resistance is shallow in that direction.

Although it is certain that the Tanna fault is near the position shown in this figure, the abnormalities considered to be based on it are not seen in electrical potential change. Since an electrical boundary is not produced even if a dislocation arises within a deposition layer of low resistance, it is not expected that electrical abnormalities appear.

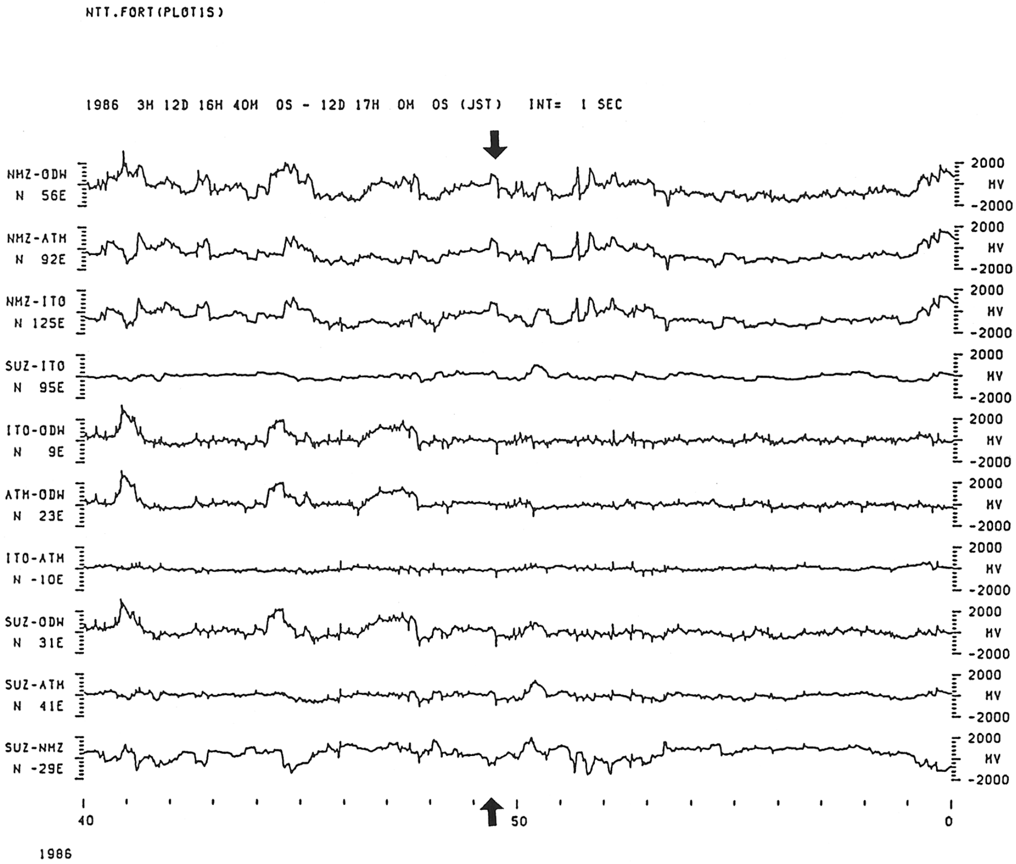

Fig. 10-4 Secondary electrical field variations at the Numazu group duration 15:40 to 17:00 on March 12, 1986.

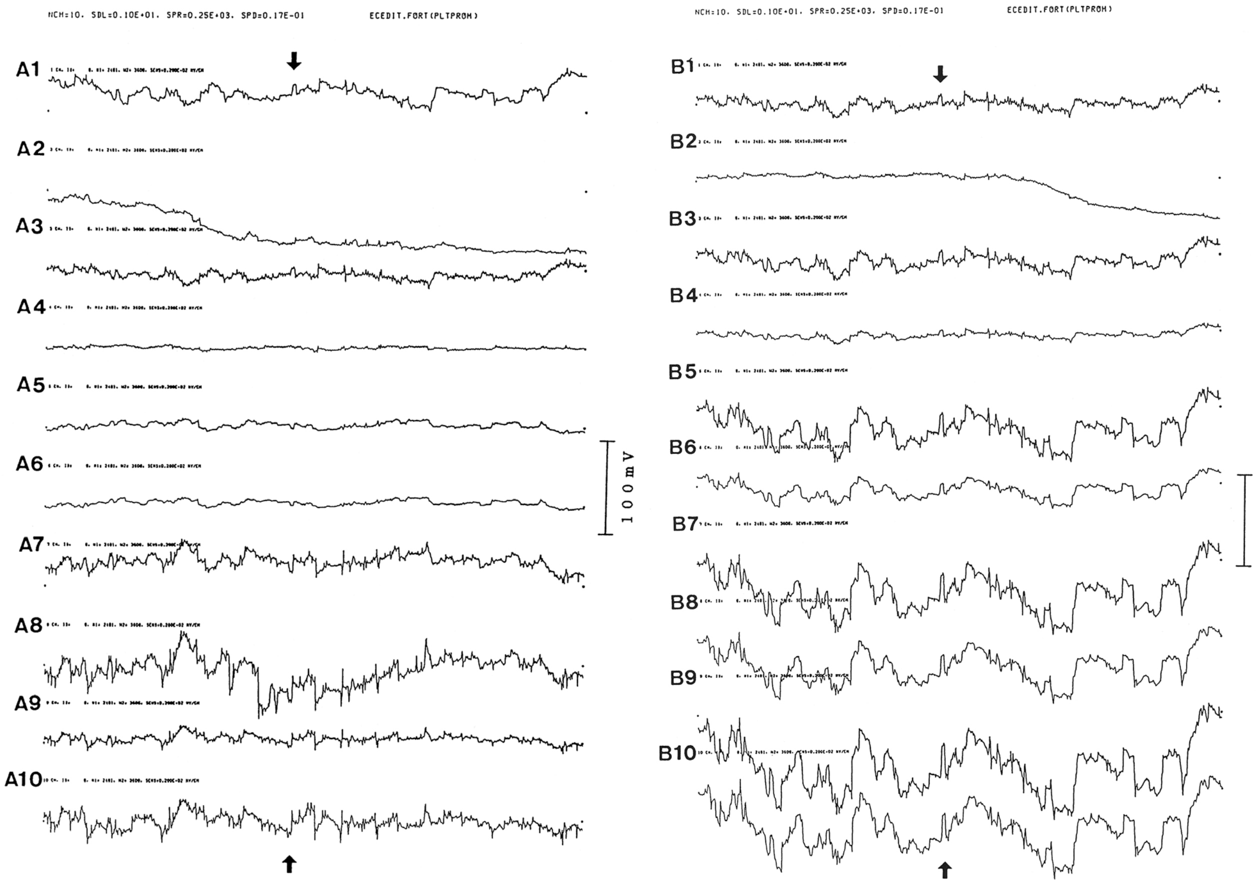

Fig. 10-5 Electrical field variations at the observation lines in and around the Tanna fault in the duration time of 20 minutes on March 12, 1986.

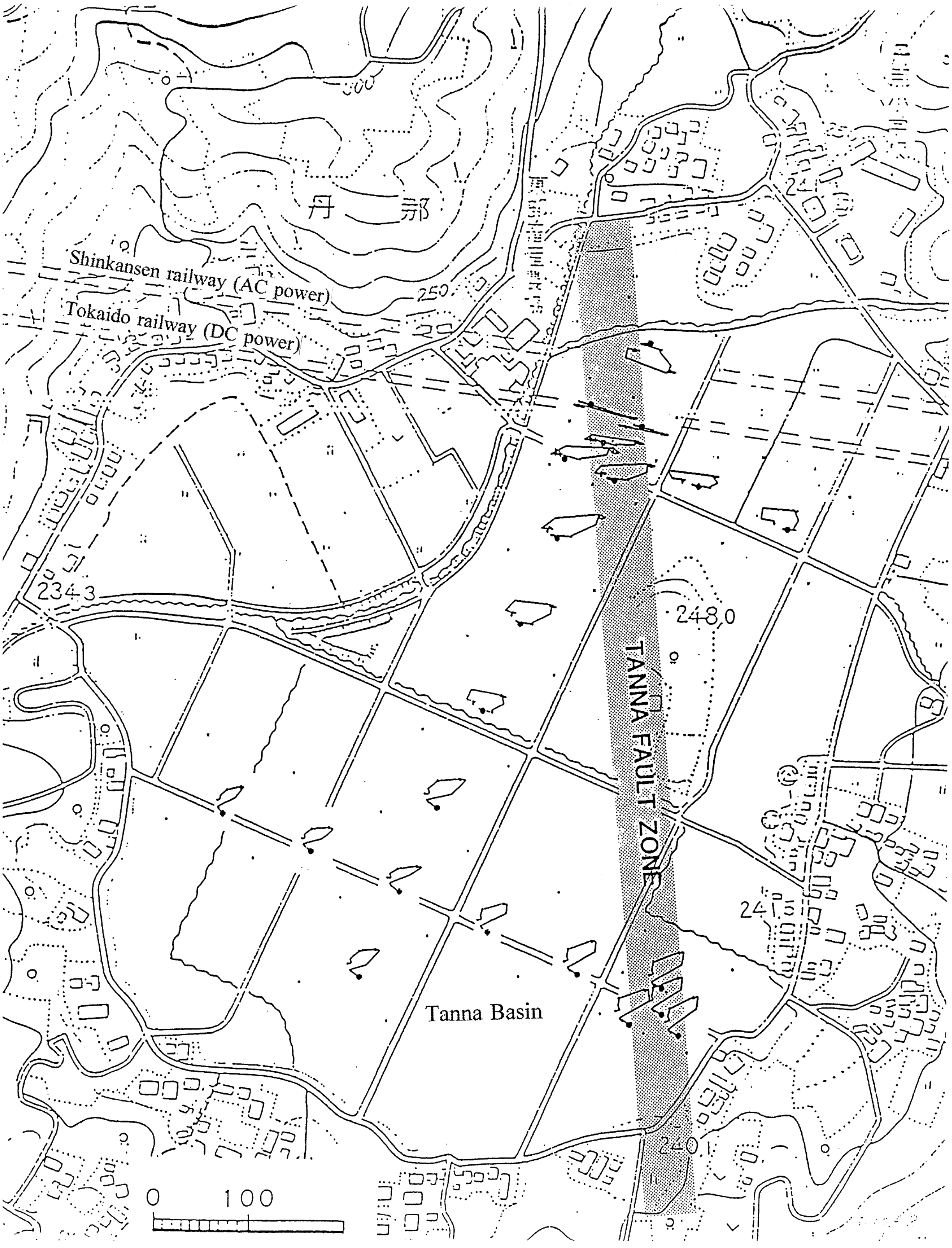

Fig. 10-6 The locus of the rectangular electrical noise changes every second for 20 and 25 seconds. The dashed lines of the north and the south side show the positions of tunnels of the JR Shinkansen railway, which is driven by alternating current, and of the JR Tokaido railway, which is driven by direct current, respectively. A depth of about 160 m has these two tunnels from surface of the earth.

10-3 Fujikawa fault

It is presumed that the Fujikawa fault is an active fault mostly prolonged toward the north from near the mouth of the Fuji River, and even the Ansei-Tokai earthquake in 1854 moved (Tsuneishi and Shiosaka, 1981). Moreover, it is thought that it is the fault which will probably cause the Tokai earthquake currently expected to start this dislocation in the near future. A good deal of drilling is performed near the Fuji River iron bridge of the Tokaido Line, and the position of the dislocation is generally confirmed. A fall of about 100 m is produced there. However, it is not clear near the mouth of the river, and the dislocation is filled in by presumption.

Observations of the magnetic total intensity by proton magnetometer, electrical resistivity with Wenner array, and artificial electrical noise were carried out near the mouth of the Fuji River.

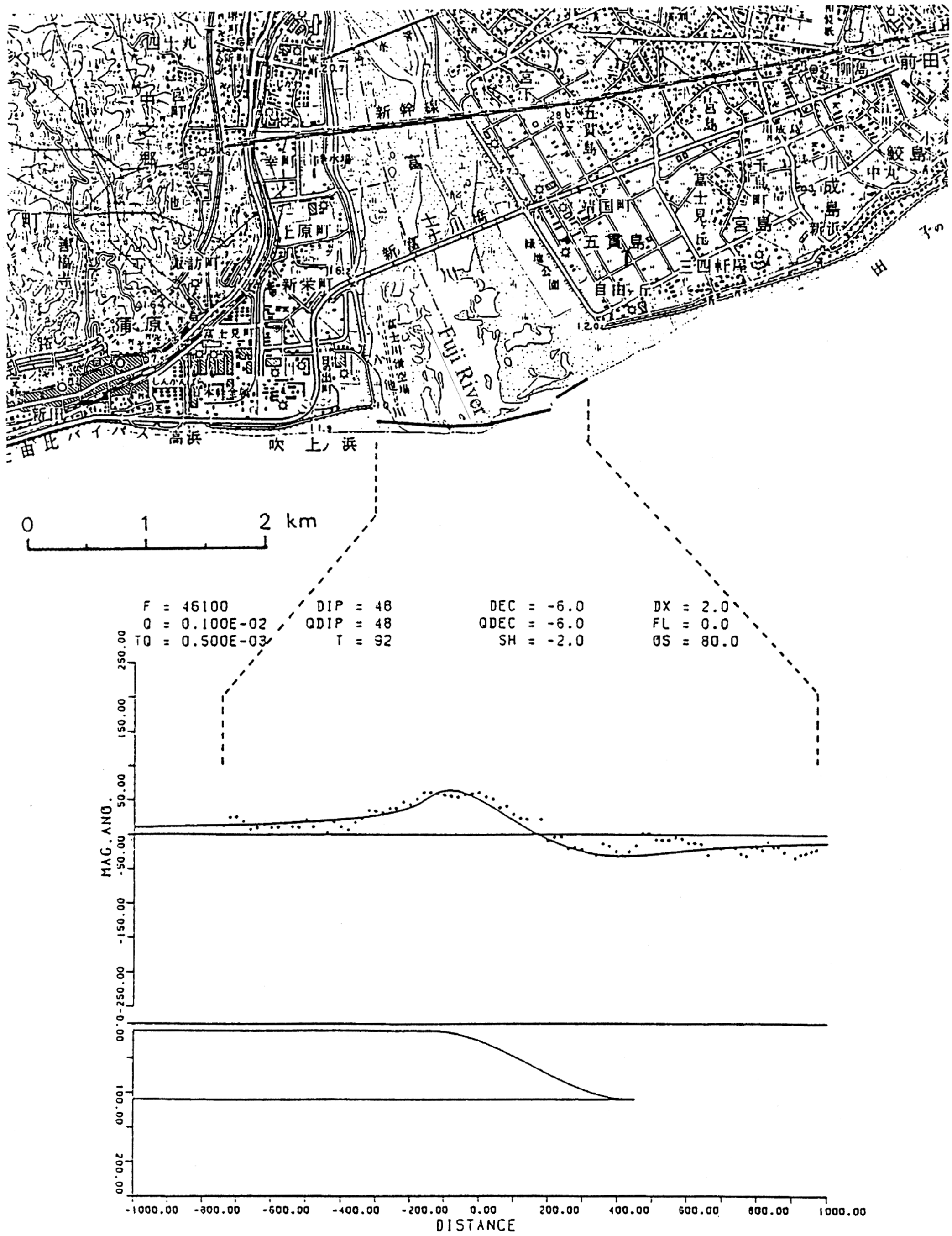

Fig. 10-7 Result of the observation of geomagnetic total intensity. The observation was conducted along the thick lines which meet the beach in the top of the figure. The point of the graph shows the observed magnetic field, and a solid line shows the profile of magnetic total intensity anomaly calculated from the subterranean anomalous magnetized body, which is shown in the bottom of the figure.

Fig. 10-7 shows the result of the observation of geomagnetic total intensity. The observation is conducted along the thick line which meets the beach because the electromagnetic noises are large in this neighborhood. The daily and short period variations of magnetic total intensity are compensated for using the magnetic variations at KAK. As shown in the middle of the figure, there is an anomalous change of around 100 nT. Magnetism, such as the lava near Fuji River, sand of the seashore, and stones and the Kanbara layer, were measured using an astatic magnetometer. The magnetic strength of the underground body is assumed by referring to the above measurement, and the underground structure as shown in the figure in the lower berth is presumed so that the observed magnetic total intensity will be suited. In the presumed model, the stratum inclines toward the east. The dislocation of an almost perpendicular fall is presumed from the drilling result near the iron bridge. Even if a fall produces geographical features by the dislocation only temporarily, it is also considered by the subsequent landslide that such a geographical feature arose. Calculation of a magnetic field is performed using magnetic permeability of 10^{-3} emu/cc by the formula from Mori et al. (1983) but not using the remaining magnetization.

Observation of electrical noise in the mouth of the Fuji River was performed with electrodes that have been arranged at 50 m intervals, as the black dots of Fig. 10-8 showed. It was carried out, as in the case of the Tanna fault, by the method of measuring the electrical potential of other points on the basis of one point, using copper-copper sulfate electrodes. Although the example of the potential record is not shown, the noise with a duration time of 5-6 seconds is chosen, and the situation of the change is shown in Fig. 10-8. A similar change was selected although No. 1-10 and No. 10-14 were not the same change, which are the points observed on another day.

Though the position of the fault presumed by the result of the observation of the magnetic total intensity is near No. 1, since it entered into the river, the east side has regrettably not been measured there. It seems that the amplitudes of the noise have changed in the west from No. 10. Since the measurements bordering on there were performed on different days, although firm belief is impossible, it is thought that a surface resistance change will be greatly reflected.

Although 1 more observation line is required in order to check the observed results of magnetic total intensity, even if it is measured by the inland side from it, it is thought that good results will not be obtained because of large artificial magnetic noises. If the size of an unusual region is taken into consideration, it will be thought that abnormalities are detectable to several 100 m in the offing. So it was considered that the measurements with a boat would be off by several 100 m, but that was regrettably unrealizable.

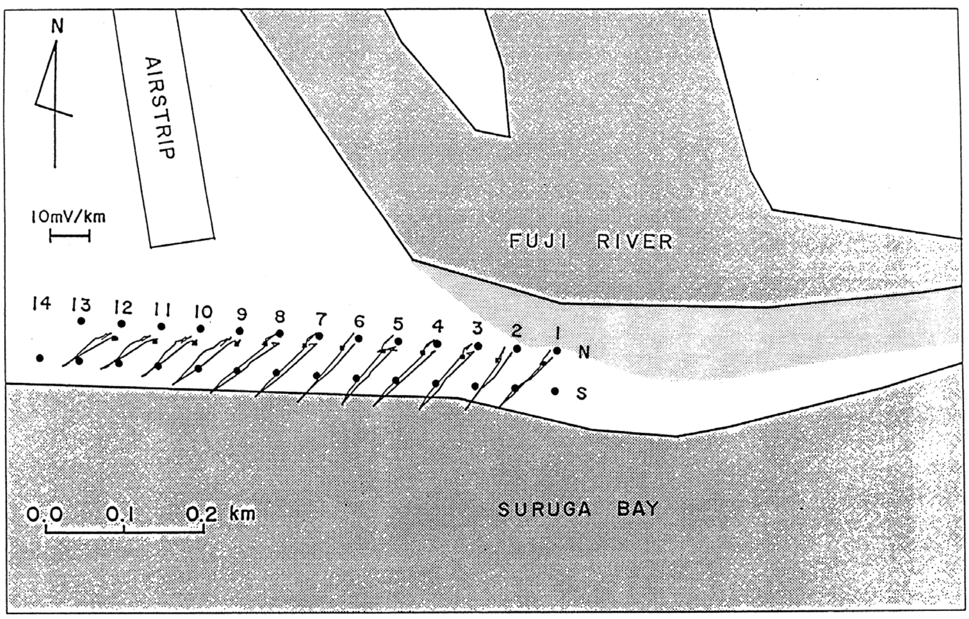

Fig. 10-8 Electrode arrangement for the observation of electrical noise in the mouth of the Fuji River, and the locus of electrical noise changes every second for 5 — 6 seconds.

11. Anomalous geoelectric change observed near CA (conductivity anomaly) boundary

It is well known that induced electrical currents tend to flow in a preferred direction. Honkura (1976) calculated how much the amplitude and directions of geoelectric variation change, when a conductivity anomalous region arose in relation to an earthquake. In his case, a base length for the observation, that is an arrangement of actual observing electrodes, was ignored. Here, when electrodes are arranged around an unusual domain, it calculates what potential difference is observed using the formula which he drew.

The case where electrical potential is observed around the unusual domain of a hemisphere (radius = a) as shown in the lower part of Fig. 11-1 is considered. The small open circles in the figure are the positions of the electrodes, and the top of the lower part of the figure looked at the unusual domain horizontally, whereas the bottom of the figure looked at it from the top.

Suppose that the uniform electrical field is built from the distant place of an unusual domain. The potential in the distance r from the center of the hemisphere is

$$Vo = A(r + K_1a^3/r^2)\cos\varphi \qquad (r>a)$$

$$Vi = ArK_2\cos\varphi \qquad (r<a).$$

Here, A is a constant, and φ the angle from the direction (the x direction) which the external field has required. If we make Ri the resistance in the hemisphere and Ro the resistance of the outside, K_1 and K_2 will be given by the following formula:

$$K_1 = (Ri - Ro) / (2Ri + Ro)$$

$$K_2 = 3Ri(2Ri + Ro) / (1 + K_1)$$

When we actually observe the electrical field, the potential differences of the directions of x (horizontal axis) and y (vertical axis) with the base lengths S centering on the distance D from the center are measured. It sets with K = Ri/Ro and a = 1, and when changing K, D and S, it calculates what potential difference (Ex and Ey) is observed.

The top of Fig. 11-1 is the example which calculated what values Ex and Ey would become for D = 1.2 and S = 0.2. A solid line shows the calculation result in K = 0.1, and a dotted line shows in K = 10, when the direction (φ) of external potential is made to change from 0 up to 90 degrees. Namely, when we observe the electrical potential immediately outside the anomalous region, the predominant direction of electrical change is perpendicular to the boundary for the low resistance anomalous region, and tangent for the high.

As K = 0.1, calculations were made to learn how an electrical field would be observed when the value of D changes when S = 0.01, 0.1 and 1.0, and show the result to the left of Fig. 11-2. A vertical axis Ex of the above graph expresses the size of the electrical field of x directions to the size of an external electrical field. The lower graph shows the degree of the predominant direction of the electrical field Ex/Ey. When an extreme value of S = 0.01 is used, the maximum value of Ex/Ey becomes ten.

As S = 0.01, calculations were made to learn how an electrical field would be observed when the value of D changes for K = 0.1, 0.2, and 0.5, and the results are shown to the right of Fig. 11-2. In this case, also, when we observe the electrical field near the CA (conductivity anomaly) boundary, the direction of the changes will show a strong predominant direction.

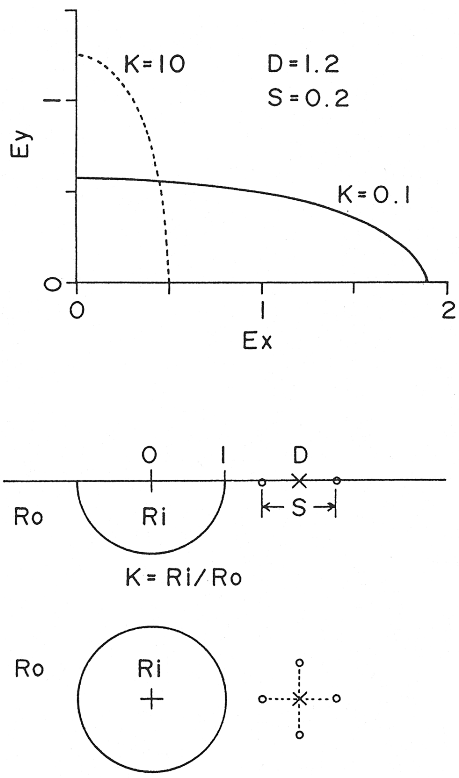

Fig. 11-1 Calculated electrical potential (top) around an unusual domain (bottom). The unusual domain has a hemisphere of a radius r, and Ri and Ro are the electrical resistances of the unusual domain and outside of it, respectively. Small open circles show the position of the electrodes. The base length for the observation is S; and D, which is a distance from the center of the hemisphere (O), is the center of the electrodes.

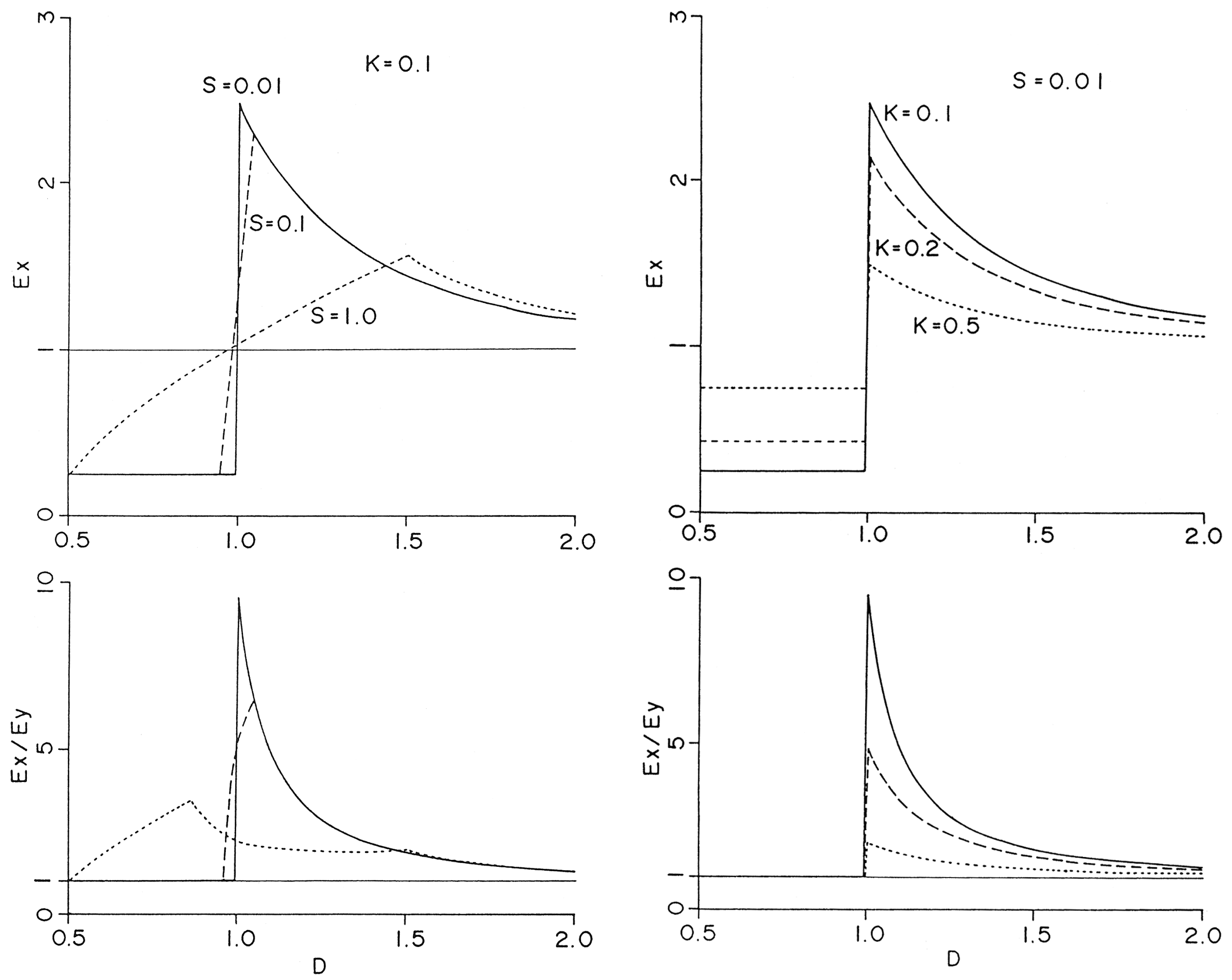

Fig. 11-2 Calculated electrical potential around an unusual domain.

The actual example of application of this calculation has electrical potential observation in the Akan lake in the eastern part of Hokkaido (Mori, 1987). The observation was performed by the north edge of the Akan caldera. If we assume that the Akan caldera has low resistance as compared with the circumference, it can explain why an electrical potential change which lay in the predominant direction of north and south was observed.

12. Electrical observation on the sea floor by making use of the power-feeding arrangement of the Permanent Ocean-Bottom Seismograph Observation System off Boso Peninsula (BSOBS)

Permanent Ocean-Bottom Seismograph Observation Systems by JMA is installed in the offing of Tokai, and the offing of Boso Peninsula (Fujisawa et. al., 1986). As shown in Fig. 2-1, the submarine systems are supplied with electric power in highly precise direct current from the power units at Omaezaki Weather Station (OMZ) and at Katsuura Weather Station (KTU) through cables. The return current flows between the sea earths (TS1 and BS1) attached near the terminal apparatus and the seashore earths (OMZ and KTU) through the sea water and the ground. Since the electrical supply voltage is controlled to compensate for the current when a potential difference arises between the sea earth and the seashore earth, if the electrical supply voltage is measured, the external potential change will be known. The case off Tokai is already described (Mori, 1982, 1987). Here, the example of electrical potential change measured about the case off Boso Peninsula is shown briefly.

Although it is not directly related to the electrical observations using NTT equipment, since it is thought that it is necessary to study the relation between the electrical field on land, and movement of sea water and the electrical field on the sea floor, it is described for reference.

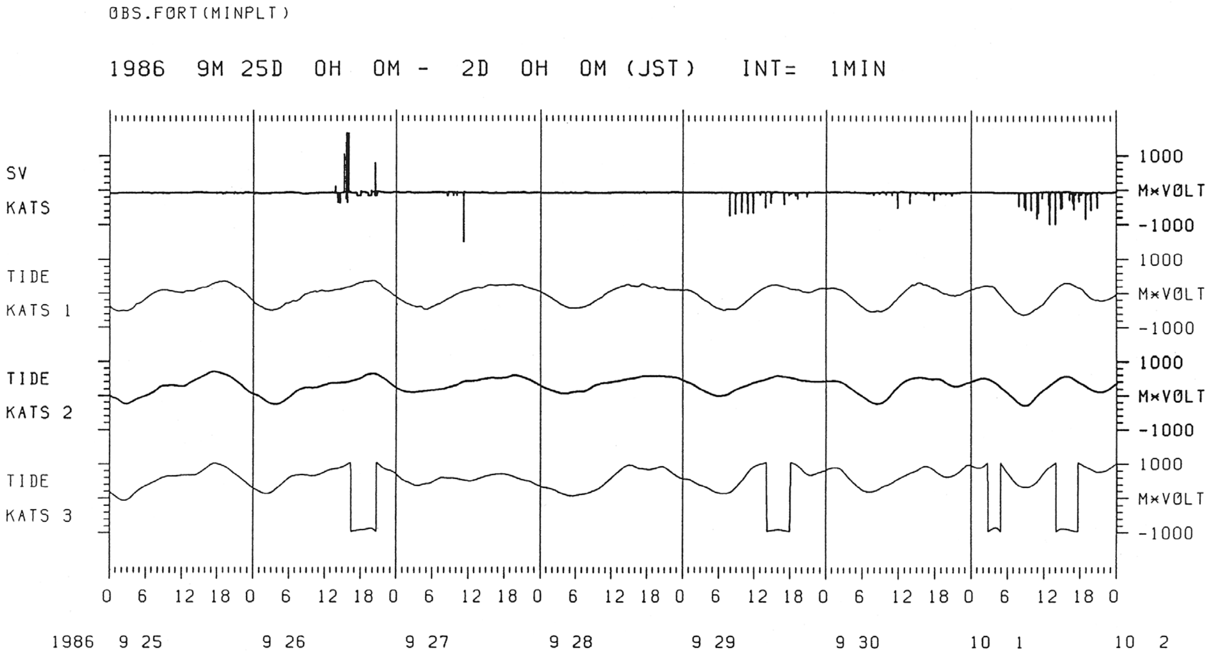

Fig. 12-1 Record of the electrical supply voltage (SV) and the tsunami meters (TIDE) in mV by BSOBS. TIDE at KATS 1, KATS 2 and KATS 3 represent the sea level at BS1, BS2 and BS3, respectively.

A part of the results are shown as recorded with the digital recorder in the Katsuura Weather Station from July to December, 1986, before being put into regular service. Fig. 12-1 shows the records of the electrical supply voltage (SV) and the tsunami meters (TIDE), and TIDE at KATS 1, KATS 2 and KATS 3 represent the sea level at BS1, BS2 and BS3, respectively.

Mustache-like noises are in the SV record in many cases in the daytime. Since it is thought that these noises are due to leak currents by the direct-current train, the relation between the variations of SV and the arrival-and-departure time of trains at the Katsuura railway station is investigated. It is confirmed that large changes of the SV correspond to the departure of a train as shown in Fig. 12-2. The state of noises changes from day to day as shown in Fig. 12-1. The cause for this is considered to be that the amount of current which is transmitted and leaks from a train's rail changes with conditions, such as humidity.

Although it is thought that it is difficult to use the data of a period of time containing that train noise, the data at night with few noises may be usable as effective data. Now, the telemeter of the data of BSOBS is carried out to the Seismological and Volcanological Department of JMA, and it is recorded there.

13. Conclusions

(1) Using the facilities of NTT Company, it is confirmed that we can obtain highly stable and noiseless geoelectric data compared to those obtained by ordinary observations. At Mito, the observed data are fairly noiseless, while at Numazu, the data contain large amplitude noises.

(2) The method of real-time detection of the anomalous geoelectric changes accompanying tectonic activity has been developed. Furthermore, in order to raise accuracy, it is thought to be required to take into consideration the use of BAYTAP-G (Ishiguro, et al., 1984), seasonal changes of geomagnetic field, etc.

(3) When it is assumed that the impulse response (impedance tensor) of the electrical variation to geomagnetic variation does not change in time and the impulse response is used for prolonged data, changes of underground electrical conductivity may also appear in the residual field as natural potential change.

(4) Though in the Mito group, unusual geoelectric change directly considered to have been related to the earthquake is not detected, a principal method for reduction of the induced component was established. However, examination of the abnormalities of short cycle changes of several hours or less is inadequate.

(5) Anomalous variations seemingly related to the earthquake swarm off the east coast of the Izu Peninsula were observed in the Numazu group. The

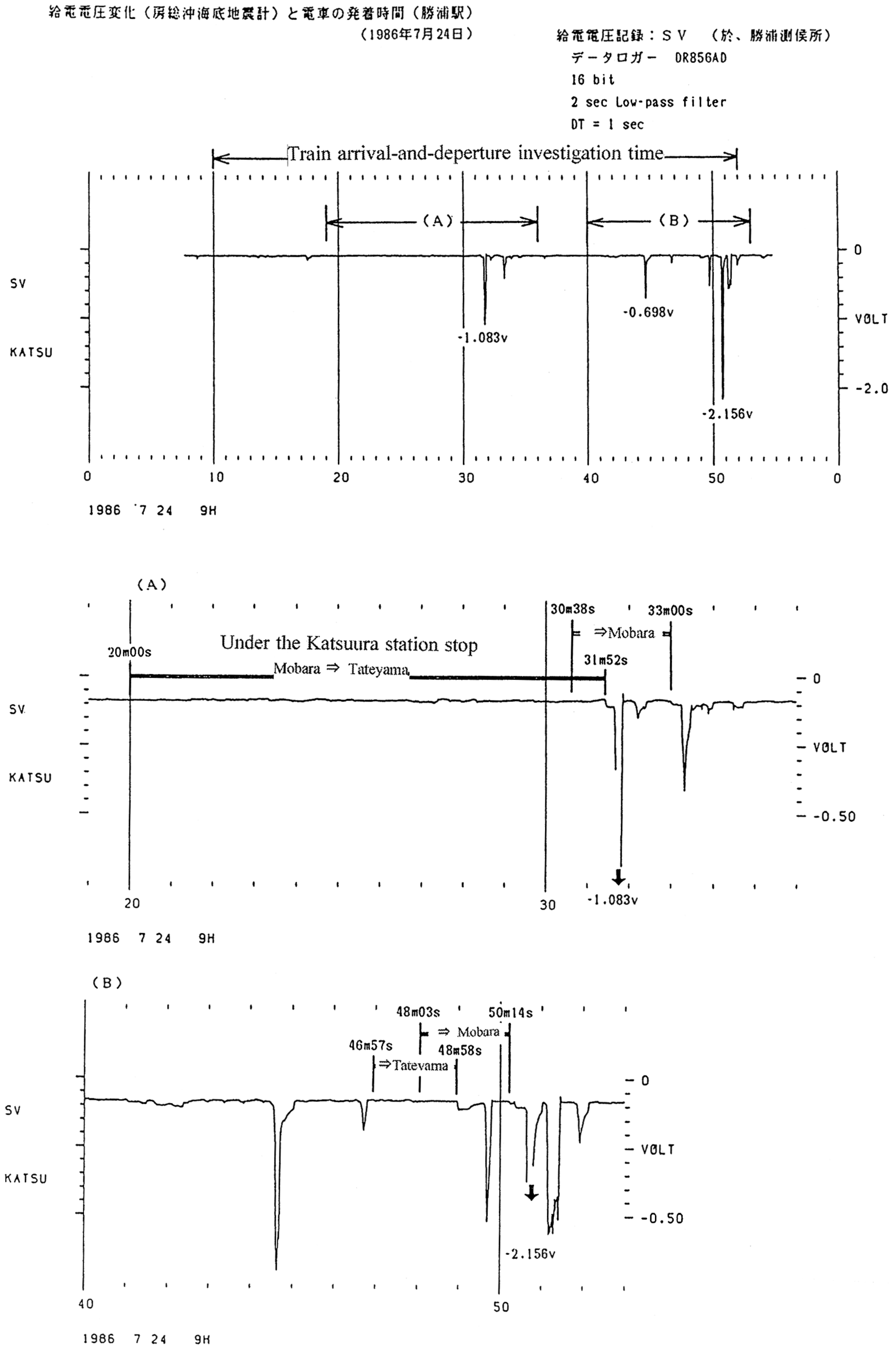

Fig. 12-2 Relation between the variations of the electrical supply voltage (SV) of BSOBS and the arrival-and-departure time of trains at the Katsuura railway station.

earthquake swarm started around October 13, 1985, when electrical potential changes of 300 mV at Atami and 100 mV at Ito and Shuzenji took place simultaneously. The volume strain meter of Higashi-Izu also changed simultaneously. Stress change applies to Shuzenji and Higashi-Izu from Atami, and it is thought that there was an electrical potential change corresponding to it. However, on the occasion of subsequent earthquake swarms (as earthquake swarms, the scales are somewhat small), changes were not detected.

(6) The Izu-Oshima volcano erupted on November 15, 1986. Before the start of the eruption, the geoelectric potentials at ODW are estimated to have decreased abruptly by 500 mV on November 6 and attained a maximum decrease of 800 mV on November 9. ODW is located at the extension of the Suruga Trough, and on the boundary of the Eurasia Plate and the Philippine Sea Plate. The flow of underground water which is caused by a change of stress acting on the boundary may possibly cause changes in the streaming potential and electrical conductivity. The change of the groundwater accompanying the stress change of a plate boundary can be considered to be the cause of this.

(7) The electrical potential changes relevant to tide level changes were detected. Around March, 1986, the tide level change was sharp, and the electrical potential changed in a way that it was thought that it was related to the electrical potential in the Numazu group. There was change relevant to a tide level with the electrical potential of the Numazu group around August 4, 1986.

(8) Constituents of geoelectric change unrelated to geomagnetic change and long cycle change were detected. Although it is thought that the constituents are based on the earth tide or a sea tide, in order to separate these, comparison observation at many points is required. The earth tide and long cycle change may express the potential change accompanying stress change.

(9) The noise by the direct-current train is observed in several 10 km, as shown by Section 10. By investigating a time change of response of electrical fields observed between baselines, it is thought that it is applicable also to detection of an underground electrical change.

(10) As shown in Section 11, the big abnormalities in electrical potential changes should be observed near the CA (conductivity anomaly) boundary. On the contrary, if earth potential is observed near the CA boundary, it will be thought possible to detect sensitively unusual phenomena relevant to tectonic activities. The pattern of daily changes of the earth potential before and behind the eruption of the Izu-Oshima volcano is considered to reflect such a state.

14. Circumstances of observation and acknowledgements

The author is indebted extensively to the staff of the Nippon Telegraph and Telephone Public Corporation (now NTT Company) for their observations, and he had many people support the cause which began with this observation.

After the author's transfer (April, 1980) to the Seismology Volcanology Research Department of Meteorological Research Institute (MRI), he was soon blessed with the opportunity to analyze the geoelectric observations on the sea floor by making use of the power-feeding arrangement of the Permanent Ocean-Bottom Seismograph Observation Systems (OBS) installed by the Japan Meteorological Agency (JMA). It was shown that the earth potential observation using the electrical supply voltage of the OBS is effective and useful for the research of earthquake prediction, oceanography, etc. (Mori, 1982). Mr. Matsumoto, who belongs to the same research section as the author, taught that NTT has adopted the same system as OBS for the electrical supply system from Ito to Izu-Oshima and Miyake-jima. The author had Mr. Matsumoto and Mr. Fujisawa, of the Earthquake Division of JMA, introduce Mr. Aoyagi, who is taking charge of system manufacture of the NEC Company, and after that visited the Engineering Department of the Kanto Telecommunications Bureau with Mr. Matsumoto and Mr. Aoyagi (July, 1983). The author explains the affair of the geoelectric observation off Tokai to Mr. Hagiwara of the Engineering Department, and allowed for an experimental observation for the submarine cable between Ito and Izu-Oshima.

Although it was decided to perform test observations from the beginning of October, 1983, in Ito, when the test record of the time of installation of NTT Corporation electrical supply system was considered, it became clear that the current supplied was seldom stable. Moreover, since the supply of current was performed from both Ito and Izu-Oshima, even if it was recorded only in Ito, it turns out that it is likely to be almost meaningless. It seemed that furthermore, temperature changes were also received. Moreover, since the cable was prolonged also to Miyake-jima, it became a conclusion that it is better to carry out simultaneous measurements also in Miyake-jima. Therefore, although it was thought that data with utility values could be taken when performing simultaneous measurements at three places, Ito, Izu-Oshima, and Miyake-jima, since measurement equipment and traveling expenses were not able to be prepared, observation had to be given up. Having considered that Miyake-jima volcano erupted on October 3, 1983, and Izu-Oshima volcano erupted on November 15, 1986, it was very regrettable.

The author visited the Kanto Telecommunications Bureau and said that he could not but give up observations and expressed his gratitude for all the cooperation he had received. At that time, the author had Mr. Hagiwara and Mr. Ban teach that there is a cable which is used for geoelectric observation also on land.

Although we had performed many extraordinary geomagnetic and geoelectric observations, the best we could do was to record up to half of the values of geoelectric observations during an observation period. Geoelectric observations have been continuously afflicted by artificial noises and the drift by change of contact potential between electrode and soil. Even if an author reads or hears a paper saying that an unusual phenomenon of earth current came out before an earthquake, therefore, do not feel that those statements can be trusted as they are. (However, the author once observed a geoelectric record which is still regarded as the sign of an earthquake.) Even if the copper-copper sulfate electrode and the lead-lead chloride electrode, which are said to have little drift, were used for geoelectric observations, the records were not shown to be the same as daily changes when they were observed at the same point (Mori, 1984). So we are beginning to think that geoelectric observations will be almost meaningless for anything besides inferring an underground structure. But if the long baseline of NTT Corporation can be used, the author thinks that it will be value to carry out test observations ashore.

Although noises, such as thunder, were causes for anxiety when observing using the line stretched in the air, it is allowed to use the subterranean buried cable which is on a direct route between telephone offices. And it was allowed to observe geoelectric fields by the route of Mito-Kasama-Shimodate near the MRI. Moreover, the author had borrowed the low-path filter of 10 seconds to several tens of minutes from Mr. Yoshino of the Earthquake Research Institute, University of Tokyo, recently. Since it was expected that the 1-second noise of a charge counter and a city artificial noise enter when the ground of a telephone office was used as an electrode, observations could not be made without the filter, but the timing was very good.

Since it became clear that Kasama was an uninhabited relay station just before the observation start, the pen recorder was installed in the Shimodate relay station, and it was decided to measure the electrical potential of Kasama and Oyama on that basis (November 29, 1983). Although the recorder sometimes caused trouble, Mr. Tomaru and persons in the Shimodate relay station very cooperatively maintained it. Although the obtained record was fragmentary, it was big harvest that checked that the record had almost no drift, and there were few artificial noises beyond anticipation in spite of having the NTT relay station located at the urban center. However, using only the record of a pen recorder, since there was a limit in the analysis, the observation was interrupted in four months.

Since the prospect which can purchase one digital recorder in March, 1985 was attached, it offered again to want to perform test observation to Mr. Hagiwara. He pleasantly consented to test the observations. It was then decided to measure the electrical potential between Ishioka, Kasama, and Hitachiota on the basis of Mito so that the directivity of the earth current could also be discussed. The reason for choosing that was based on the following reason. Since it is a new method, it was necessary first to compare with the data of the Magnetic Observatory, and this area was chosen since there are probably comparatively few noises because of an alternating current train. Observation was started from January, 1985, using the multi-pen recorder. Also adding to the March record by the newly-purchased digital recorder, electrical potential came to be able to carry out digital inclusion. The head, Mr. Miyazawa, the Examination Division chief, Mr. Tsukui, and other personnel also of the Mito Telephone Office got very much interested in earth current observation, and they cooperated very much with the trouble of a recording form and the pen of a pen recorder and entry of time, etc.

Nippon Telegraph and Telephone Public Corporation became Nippon Telegraph and Telephone Company (NTT) from April, 1985; however it was convenient to make geoelectric observations anyway. Since the prospects of purchasing the 2nd digital recorder seemed much stronger, an offer was made to carry out observations, starting with continuing observations in Mito and another point at the Kanto Telecommunications Bureau in March, 1985. There was very good cooperation, although Mr. Toyoda and Mr. Terashima became negotiation partners, instead of Mr. Hagiwara, on the Kanto Communication Bureau side at this time. Since the Fujinomiya telephone office, which was the next place desired for ground observations, was under the jurisdiction of the Tokai Telecommunications Bureau, they introduced Mr. Mimura of the Facilities Department, the Tokai Telecommunications Bureau.

When the plan to do observations in Fujinomiya was formed in April, 1985, the person in charge of the Tokai Telecommunications Bureau had replaced Mr. Serizawa at this time. As a result of expressing to him by telephone our desire to carry out the start of observations, he pleasantly consented. In addition, the organization of NTT was changed, the Mito telephone office came under the jurisdiction of the Kanto Total Branch, and the Fujinomiya telephone office came under the jurisdiction of the Tokai Total Branch from April.

When it was determined that observation in Fujinomiya would start from June 10, 1985, the underground metallic cable of the Fujinomiya-Minobu-Kofu route was already due to be transposed to the optical fiber cable at this time. Although the author had agreed on waiting until the cable was replaced for good conditions to observe, the cable was flooded out by the heavy rain from the typhoon on June 30. Since Mr. Serizawa proposed the continuation of observation at another point, the author chose Numazu and is also continuing observations there now.

Although the Numazu, Shuzenji, Ito, and Atami telephone offices belonged to the jurisdiction range of the Tokai Total Branch and Odawara belonged to the Kanto Total Branch, both the total branches cooperated willingly. After that the division system of NTT was changed further, and the Mito, Kasama, and Hitachiota telephone office came to belong to a Central Network Branch. I had Manager Kawasaki of the Engineering Department of the Kanto Total Branch introduce the Central Network Branch, and had him become the negotiation partners to Mr. Seki and Mr. Noguchi of the First Equipment Part.

Personnel movement of NTT was very intense, and the negotiation person in charge was replaced in several months. However, irrespective of that, there was no trouble in the observation. Since the Tokai Total Branch was located in Nagoya-shi, correspondence about the observation was performed by telephone and letter. The author took advantage of his attending the general meeting of the Seismological Society of Japan in Gifu University in October, 1986, to call on the Tokai Total Branch in Nagoya-shi and was allowed to explain the observation results, etc., to about ten personnel. At this time, it was conversely encouraged by Mr. Ide and Mr. Yamaguchi of the Technology Planning Part, who had become the negotiation partners.

In the Numazu and Mito telephone office, geoelectric observations have been performed with digital recorders and the monitor record was made by multi-pen recorders. Using the digital recorders are most convenient, while the paper sendings and the pens of the multi-pen recorders sometimes get out of condition. Although it was kept in mind so that trouble might seldom be made for the personnel of NTT, they corrected the trouble of paper sendings or pens in practice. They show interest also about the records and fill in time, etc., independently. We are especially indebted to The First Transmission Radio Engineering Division Section chief, Mr. Suzuki in Numazu, and The General Planning and Policy Division Section chief, Mr. Hinohara in Mito.

The third laboratory for studying the tectonic activities relevant to an earthquake was installed in the Seismology Volcanology Research Department of MRI in October, 1984. The author will belong to the third laboratory from the first laboratory and will take charge also of the research on electromagnetism thereafter. The following three persons will cooperate in this research, Mr. Takayama, who transferred from the Seismological Observatory of JMA, Dr. Yoshikawa, who was employed from the Earthquake Research Institute, University of Tokyo and Mr. Koizumi of the second laboratory. Especially, the analyses of the removal of induced electrical potential change and the dislocation inquiry have the large contribution by Mr. Takayama. Moreover, the author had Dr. Katsumata and Dr. Seino of the first laboratory and Mr. Takahashi and Mr. Sato of the Planning Office cooperate in the maintenance of apparatus, etc.

The author was transferred to the Kakioka Magnetic Observatory in April, 1987, and belongs to also the MRI will continue observation further simultaneously with MRI. The observation is taken over pleasantly by the personnel of the Magnetic Observatory. When summarizing this article especially, Dr. Ozima cooperated very much.

Finally the author is deeply thankful to the above-mentioned people.

In addition, the author's place was changed in the Seismological and Volcanological Department of JMA in October, 1987. This paper is described based on the memorandum described in September, 1987.

References

Akaike, H., Power spectrum estimation through auto-regressive model fitting, Ann. Inst. Statist. Math., 21, 407-419, 1969.

Akaike, H., Information theory and an extension of the maximum likelihood principle. In: B.N. Petrov and F. Csaki (Editors), 2nd Inst. Symp. on Information Theory. Akademiai Kiado, Budapest, 267-281, 1973.

Ashida, Y., and M. Saito, Design of digital Chebyshev filter, Geophysical Exploration 23, 6-19, 1970 (in Japanese).

Barlow, W. H., On the spontaneous electrical currents observed in the wires of the electric telegraph, Phil. Trans. Roy. Soc. London, A 61, 61-72, 1849.

Chapman, S., and J. Bartels, Geomagnetism, Oxford Univ. Press, London, 417-448, 1940.

Corwin, R. F., and H. F. Morrison, Self-potential variations preceding earthquakes in Central California, Geophys. Res. Lett., 4, 171-174, 1977.

Earthquake Research Institute, University of Tokyo, Variation in the Electrical Resistivity of the Fujikawa Fault (March, 1984 - December, 1986), Report of the Coordinating Committee for Earthquake Prediction, 38, 391-393, 1987 (in Japanese).

Electromagnetic Research Group for the Active Fault, Low electrical resistivity along an active fault, J. Geomag. Geoelectr., 34, 103-127, 1982.

Fujisawa, I., S. Tateyama and J. Funasaki, Permanent Ocean-Bottom Earthquake and Tsunami Observation System off the Boso Peninsula, Sokko-Jiho, 53.3, 1-40, 1986 (in Japanese).

Garland, G. D., Earth currents, in Methods and Techniques in Geophysics, edited by S. K. Runcorn, Interscience, New York, 1, 277-307, 1960.

Hatakeyama, H., Earth current. Physics, Iwanami, C, 1-6, 1940 (Japanese)

Honkura, Y., Perturbation of the electric current by a resistivity anomaly and its application to earthquake prediction, J. Geomag. Geoelectr., 28, 47-57, 1976.

Ishiguro, M., T. Sato, Y. Tamura, M. Ooe, Tidal data analysis - An introduction to BAYTAP-G, Proceedings of the Institute of Statistical Mathematics, 32, 71-85, 1984 (in Japanese)

Japan Meteorological Agency, Seismic activity in and around the Izu peninsula, November, 1986 - May, 1987, Report of the Coordinating Committee for Earthquake Prediction, 38, 237-246, 1987 (in Japanese).

Matsuda, T., 1930 Earthquake fault of the Kita-Izu earthquake, Izu, Tokai University Press, 73-93, 1972 (in Japanese).

Molnar, P., T. Hanks, A. Nur, B. Raleigh, F. Wu, J. Savage, C. Scholz, H. Craig, R. Turner and G. Benett, Prediction of the Haicheng earthquake. EOS (Trans. Am. Geophys. Union), 58, 236-272, 1977

Mori, T., and K. Hasegawa, On Earth current 1Hz noise in Yasutomi-cho, Hyogo, The Technical Report of the Kakioka Magnetic Observatory, 19, 1, 27-33, 1979 (in Japanese).

Mori, T., Electrical field fluctuations on the seafloor of the Tokai-oki, -Use of the Ocean Bottom Seismograph Observation System -, Zisin, 35, 213-221, 1982 (in Japanese).

Mori, T., M. Kawamura, K. Ohchi and Y. Mizuno, Electric and magnetic structure of the Kushibiki fault, Papers in Meteorology and Geophysics, 34, 95-104, 1983 (in Japanese).

Mori, T., Electric potential parallel observation by three kinds of electrode, Report of Conductivity Anomaly Research Group, 287- 292, 1984 (in Japanese).

Mori, T., A test observation of geoelectric field with a long electrode span. Paper in Meteorology and Geophysics, 36, 149-15, 1985. (in Japanese)

Mori, T., Variations in the geoelectric field with relation to crustal conditions of the earth, Geophysical Magazine, 42, 41-104, 1987.

Myachkin, V. I., G. A. Sobolev, N. A. Dolbilkina, V. N. Morozow, and V. B. Preobrazensky, The study of variations in geophysical fields near focal zones of Kamchatka, Tectonophysics, 14, 287-293, 1972.

Ono, Y., and T. Uchida, Research on the underground resistance structure of the Sennya fault and its circumference, Research of the degree of dislocation activity by the earth electromagnetic technique. 58-63, 1982 (in Japanese).

Rikitake, T., and I. Yokoyama, The anomalous behavior of geomagnetic variations of short period in Japan and its relation to the subterranean structure. The 6th report. (The results of further observations and some considerations concerning the influences of the sea on geomagnetic variations). Bull. Earthq. Res. Inst., Univ. Tokyo, 33, 297-331, 1955.

Sakamoto, Y., M. Ishiguro and G. Kiatgawa, Akaike Information Criterion statistics, KTK Scientific Publishers, 290 pp, 1986.

Shyda, R., On earth currents, Transaction of the Seismological Society of Japan, 9, 32-50, 1886.

Sobolev, G. A., Application of electric method to the tentative short term forecast of Kamchatka Earthquake, Pure Appl. Geophys., 113, 229-235, 1975.

Takayama, H., and T. Mori, A trial of elimination of geoelectric field variations induced by geomagnetic variations, Papers in Meteorology and Geophysics, 38, 17-28, 1987. (in Japanese)

Tsuneishi, Y., and K. Shiosaka, The Fujikawa fault and the Tokai earthquake, Engineering Geology, 22, 52-66, 1981 (in Japanese).

Varotsos, P., and K. Alexopoulos, Physical properties of the variations of the electric field of the earth preceding earthquakes. Determination of epicenter and magnitude, Tectonophysics, 110, 99-125, 1984.